

This report was prepared as an account of work sponsored by an agency of the United States Government. Neither the United States Government nor any agency thereof, nor any of their employees, makes any warranty, express or implied, or assumes any legal liability or responsibility for the accuracy, completeness, or usefulness of any information, apparatus, product, or process disclosed, or represents that its use would not infringe privately owned rights. Reference herein to any specific commercial product, process, or service by trade name, trademark, manufacturer, or otherwise does not necessarily constitute or imply its endorsement, recommendation, or favoring by the United States Government or any agency thereof. The views and opinions of authors expressed herein do not necessarily state or reflect those of the United States Government or any agency thereof.

METALLIC FUELS HANDBOOK

Compiled by

G. L. Hofman, L. Leibowitz, J. M. Kramer,  
M. C. Billone, and J. F. Koenig

Argonne National Laboratory  
9700 South Cass Avenue  
Argonne, Illinois 60439

ANL-IFR--29

TI86 025342

~~NOTICE  
This report contains information of a preliminary nature and was prepared primarily for internal use at the originating installation. It is subject to revision and therefore does not represent a final report. It is passed to the recipient in confidence and should not be abstracted or further disclosed without the approval of the originating installation or USDOE Office of Scientific and Technical Information, Oak Ridge, TN 37830.~~

IFR TECHNICAL MEMORANDUM NO. 29

~~Results reported in the IFR-TM series of memoranda frequently are preliminary and subject to revision. Consequently they should not be quoted or referenced without the authors' permission.~~

~~APPLIED TECHNOLOGY  
Any Further Distribution by any Holder of this Document or of the Data Therein to Third Parties Representing Foreign Interests, Foreign Governments, Foreign Companies and Foreign Subsidiaries or Foreign Branches of U.S. Companies Should Be Coordinated with the Deputy Assistant Secretary for Breeder Reactor Programs, Department of Energy.~~

~~APPLIED TECHNOLOGY  
Any further distribution by any holder of this document or of the data therein to third parties representing foreign interests, foreign governments, foreign companies and foreign subsidiaries or foreign branches of U.S. companies should be coordinated with the Deputy Assistant Secretary for Breeder Reactor Programs, Department of Energy.~~

Distribution of this report is Unlimited, David Hamrin, OSTI, 12/09/2016

~~Released for announcement  
in the Distribution Program to  
participants in the LMFBR  
program. Others request from  
DOE~~

*Handwritten signature*

## **DISCLAIMER**

**This report was prepared as an account of work sponsored by an agency of the United States Government. Neither the United States Government nor any agency Thereof, nor any of their employees, makes any warranty, express or implied, or assumes any legal liability or responsibility for the accuracy, completeness, or usefulness of any information, apparatus, product, or process disclosed, or represents that its use would not infringe privately owned rights. Reference herein to any specific commercial product, process, or service by trade name, trademark, manufacturer, or otherwise does not necessarily constitute or imply its endorsement, recommendation, or favoring by the United States Government or any agency thereof. The views and opinions of authors expressed herein do not necessarily state or reflect those of the United States Government or any agency thereof.**

## **DISCLAIMER**

**Portions of this document may be illegible in electronic image products. Images are produced from the best available original document.**



## TABLE OF CONTENTS

	<u>Page</u>
A. GENERAL.....	A.1-1
B. THERMODYNAMICS	
B.1 Enthalpy and Heat Capacity	
B.1.1 Uranium-Zirconium Alloys .....	B.1-1
B.1.2 Uranium-Plutonium-Zirconium Alloys .....	B.1-5
B.1.3 Others .....	B.1-10
REFERENCES - Section B.1 .....	B.1-27
B.2 Phase Equilibria	
B.2.1 Uranium-Zirconium Alloys .....	B.2-1
B.2.2 Uranium-Plutonium-Zirconium Alloys .....	B.2-6
B.2.3 Others .....	B.2-32
REFERENCES - Section B.2 .....	B.2-36
B.3 Density and Thermal Expansion	
B.3.1 Uranium-Zirconium Alloys .....	B.3-3
B.3.2 Uranium-Plutonium-Zirconium Alloys .....	B.3-6
B.3.3 Others .....	B.3-9
REFERENCES - Section B.3 .....	B.3-17
B.4 Surface Tension (This section is incomplete at this time.)	
B.4.1 Uranium-Zirconium Alloys .....	B.4-
B.4.2 Uranium-Plutonium-Zirconium Alloys .....	B.4-
B.4.3 Others .....	B.4-
REFERENCES - Section B.4 .....	B.4-

TABLE OF CONTENTS (cont'd)

	<u>Page</u>
C. TRANSPORT	
C.1 Thermal Conductivity	
C.1.1 Uranium-Zirconium Alloys .....	C.1-1
C.1.2 Uranium-Plutonium-Zirconium Alloys .....	C.1-6
C.1.3 Others .....	C.1-10
REFERENCES - Section C.1 .....	C.1-22
C.2 Viscosity (This section is incomplete at this time.)	
C.2.1 Uranium-Zirconium Alloys .....	C.2-
C.2.2 Uranium-Plutonium-Zirconium Alloys .....	C.2-
C.2.3 Others .....	C.2-
REFERENCES - Section C.2 .....	C.2-
C.3 Diffusion Coefficients	
C.3.1 Uranium-Zirconium Alloys .....	C.3-1
C.3.2 Uranium-Plutonium-Zirconium Alloys .....	C.3-4
C.3.3 Others .....	C.3-5
REFERENCES - Section C.3 .....	C.3-13
D. MECHANICAL	
D.1 Elastic Constants	
D.1.1 Uranium-Zirconium Alloys .....	D.1-1
D.1.2 Uranium-Plutonium-Zirconium Alloys .....	D.1-9
D.1.3 Others .....	D.1-11
REFERENCES - Section D 1.....	D.1-12

TABLE OF CONTENTS (cont'd)

	<u>Page</u>
D.2 Creep	
D.2.1 Uranium-Zirconium Alloys .....	D.2-1
D.2.2 Uranium-Plutonium-Zirconium Alloys .....	D.2-2
D.2.3 Others .....	D.2-4
REFERENCES - Section D.2 .....	D.2-12

LIST OF FIGURES

		<u>Page</u>
B.1-1	Enthalpy, $H(T) - H(298)$ , $\text{kJ mol}^{-1}$ , of U-10 wt % Zr.....	B.1-4
B.1-2	Enthalpy, $H(T) - H(298)$ $\text{kJ mol}^{-1}$ , for Uranium, U-10 wt % Zr, and U-15 wt % Pu-10 wt % Zr .....	B.1-8
B.1-3	Enthalpy, $H(T) - H(298)$ $\text{kJ mol}^{-1}$ , for U-15 wt % Pu-10 wt % Zr Compared with Mole-average Values .....	B.1-9
B.1-4	Heat-capacity Data for Uranium for Various Investigators..	B.1-12
B.1-5	Enthalpy, $H(T) - H(298)$ $\text{kJ mol}^{-1}$ for Uranium .....	B.1-16
B.1-6	Heat-capacity Data for Plutonium from Various Investigators .....	B.1.18
B.1-7	Enthalpy, $H(T) - H(298)$ $\text{kJ mol}^{-1}$ , for Plutonium .....	B.1-23
B.1-8	Enthalpy, $H(T) - H(298)$ $\text{kJ mol}^{-1}$ , for Zirconium .....	B.1-26
B.2-1	Phase Diagram of the System Uranium-Zirconium .....	B.2-2
B.2-2	Phase Diagram of the System Plutonium-Uranium .....	B.2-3
B.2-3	Phase Diagram of the Plutonium-Zirconium System .....	B.2-4
B.2-4a	Uranium-Plutonium-Zirconium Phase Diagram .....	B.2-8
B.2-4b	Uranium-Plutonium-Zirconium Phase Diagram .....	B.2-9
B.2-4c	Uranium-Plutonium-Zirconium Phase Diagram .....	B.2-10
B.2-4d	Uranium-Plutonium-Zirconium Phase Diagram .....	B.2-11
B.2-4e	Uranium-Plutonium-Zirconium Phase Diagram .....	B.2-12
B.2-4f	Uranium-Plutonium-Zirconium Phase Diagram .....	B.2-13
B.2-4g	Uranium-Plutonium-Zirconium Phase Diagram .....	B.2-14
B.2-4h	Uranium-Plutonium-Zirconium Phase Diagram .....	B.2-15
B.2-4i	Uranium-Plutonium-Zirconium Phase Diagram .....	B.2-16
B.2-5	Calculated Section of the Pu-U-Zr Phase Diagram (mol %); 700°C .....	B.2-17
B.2-6	Calculated Section of the Pu-U-Zr Phase Diagram (mol %); 800°C .....	B.2-18
B.2-7	Calculated Section of the Pu-U-Zr Phase Diagram (mol %); 900°C .....	B.2-19

LIST OF FIGURES (cont'd)

	<u>Page</u>
B.2-8	Calculated Section of the Pu-U-Zr Phase Diagram (mol %); 1000°C ..... B.2-20
B.2-9	Calculated Section of the Pu-U-Zr Phase Diagram (mol %); 1050°C ..... B.2-21
B.2-10	Calculated Section of the Pu-U-Zr Phase Diagram (mol %); 1100°C ..... B.2-22
B.2-11	Calculated Section of the Pu-U-Zr Phase Diagram (mol %); 1150°C ..... B.2-23
B.2-12	Calculated Section of the Pu-U-Zr Phase Diagram (mol %); 1200°C ..... B.2-24
B.2-13	Calculated Section of the Pu-U-Zr Phase Diagram (mol %); 1250°C ..... B.2-25
B.2-14	Calculated Section of the Pu-U-Zr Phase Diagram (mol %); 1300°C ..... B.2-26
B.2-15	Calculated Section of the Pu-U-Zr Phase Diagram (mol %); 1400°C ..... B.2-27
B.2-16	Calculated Section of the Pu-U-Zr Phase Diagram (mol %); 1500°C ..... B.2-28
B.2-17	Calculated Section of the Pu-U-Zr Phase Diagram (mol %); 1600°C ..... B.2-29
B.2-18	Calculated Section of the Pu-U-Zr Phase Diagram (mol %); 1700°C ..... B.2-30
B.2-19	The 14 Space Lattices Illustrated by a Unit Cell ..... B.2-34
B.3-1	Mean Linear Thermal Expansion ( $\Delta L/L_0, \%$ ) for Uranium U-10 wt % Zr, and U-20 wt % Zr ..... B.3-4
B.3-2	Mean Linear Thermal-expansion Coefficients ( $\Delta L/L_0, \%$ ) for Uranium, U-10 wt % Zr, and U-15 wt % Pu-10 wt % ..... B.3-8
B.3-3	Mean Linear Thermal-expansion ( $\Delta L/L_0, \%$ ) of Uranium, Plutonium, and Zirconium ..... B.3-10
B.3-4	Density of Solid and Liquid Uranium ..... B.3-15
C.1-1	Comparison Between U-Zr Thermal Conductivity Data and the Recommended Correlation (Eq. 1) ..... C.1-3

LIST OF FIGURES (cont'd)

	<u>Page</u>
C.1-2 Comparison Between Correlation Predictions (Dashed-Lines) and Data for Thermal Conductivity of Unirradiated, 100%-Dense U-Pu-Zr Alloys .....	C.1-8
C.1-3 Comparison Between Measured Thermal Conductivities of Unirradiated, 100%-Dense U-5Fs and Values Calculated from the Correlation (Eq. 1) .....	C.1-11
C.1-4 Comparison Between Analytical Porosity-Correction Factor $f_p = k/k_o = (1 - P)/(1 + \beta P)$ , and the Data of di Novi [5] for $\beta = 2.5$ .....	C.1-19
C.1-5 Comparison of the Analytical Porosity-Correction Factor, $f_p = k/k_o = (1 - p)/(1 - \beta p)$ , with the Inreactor Data of Beck and Fousek for $\beta = 1.5$ and $\beta .25$ .....	C.1-21
C.3-1 Intrinsic Diffusion Coefficients of Uranium and Zirconium in Gamma U-Zr .....	C.3-3
C.3-2 Self-Diffusion Coefficients of Uranium .....	C.3-6
C.3-3 Self-Diffusion Coefficients in Plutonium .....	C.3-7
C.3-4 Xenon-Diffusion Coefficients in Uranium .....	C.3-8
D.1-1 Variation of Dynamic Modulus of Elasticity at Various Temperatures with Uranium Content in Induction-melted U-Zr Alloys .....	D.1-2
D.1-2 Variation of Dynamic Modulus of Elasticity at Various Temperatures with Uranium Content in Arc-melted U-Zr Alloys .....	D.1-3
D.1-3 Effect of Temperature on Elastic Moduli of Uranium .....	D.1-7
D.2-1 Secondary Creep of Metal Fuels .....	D.2-6
D.2-2 Secondary Creep of U-Pu-Zr Alloys .....	D.2-8

LIST OF TABLES

	<u>Page</u>
A-1	Conversion Factors for the U.S. Customary System, Metric System, and International System ..... A-1
A-2	Conversion Factors for the U.S. Customary System, Metric System, and International System (cont'd) ..... A-2
A-3	Conversion Factors for the U.S. Customary System, Metric System, and International System (cont'd) ..... A-3
A-4	Temperatures, Celsius to Fahrenheit Conversion Table ..... A-4
A-5	Temperatures, Celsius to Fahrenheit Conversion Table (cont'd) ..... A-5
A-6	Temperatures, Celsius to Fahrenheit Conversion Table (cont'd) ..... A-6
A-7	Temperatures, Celsius to Fahrenheit Conversion Table (cont'd) ..... A-7
A-8	Temperatures, Celsius to Fahrenheit Conversion Table (cont'd) ..... A-8
A-9	Densities of the Elements ..... A-9
A-10	Densities of the Elements (cont'd) ..... A-10
A-11	Melting and Boiling Points of Elements ..... A-11
A-12	Melting and Boiling Points of Elements [cont'd]..... A-12
A-13	Vapor Pressure Equations for Elements ..... A-13
A-14	Vapor Pressure Equations for Elements (cont'd) ..... A-14
A-15	Vapor Pressure Equations for Elements (cont'd) ..... A-15
B.1-1	Enthalpy and Heat Capacity of U-10 wt % Zr ..... B.1-3
B.1-2	Enthalpy of U-15 wt % Pu-10 wt % ..... B.1-5
B.1-3	Enthalpy and Heat Capacity of U-15 wt % Pu-10 wt % Zr .... B.1-7
B.1-4	High-Temperatures Heat Capacity and Enthalpy of Uranium .. B.1-10
B.1-5	Enthalpies of Transition for Uranium ..... B.1-13
B.1-6	High-Temperature Heat Capacity and Enthalpy of Plutonium . B.1-17
B.1-7	Temperature and Enthalpy of Plutonium Transitions ..... B.1-21
B.1-8	High-Temperature Heat Capacity and Enthalpy of Zr..... B.1-24
B.2-1	Phase Transitions and Structures in U, Pu, and Zr ..... B.2-33

LIST OF TABLES (cont'd)

	<u>Page</u>
B.2-2	The Crystal System [6] ..... B.2-33
B.3-1	Density and Linear Thermal Expansion of U-10 wt % Zr ..... B.3-5
B.3-2	Density and Linear Thermal Expansion of U-20 wt % Zr ..... B.3-5
B.3-3	Density and Thermal-Expansion Coefficients of U-Pu-Zr Alloys ..... B.3-7
B.3-4	Density and Linear Expansion of U-15 wt % Pu-10 wt % Zr .. B.3-7
B.3-5	Density and Linear Expansion of Uranium ..... B.3-11
B.3-6	Density and Linear Thermal Expansion of Zirconium ..... B.3-12
B.3-7	Density and Linear Thermal Expansion of Plutonium ..... B.3-13
B.3-8	Measurements of Density of Liquid Uranium, $\rho(\text{g}/\text{cm}^3) = \alpha - bT(\text{k})$ ..... B.3-14
B.3-9	Density and Volume of Solid and Liquid Uranium ( $T=T_m$ ) .... B.3-16
C.1-1	Summary of U-Zr Alloy Thermal-conductivity Data and Values (in Parenthesis) Calculated from Eq. 1 ..... C.1-2
C.1-2	Summary of Thermal-conductivity Data for Unirradiated, 100%-Dense U-Pu-Zr Alloys ..... C.1-7
C.1-3	Correlation Values and Uncertainty Estimates for the Thermal Conductivity of Unirradiated, 100%-Dense U-5FS ... C.1-10
C.1-4	Measured Thermal Conductivities of U-5 wt % Fs ..... C.1-12
C.1-5	Summary of di Novi [5] Data ( $28 < T < 595^\circ\text{C}$ ) ..... C.1-18
C.3-1	Diffusion Coefficients in Gamma U-Zr ..... C.3-1
C.3-2	Diffusion Coefficients in U-Pu Alloys Between $400^\circ\text{C}$ and $540^\circ\text{C}$ ..... C.3-10
D.1-1	Comparison between the Correlation Values and Experimental Data (from (Fig. D.1-1) for U-Zr Alloys ..... D.1-4
D.1-2	Static Young's-Modulus Values for Several U-Pu-Zr Compositions ..... D.1-10
D.2-1	Time (Minutes) to Attain 2% Strain in U-Pu-Zr Alloys ..... D.2-3
D.2-2	Measured and Calculated Minimum Creep Rates of Low-Zirconium Binary U-Zr Alloys at $818^\circ\text{C}$ ..... D.2-9

# METALLIC FUELS HANDBOOK

Compiled by

G. L. Hofman, L. Leibowitz, J. M. Kramer,  
M. C. Billone, and J. F. Koenig

## PREFACE

This compilation of Thermophysical and Mechanical Properties of certain metallic fuels is meant to be used as a common source of data in work related to the **Integral Fast Reactor**. Because research on these properties is an ongoing effort, this handbook must be continuously updated in order to provide the best data set to all involved in the IFR program. The use of common source of properties will facilitate comparison of various analyses of fuel behavior performed within the program. It also will facilitate uncovering of gaps and weaknesses in the data base, and thus enable better direction for future work on experimental properties.

This handbook focuses on the two fuel compositions chosen for the IFR; namely, Uranium-Zirconium and Uranium-Plutonium-Zirconium.

Because of the paucity of data in some areas on these specific alloys, data on the elements as well as related alloys are presented to aid the user in estimating property values that are not available.

The selection of properties to be included in the handbook was based on a survey of all IFR participants.

The Properties Evaluation Working Group will consider any requests for inclusion of additional properties, and solicits critiques of the present work as well as submittal of additional data that the user may encounter.

### Property Evaluation Working Group

**Chairman:** G. L. Hofman, EBR-II Division

**Members:** L. Leibowitz, Chemical Technology Division

J. M. Kramer, Reactor Analysis & Safety Division

M. C. Billone, Material Science & Technology Division

J. F. Koenig, EBR-II Division

**CONVERSION FACTORS FOR THE U.S. CUSTOMARY SYSTEM,  
METRIC SYSTEM, AND INTERNATIONAL SYSTEM**

**A. UNITS OF LENGTH**

Units	cm	m	in.	ft	yd	mile
1 cm	= 1	0.01*	0.3937008	0.03280840	0.01093613	6.213712x10 <sup>-8</sup>
1 m	= 100.	1	39.37008	3.280840	1.093613	6.213712x10 <sup>-6</sup>
1 in.	= 2.54*	0.0254	1	0.08333333...	0.02777777...	1.578283x10 <sup>-8</sup>
1 ft	= 30.48	0.3048	12.*	1	0.3333333...	1.899999x10 <sup>-7</sup>
1 yd	= 91.44	0.9144	36.	3.*	1	5.681818x10 <sup>-7</sup>
1 mile	= 1.609344x10 <sup>5</sup>	1.609344x10 <sup>3</sup>	6.336x10 <sup>4</sup>	5280.*	1760.	1

**B. UNITS OF AREA**

Units	cm <sup>2</sup>	m <sup>2</sup>	in. <sup>2</sup>	ft <sup>2</sup>	yd <sup>2</sup>	mile <sup>2</sup>
1 cm <sup>2</sup>	= 1	10 <sup>-4</sup> *	0.1550003	1.076391x10 <sup>-3</sup>	1.195990x10 <sup>-6</sup>	3.861022x10 <sup>-11</sup>
1 m <sup>2</sup>	= 10 <sup>4</sup>	1	1550.003	10.76391	1.195990	3.861022x10 <sup>-7</sup>
1 in. <sup>2</sup>	= 6.4516*	6.4516x10 <sup>-6</sup>	1	6.944444x10 <sup>-8</sup>	7.716049x10 <sup>-8</sup>	2.490977x10 <sup>-10</sup>
1 ft <sup>2</sup>	= 929.0304	0.09290304	144.*	1	0.11111111...	3.587007x10 <sup>-8</sup>
1 yd <sup>2</sup>	= 8361.273	0.8361273	1296.	9.*	1	3.228306x10 <sup>-7</sup>
1 mile <sup>2</sup>	= 2.589988x10 <sup>10</sup>	2.589988x10 <sup>6</sup>	4.014490x10 <sup>9</sup>	2.78784x10 <sup>7</sup> *	3.0976x10 <sup>6</sup>	1

**C. UNITS OF VOLUME**

Units	cm <sup>3</sup>	liter	in. <sup>3</sup>	ft <sup>3</sup>	qt	gal
1 cm <sup>3</sup>	= 1	10 <sup>-3</sup>	0.06102374	3.531467x10 <sup>-8</sup>	1.056688x10 <sup>-3</sup>	2.641721x10 <sup>-4</sup>
1 liter	= 1000.*	1	61.02374	0.03531467	1.056688	0.2641721
1 in. <sup>3</sup>	= 16.38706*	0.01638706	1	5.787037x10 <sup>-8</sup>	0.01731602	4.329004x10 <sup>-3</sup>
1 ft <sup>3</sup>	= 28316.05	28.31605	1728.*	1	2.992208	7.480520
1 qt	= 946.353	0.946353	57.75	0.0342014	1	0.25
1 gal (U.S.)	= 3785.412	3.785412	231.*	0.1336806	4.*	1

CONVERSION FACTORS FOR THE U.S. CUSTOMARY SYSTEM,  
METRIC SYSTEM, AND INTERNATIONAL SYSTEM (contd)

D. UNITS OF MASS

Units	g	kg	oz	lb	metric ton	ton
1 g	= 1	$10^{-3}$	0.03527396	$2.204623 \times 10^{-3}$	$10^{-6}$	$1.102311 \times 10^{-6}$
1 kg	= 1000.	1	35.27396	2.204623	$10^{-3}$	$1.102311 \times 10^{-3}$
1 oz (avdp)	= 28.34952	0.02834952	1	0.0625	$2.834952 \times 10^{-5}$	$5 \times 10^{-5}$
1 lb (avdp)	= 453.5924	0.4535924	16.*	1	$4.535924 \times 10^{-4}$	0.0005
1 metric ton	= $10^6$	1000.*	35273.96	2204.623	1	1.102311
1 ton	= 907184.7	907.1847	32000.	2000.*	0.9071847	1

E. UNITS OF DENSITY

Units	$\text{g cm}^{-3}$	$\text{g l.}^{-1}$	$\text{oz in.}^{-3}$	$\text{lb in.}^{-3}$	$\text{lb ft.}^{-3}$	$\text{lb gal.}^{-1}$
1 $\text{g cm}^{-3}$	= 1	1000.	0.5780365	0.03612728	62.42795	8.345403
1 $\text{g l.}^{-1}$	= $10^{-3}$	1	$5.780365 \times 10^{-4}$	$3.612728 \times 10^{-5}$	0.06242795	$8.345403 \times 10^{-3}$
1 $\text{oz in.}^{-3}$	= 1.729994	1729.994	1	0.0625	108.	14.4375
1 $\text{lb in.}^{-3}$	= 27.67991	27679.91	16.	1	1728.	231.
1 $\text{lb ft.}^{-3}$	= 0.01601847	16.01847	$9.259259 \times 10^{-3}$	$5.7870370 \times 10^{-4}$	1	0.1336806
1 $\text{lb gal.}^{-1}$	= 0.1198264	119.8264	$4.789536 \times 10^{-3}$	$4.3290043 \times 10^{-3}$	7.480519	1

F. UNITS OF PRESSURE

Units	$\text{dyn cm}^{-2}$	bar	atm	$\text{kg(wt) cm}^{-2}$	mmHg (Torr)	in. Hg	$\text{lb(wt) in.}^{-2}$
1 $\text{dyn cm}^{-2}$	= 1	$10^{-6}$	$9.869233 \times 10^{-7}$	$1.019716 \times 10^{-6}$	$7.500617 \times 10^{-8}$	$2.952999 \times 10^{-8}$	$1.450377 \times 10^{-8}$
1 bar	= $10^6$	1	0.9869233	1.019716	750.0617	29.52999	14.50377
1 atm	= 1013250.*	1.013250	1	1.033227	760.	29.92126	14.69595
1 $\text{kg(wt) cm}^{-2}$	= 980665.	0.980665	0.9678411	1	735.5592	28.95903	14.22334
1 mmHg (Torr)	= 1333.224	$1.333224 \times 10^3$	$1.3157895 \times 10^3$	$1.8595099 \times 10^3$	1	0.03937008	0.01933678
1 in. Hg	= 33863.88	0.03386388	0.03342105	0.03453155	25.4	1	0.4911541
1 $\text{lb(wt) in.}^{-2}$	= 68947.57	0.06894757	0.06804596	0.07030696	51.71493	2.036021	1

CONVERSION FACTORS FOR THE U.S. CUSTOMARY SYSTEM,  
METRIC SYSTEM, AND INTERNATIONAL SYSTEM (contd)

C. UNITS OF ENERGY

Units	g mass (energy equiv)	J	intJ	cal	cal <sub>IT</sub>	Btu <sub>IT</sub>	kW hr	hp hr	ft-lb (wt)	cu ft- lb (wt) in. <sup>-2</sup>	1 atm
1 g mass (energy equiv)	=1	8.987554 x 10 <sup>13</sup>	8.986071 x 10 <sup>13</sup>	2.148077 x 10 <sup>13</sup>	2.146640 x 10 <sup>13</sup>	8.518558 x 10 <sup>13</sup>	2.496543 x 10 <sup>7</sup>	3.347919 x 10 <sup>7</sup>	6.628880 x 10 <sup>13</sup>	4.603399 x 10 <sup>11</sup>	8.870026 x 10 <sup>11</sup>
1 J	=1.112650 x 10 <sup>-13</sup>	1	0.999835	0.2390057	0.2388459	9.478172 x 10 <sup>-6</sup>	2.777777... x 10 <sup>-7</sup>	3.725062	0.7375622	5.121960 x 10 <sup>-3</sup>	9.869233 x 10 <sup>-8</sup>
1 int J	=1.112833 x 10 <sup>-13</sup>	1.000165	1	0.2390452	0.2388853	9.479735 x 10 <sup>-6</sup>	2.778236 x 10 <sup>-7</sup>	3.725676 x 10 <sup>-7</sup>	0.7376839	5.122805 x 10 <sup>-3</sup>	9.870862 x 10 <sup>-8</sup>
1 cal	=4.655327 x 10 <sup>-13</sup>	4.184	4.183310	1	0.9993312	3.965667 x 10 <sup>-3</sup>	1.162222... x 10 <sup>-3</sup>	1.558562 x 10 <sup>-3</sup>	3.085960	2.143028 x 10 <sup>-2</sup>	0.04129287
1 cal <sub>IT</sub>	=4.658442 x 10 <sup>-13</sup>	4.1868	4.186109	1.000669	1	3.968321 x 10 <sup>-3</sup>	1.163000 x 10 <sup>-3</sup>	1.559609 x 10 <sup>-3</sup>	3.088025	2.144462 x 10 <sup>-2</sup>	0.04132050
1 Btu <sub>IT</sub>	=1.173908 x 10 <sup>-11</sup>	1055.056	1054.882	252.1644	251.9958*	1	2.930711 x 10 <sup>-4</sup>	3.930148 x 10 <sup>-4</sup>	778.1693	5.403953	10.41259
1 kW hr	=4.005539 x 10 <sup>-9</sup>	3600000.*	3599406.	860420.7	859845.2	3412.142	1	1.341022	2655224.	18439.06	35529.24
1 hp hr	=2.986930 x 10 <sup>-9</sup>	2684519.	2684077.	641615.6	641186.5	2544.33	0.7456998	1	1980000.*	13750.	26494.15
1 ft-lb (wt)	=1.508550 x 10 <sup>-13</sup>	1.355818	1.355594	0.3240483	0.3238315	1.285067 x 10 <sup>-3</sup>	3.766161 x 10 <sup>-7</sup>	5.050505... x 10 <sup>-7</sup>	1	6.944444... x 10 <sup>-3</sup>	0.0133805
1 cu ft-lb (wt) in. <sup>-2</sup>	=2.172313 x 10 <sup>-12</sup>	195.2378	195.2056	46.66295	46.63174	0.1850497	5.423272 x 10 <sup>-3</sup>	7.272727... x 10 <sup>-3</sup>	144.*	1	1.926847
11 atm	=1.1127392 x 10 <sup>-12</sup>	101.3250	101.3083	24.21726	24.20106	0.09603757	2.814583 x 10 <sup>-3</sup>	3.774419 x 10 <sup>-3</sup>	74.73349	0.5189825	1

**TEMPERATURES, CELSIUS TO FAHRENHEIT**  
Conversion Table

The values in the body of this table give, in degrees Fahrenheit, the temperatures indicated in degrees Celsius at the top and side.

1°C = 1.8°F  
For temperatures below 0°C

Temp. °C	0	1	2	3	4	5	6	7	8	9
0	+32.0	30.2	28.4	26.6	24.8	23.0	21.2	19.4	17.6	15.8
-10	+14.0	12.2	10.4	8.6	6.8	5.0	3.2	+1.4	-0.4	-2.2
-20	-4.0	5.8	7.6	9.4	11.2	13.0	14.8	16.6	18.4	20.2
-30	-22.0	23.8	25.6	27.4	29.2	31.0	32.8	34.6	36.4	38.2
-40	-40.0	41.8	43.6	45.4	47.2	49.0	50.8	52.6	54.4	56.2
-50	-58.0	59.8	61.6	63.4	65.2	67.0	68.8	70.6	72.4	74.2
-60	-76.0	77.8	79.6	81.4	83.2	85.0	86.8	88.6	90.4	92.2
-70	-94.0	95.8	97.6	99.4	101.2	103.0	104.8	106.6	108.4	110.2
-80	-112.0	113.8	115.6	117.4	119.2	121.0	122.8	124.6	126.4	128.2
-90	-130.0	131.8	133.6	135.4	137.2	139.0	140.8	142.6	144.4	146.2
-100	-148.0	149.8	151.6	153.4	155.2	157.0	158.8	160.6	162.4	164.2
-110	-166.0	167.8	169.6	171.4	173.2	175.0	176.8	178.6	180.4	182.2
-120	-184.0	185.8	187.6	189.4	191.2	193.0	194.8	196.6	198.4	200.2
-130	-202.0	203.8	205.6	207.4	209.2	211.0	212.8	214.6	216.4	218.2
-140	-220.0	221.8	223.6	225.4	227.2	229.0	230.8	232.6	234.4	236.2
-150	-238.0	239.8	241.6	243.4	245.2	247.0	248.8	250.6	252.4	254.2
-160	-256.0	257.8	259.6	261.4	263.2	265.0	266.8	268.6	270.4	272.2
-170	-274.0	275.8	277.6	279.4	281.2	283.0	284.8	286.6	288.4	290.2
-180	-292.0	293.8	295.6	297.4	299.2	301.0	302.8	304.6	306.4	308.2
-190	-310.0	311.8	313.6	315.4	317.2	319.0	320.8	322.6	324.4	326.2
-200	-328.0	329.8	331.6	333.4	335.2	337.0	338.8	340.6	342.4	344.2
-210	-346.0	347.8	349.6	351.4	353.2	355.0	356.8	358.6	360.4	362.2
-220	-364.0	365.8	367.6	369.4	371.2	373.0	374.8	376.6	378.4	380.2
-230	-382.0	383.8	385.6	387.4	389.2	391.0	392.8	394.6	396.4	398.2
-240	-400.0	401.8	403.6	405.4	407.2	409.0	410.8	412.6	414.4	416.2
-250	-418.0	419.8	421.6	423.4	425.2	427.0	428.8	430.6	432.4	434.2
-260	-436.0	437.8	439.6	441.4	443.2	445.0	446.8	448.6	450.4	452.2
-270	-454.0	455.8	457.6	459.4	—	—	—	—	—	—

TEMPERATURES, CELSIUS TO FAHRENHEIT (contd)

For temperatures above 0°C

Temp. °C	0	1	2	3	4	5	6	7	8	9
0	32.0	33.8	35.6	37.4	39.2	41.0	42.8	44.6	46.4	48.2
10	50.0	51.8	53.6	55.4	57.2	59.0	60.8	62.6	64.4	66.2
20	68.0	69.8	71.6	73.4	75.2	77.0	78.8	80.6	82.4	84.2
30	86.0	87.8	89.6	91.4	93.2	95.0	96.8	98.6	100.4	102.2
40	104.0	105.8	107.6	109.4	111.2	113.0	114.8	116.6	118.4	120.2
50	122.0	123.8	125.6	127.4	129.2	131.0	132.8	134.6	136.4	138.2
60	140.0	141.8	143.6	145.4	147.2	149.0	150.8	152.6	154.4	156.2
70	158.0	159.8	161.6	163.4	165.2	167.0	168.8	170.6	172.4	174.2
80	176.0	177.8	179.6	181.4	183.2	185.0	186.8	188.6	190.4	192.2
90	194.0	195.8	197.6	199.4	201.2	203.0	204.8	206.6	208.4	210.2
100	212.0	213.8	215.6	217.4	219.2	221.0	222.8	224.6	226.4	228.2
110	230.0	231.8	233.6	235.4	237.2	239.0	240.8	242.6	244.4	246.2
120	248.0	249.8	251.6	253.4	255.2	257.0	258.8	260.6	262.4	264.2
130	266.0	267.8	269.6	271.4	273.2	275.0	276.8	278.6	280.4	282.2
140	284.0	285.8	287.6	289.4	291.2	293.0	294.8	296.6	298.4	300.2
150	302.0	303.8	305.6	307.4	309.2	311.0	312.8	314.6	316.4	318.2
160	320.0	321.8	323.6	325.4	327.2	329.0	330.8	332.6	334.4	336.2
170	338.0	339.8	341.6	343.4	345.2	347.0	348.8	350.6	352.4	354.2
180	356.0	357.8	359.6	361.4	363.2	365.0	366.8	368.6	370.4	372.2
190	374.0	375.8	377.6	379.4	381.2	383.0	384.8	386.6	388.4	390.2
200	392.0	393.8	395.6	397.4	399.2	401.0	402.8	404.6	406.4	408.2
210	410.0	411.8	413.6	415.4	417.2	419.0	420.8	422.6	424.4	426.2
220	428.0	429.8	431.6	433.4	435.2	437.0	438.8	440.6	442.4	444.2
230	446.0	447.8	449.6	451.4	453.2	455.0	456.8	458.6	460.4	462.2
240	464.0	465.8	467.6	469.4	471.2	473.0	474.8	476.6	478.4	480.2
250	482.0	483.8	485.6	487.4	489.2	491.0	492.8	494.6	496.4	498.2
260	500.0	501.8	503.6	505.4	507.2	509.0	510.8	512.6	514.4	516.2
270	518.0	519.8	521.6	523.4	525.2	527.0	528.8	530.6	532.4	534.2
280	536.0	537.8	539.6	541.4	543.2	545.0	546.8	548.6	550.4	552.2
290	554.0	555.8	557.6	559.4	561.2	563.0	564.8	566.6	568.4	570.2
300	572.0	573.8	575.6	577.4	579.2	581.0	582.8	584.6	586.4	588.2
310	590.0	591.8	593.6	595.4	597.2	599.0	600.8	602.6	604.4	606.2
320	608.0	609.8	611.6	613.4	615.2	617.0	618.8	620.6	622.4	624.2
330	626.0	627.8	629.6	631.4	633.2	635.0	636.8	638.6	640.4	642.2
340	644.0	645.8	647.6	649.4	651.2	653.0	654.8	656.6	658.4	660.2
350	662.0	663.8	665.6	667.4	669.2	671.0	672.8	674.6	676.4	678.2
360	680.0	681.8	683.6	685.4	687.2	689.0	690.8	692.6	694.4	696.2
370	698.0	699.8	701.6	703.4	705.2	707.0	708.8	710.6	712.4	714.2
380	716.0	717.8	719.6	721.4	723.2	725.0	726.8	728.6	730.4	732.2
390	734.0	735.8	737.6	739.4	741.2	743.0	744.8	746.6	748.4	750.2

-273.10°C = -450.72°F = absolute zero

For	°C	0.1	0.2	0.3	0.4	0.5	0.6	0.7	0.8	0.9	1.0
Interpolation	°F	0.18	0.36	0.54	0.72	0.90	1.08	1.26	1.44	1.62	1.80

TEMPERATURES, CELSIUS TO FAHRENHEIT (contd)

For temperatures above 0°C.

Temp. °C	0	1	2	3	4	5	6	7	8	9	
400	752.0	753.8	755.6	757.4	759.2	761.0	762.8	764.6	766.4	768.2	
410	770.0	771.8	773.6	775.4	777.2	779.0	780.8	782.6	784.4	786.2	
420	788.0	789.8	791.6	793.4	795.2	797.0	798.8	800.6	802.4	804.2	
430	806.0	807.8	809.6	811.4	813.2	815.0	816.8	818.6	820.4	822.2	
440	824.0	825.8	827.6	829.4	831.2	833.0	834.8	836.6	838.4	840.2	
450	842.0	843.8	845.6	847.4	849.2	851.0	852.8	854.6	856.4	858.2	
460	860.0	861.8	863.6	865.4	867.2	869.0	870.8	872.6	874.4	876.2	
470	878.0	879.8	881.6	883.4	885.2	887.0	888.8	890.6	892.4	894.2	
480	896.0	897.8	899.6	901.4	903.2	905.0	906.8	908.6	910.4	912.2	
490	914.0	915.8	917.6	919.4	921.2	923.0	924.8	926.6	928.4	930.2	
500	932.0	933.8	935.6	937.4	939.2	941.0	942.8	944.6	946.4	948.2	
510	950.0	951.8	953.6	955.4	957.2	959.0	960.8	962.6	964.4	966.2	
520	968.0	969.8	971.6	973.4	975.2	977.0	978.8	980.6	982.4	984.2	
530	986.0	987.8	989.6	991.4	993.2	995.0	996.8	998.6	1000.4	1002.2	
540	1004.0	1005.8	1007.6	1009.4	1011.2	1013.0	1014.8	1016.6	1018.4	1020.2	
550	1022.0	1023.8	1025.6	1027.4	1029.2	1031.0	1032.8	1034.6	1036.4	1038.2	
560	1040.0	1041.8	1043.6	1045.4	1047.2	1049.0	1050.8	1052.6	1054.4	1056.2	
570	1058.0	1059.8	1061.6	1063.4	1065.2	1067.0	1068.8	1070.6	1072.4	1074.2	
580	1076.0	1077.8	1079.6	1081.4	1083.2	1085.0	1086.8	1088.6	1090.4	1092.2	
590	1094.0	1095.8	1097.6	1099.4	1101.2	1103.0	1104.8	1106.6	1108.4	1110.2	
600	1112.0	1113.8	1115.6	1117.4	1119.2	1121.0	1122.8	1124.6	1126.4	1128.2	
610	1130.0	1131.8	1133.6	1135.4	1137.2	1139.0	1140.8	1142.6	1144.4	1146.2	
620	1148.0	1149.8	1151.6	1153.4	1155.2	1157.0	1158.8	1160.6	1162.4	1164.2	
630	1166.0	1167.8	1169.6	1171.4	1173.2	1175.0	1176.8	1178.6	1180.4	1182.2	
640	1184.0	1185.8	1187.6	1189.4	1191.2	1193.0	1194.8	1196.6	1198.4	1200.2	
650	1202.0	1203.8	1205.6	1207.4	1209.2	1211.0	1212.8	1214.6	1216.4	1218.2	
660	1220.0	1221.8	1223.6	1225.4	1227.2	1229.0	1230.8	1232.6	1234.4	1236.2	
670	1238.0	1239.8	1241.6	1243.4	1245.2	1247.0	1248.8	1250.6	1252.4	1254.2	
680	1256.0	1257.8	1259.6	1261.4	1263.2	1265.0	1266.8	1268.6	1270.4	1272.2	
690	1274.0	1275.8	1277.6	1279.4	1281.2	1283.0	1284.8	1286.6	1288.4	1290.2	
700	1292.0	1293.8	1295.6	1297.4	1299.2	1301.0	1302.8	1304.6	1306.4	1308.2	
710	1310.0	1311.8	1313.6	1315.4	1317.2	1319.0	1320.8	1322.6	1324.4	1326.2	
720	1328.0	1329.8	1331.6	1333.4	1335.2	1337.0	1338.8	1340.6	1342.4	1344.2	
730	1346.0	1347.8	1349.6	1351.4	1353.2	1355.0	1356.8	1358.6	1360.4	1362.2	
740	1364.0	1365.8	1367.6	1369.4	1371.2	1373.0	1374.8	1376.6	1378.4	1380.2	
750	1382.0	1383.8	1385.6	1387.4	1389.2	1391.0	1392.8	1394.6	1396.4	1398.2	
760	1400.0	1401.8	1403.6	1405.4	1407.2	1409.0	1410.8	1412.6	1414.4	1416.2	
770	1418.0	1419.8	1421.6	1423.4	1425.2	1427.0	1428.8	1430.6	1432.4	1434.2	
780	1436.0	1437.8	1439.6	1441.4	1443.2	1445.0	1446.8	1448.6	1450.4	1452.2	
790	1454.0	1455.8	1457.6	1459.4	1461.2	1463.0	1464.8	1466.6	1468.4	1470.2	
For interpolation	°C	0.1	0.2	0.3	0.4	0.5	0.6	0.7	0.8	0.9	1.0
	°F	0.18	0.36	0.54	0.72	0.90	1.08	1.26	1.44	1.62	1.80

TEMPERATURES, CELSIUS TO FAHRENHEIT (cont'd)

For temperatures above 0°C

Temp. °C	0	1	2	3	4	5	6	7	8	9
800	1472.0	1473.8	1475.6	1477.4	1479.2	1481.0	1482.8	1484.6	1486.4	1488.2
810	1490.0	1491.8	1493.6	1495.4	1497.2	1499.0	1500.8	1502.6	1504.4	1506.2
820	1508.0	1509.8	1511.6	1513.4	1515.2	1517.0	1518.8	1520.6	1522.4	1524.2
830	1526.0	1527.8	1529.6	1531.4	1533.2	1535.0	1536.8	1538.6	1540.4	1542.2
840	1544.0	1545.8	1547.6	1549.4	1551.2	1553.0	1554.8	1556.6	1558.4	1560.2
850	1562.0	1563.8	1565.6	1567.4	1569.2	1571.0	1572.8	1574.6	1576.4	1578.2
860	1580.0	1581.8	1583.6	1585.4	1587.2	1589.0	1590.8	1592.6	1594.4	1596.2
870	1598.0	1599.8	1601.6	1603.4	1605.2	1607.0	1608.8	1610.6	1612.4	1614.2
880	1616.0	1617.8	1619.6	1621.4	1623.2	1625.0	1626.8	1628.6	1630.4	1632.2
890	1634.0	1635.8	1637.6	1639.4	1641.2	1643.0	1644.8	1646.6	1648.4	1650.2
900	1652.0	1653.8	1655.6	1657.4	1659.2	1661.0	1662.8	1664.6	1666.4	1668.2
910	1670.0	1671.8	1673.6	1675.4	1677.2	1679.0	1680.8	1682.6	1684.4	1686.2
920	1688.0	1689.8	1691.6	1693.4	1695.2	1697.0	1698.8	1700.6	1702.4	1704.2
930	1706.0	1707.8	1709.6	1711.4	1713.2	1715.0	1716.8	1718.6	1720.4	1722.2
940	1724.0	1725.8	1727.6	1729.4	1731.2	1733.0	1734.8	1736.6	1738.4	1740.2
950	1742.0	1743.8	1745.6	1747.4	1749.2	1751.0	1752.8	1754.6	1756.4	1758.2
960	1760.0	1761.8	1763.6	1765.4	1767.2	1769.0	1770.8	1772.6	1774.4	1776.2
970	1778.0	1779.8	1781.6	1783.4	1785.2	1787.0	1788.8	1790.6	1792.4	1794.2
980	1796.0	1797.8	1799.6	1801.4	1803.2	1805.0	1806.8	1808.6	1810.4	1812.2
990	1814.0	1815.8	1817.6	1819.4	1821.2	1823.0	1824.8	1826.6	1828.4	1830.2
1000	1832.0	1833.8	1835.6	1837.4	1839.2	1841.0	1842.8	1844.6	1846.4	1848.2
1010	1850.2	1851.8	1853.6	1855.4	1857.2	1859.0	1860.8	1862.6	1864.4	1866.2
1020	1868.0	1869.8	1871.6	1873.4	1875.2	1877.0	1878.8	1880.6	1882.4	1884.2
1030	1886.0	1887.8	1889.6	1891.4	1893.2	1895.0	1896.8	1898.6	1900.4	1902.2
1040	1904.0	1905.8	1907.6	1909.4	1911.2	1913.0	1914.8	1916.6	1918.4	1920.2
1050	1922.0	1923.8	1925.6	1927.4	1929.2	1931.0	1932.8	1934.6	1936.4	1938.2
1060	1940.0	1941.8	1943.6	1945.4	1947.2	1949.0	1950.8	1952.6	1954.4	1956.2
1070	1958.0	1959.8	1961.6	1963.4	1965.2	1967.0	1968.8	1970.6	1972.4	1974.2
1080	1976.0	1977.8	1979.6	1981.4	1983.2	1985.0	1986.8	1988.6	1990.4	1992.2
1090	1994.0	1995.8	1997.6	1999.4	2001.2	2003.0	2004.8	2006.6	2008.4	2010.2
1100	2012.0	2013.8	2015.6	2017.4	2019.2	2021.0	2022.8	2024.6	2026.4	2028.2
1110	2030.0	2031.8	2033.6	2035.4	2037.2	2039.0	2040.8	2042.6	2044.4	2046.2
1120	2048.0	2049.8	2051.6	2053.4	2055.2	2057.0	2058.8	2060.6	2062.4	2064.2
1130	2066.0	2067.8	2069.6	2071.4	2073.2	2075.0	2076.8	2078.6	2080.4	2082.2
1140	2084.0	2085.8	2087.6	2089.4	2091.2	2093.0	2094.8	2096.6	2098.4	2100.2
1150	2102.0	2103.8	2105.6	2107.4	2109.2	2111.0	2112.8	2114.6	2116.4	2118.2
1160	2120.0	2121.8	2123.6	2125.4	2127.2	2129.0	2130.8	2132.6	2134.4	2136.2
1170	2138.0	2139.8	2141.6	2143.4	2145.2	2147.0	2148.8	2150.6	2152.4	2154.2
1180	2156.0	2157.8	2159.6	2161.4	2163.2	2165.0	2166.8	2168.6	2170.4	2172.2
1190	2174.0	2175.8	2177.6	2179.4	2181.2	2183.0	2184.8	2186.6	2188.4	2190.2

For interpolation °C 0.1 0.2 0.3 0.4 0.5 0.6 0.7 0.8 0.9 1.0  
 °F 0.18 0.36 0.54 0.72 0.90 1.08 1.26 1.44 1.62 1.80

TEMPERATURES, CELSIUS TO FAHRENHEIT (cont'd)

For temperatures above 0°C.

Temp. °C	0	1	2	3	4	5	6	7	8	9	
1200	2192.0	2193.8	2195.6	2197.4	2199.2	2201.0	2202.8	2204.6	2206.4	2208.2	
1210	2210.0	2211.8	2213.6	2215.4	2217.2	2219.0	2220.8	2222.6	2224.4	2226.2	
1220	2228.0	2229.8	2231.6	2233.4	2235.2	2237.0	2238.8	2240.6	2242.4	2244.2	
1230	2246.0	2247.8	2249.6	2251.4	2253.2	2255.0	2256.8	2258.6	2260.4	2262.2	
1240	2264.0	2265.8	2267.6	2269.4	2271.2	2273.0	2274.8	2276.6	2278.4	2280.2	
1250	2282.0	2283.8	2285.6	2287.4	2289.2	2291.0	2292.8	2294.6	2296.4	2298.2	
1260	2300.0	2301.8	2303.6	2305.4	2307.2	2309.0	2310.8	2312.6	2314.4	2316.2	
1270	2318.0	2319.8	2321.6	2323.4	2325.2	2327.0	2328.8	2330.6	2332.4	2334.2	
1280	2336.0	2337.8	2339.6	2341.4	2343.2	2345.0	2346.8	2348.6	2350.4	2352.2	
1290	2354.0	2355.8	2357.6	2359.4	2361.2	2363.0	2364.8	2366.6	2368.4	2370.2	
1300	2372.0	2373.8	2375.6	2377.4	2379.2	2381.0	2382.8	2384.6	2386.4	2388.2	
1310	2390.0	2391.8	2393.6	2395.4	2397.2	2399.0	2400.8	2402.6	2404.4	2406.2	
1320	2408.0	2409.8	2411.6	2413.4	2415.2	2417.0	2418.8	2420.6	2422.4	2424.2	
1330	2426.0	2427.8	2429.6	2431.4	2433.2	2435.0	2436.8	2438.6	2440.4	2442.2	
1340	2444.0	2445.8	2447.6	2449.4	2451.2	2453.0	2454.8	2456.6	2458.4	2460.2	
1350	2462.0	2463.8	2465.6	2467.4	2469.2	2471.0	2472.8	2474.6	2476.4	2478.2	
1360	2480.0	2481.8	2483.6	2485.4	2487.2	2489.0	2490.8	2492.6	2494.4	2496.2	
1370	2498.0	2499.8	2501.6	2503.4	2505.2	2507.0	2508.8	2510.6	2512.4	2514.2	
1380	2516.0	2517.8	2519.6	2521.4	2523.2	2525.0	2526.8	2528.6	2530.4	2532.2	
1390	2534.0	2535.8	2537.6	2539.4	2541.2	2543.0	2544.8	2546.6	2548.4	2550.2	
For interpolation	°C	0.1	0.2	0.3	0.4	0.5	0.6	0.7	0.8	0.9	1.0
	°F	0.18	0.36	0.54	0.72	0.90	1.08	1.26	1.44	1.62	1.80

DENSITIES OF THE ELEMENTS

Source: CRC Handbook of Chemistry and Physics, R. C. Weast, M. J. Astle, and W. H. Beyer, eds., CRC Press, Boca Raton, FL (1984).

Element	Density, g/cm <sup>3</sup>	Temp., °C	Element	Density, g/cm <sup>3</sup>	Temp., °C
Ac	10.07	20	Hg	1.738	20
Ag	10.50	20	Mn	7.20	20
Al	2.6989	20	Mo	10.22	20
Am	13.67	20	Na	0.971	20
As (yellow)	1.97	20	Nb	8.57	20
As (gray)	5.73	20	Nd (cub)	6.80	20
Au	18.88	20	Nd (hex)	7.007	20
B (amorph)	2.37	20	NI	8.902	25
B (cryst)	2.34	20	Np	20.25	20
Ba	3.51	20	Os	22.57	20
Be	1.848	20	P (white)	1.82	20
Bi	9.787	20	P (red)	2.20	20
C (amorph)	1.8-2.1	20	P (black)	2.25-2.69	20
C (graph)	1.9-2.3	20	Pa	15.37	20
C (diam)	3.15-3.53	20	Pb	11.35	20
Ca	1.55	20	Pd	12.02	20
Cd	8.65	20	Pm	7.22	25
Ce	6.657	25	Po (a)	19.84	25
Cm	13.51	20	Pr (a)	6.773	20
Co	8.9	20	Pr (β)	6.64	20
Cr	7.18-7.20	20	Pt	21.45	20
Cs	1.873	20	Pu (a)	19.84	20
Cu	8.96	20	Ra	(5)	20
Dy	8.550	20	Rb	1.532	20
Er	9.066	25	Re	21.02	20
Eu	5.243	25	Rh	12.41	20
Fe	7.874	20	Ru	12.41	20
Ga (sol)	5.904	29.6	S (rhom)	2.07	20
Ga (liq)	6.095	29.6	S (monocl)	1.957	20
Gd	7.9004	25	Sb	6.691	20
Ge	5.323	25	Sc	2.989	25
Hf	13.31	20	Se (gray)	4.79	20
Hg	13.546	20	Se (vitr)	4.28	20
Hb	8.795	25	Si	2.33	25
In	7.31	20	Sm (a)	7.520	20
Ir	22.42	17	Sm (β)	7.40	20
K	0.862	20	Sn (gray)	5.75	20
La	6.145	25	Sn (white)	5.75	20
Li	0.534	20	Sr	2.54	20
Lu	9.840	25	Ta	16.654	20

DESCRIPTS OF THE ELEMENTS (contd)

Element	Density, g/cm <sup>3</sup>	Temp., °C	Element	Density, g/cm <sup>3</sup>	Temp., °C
Tb	8.229	20			
Tc	11.50	20			
Te	6.24	20			
Th	11.72	20			
Tl	4.54	20			
Tl	11.85	20			
Tm	9.321	25			
U	18.95	20			
V	6.11	18.7			
W	19.3	20			
Y	4.469	20			
Yb (a)	6.965	20			
Yb (B)	6.54	20			
Zn	7.153	25			
Zr	6.506	20			

MELTING AND BOILING POINTS OF ELEMENTS

Source: CRC Handbook of Chemistry and Physics, R. C. Weast, M. J. Astle, and W. H. Beyer, eds., CRC Press, Boca Raton, FL (1984).

Element	Melt. Pt., °C	Boil. Pt., °C	Element	Melt. Pt., °C	Boil. Pt., °C
Ac	1050	3200	K	63.25	760
Ag	960.8	2212	Kr	-156.6	-152.30
Al	660.37	2467	La	921	3457
Am	994	2607	Li	180.54	1342
Ar	-189.2	-185.7	Lu	1663	3395
As	—	subl 613	Mg	648.8	1090
At	302	(337)	Mn	1244	1962
Au	1064.43	3080	Mo	2617	4612
B	2300	2550	N	-209.86	-195.8
Ba	725	1640	Na	97.81	882.9
Be	1278	2970	Nb	2468	4742
Bi	271.3	1560	Nd	1021	3068
Br	-7.2	58.78	Ne	-248.67	-246.048
C	-3550		Ni	1453	2732
Ca	839	1484	Np	640	3902
Cd	320.9	765	O	-218.4	-182.962
Ce	799	3426	Os	3045	5027
Cl	-100.98	-34.6	P	44.1	280
Co	1495	2670	Pb	327.502	1740
Cm	(247)	1340	Pd	1554	2970
Cr	1857	2672	Pm	1168	2460
Cs	28.40	669.3	Po	254	962
Cu	1083.4	2567	Pr	931	3512
Dy	1412	2562	Pt	1772	3827
Er	159	2863	Pu	641	3232
Eu	822	1597	Ra	700	1140
F	-219.62	-188.14	Rb	38.89	686
Fe	1535	2750	Re	3180	(5627)
Fr	27	677	Rh	1966	3727
Ga	29.78	2403	Rn	-71	-61.8
Gd	1313	3266	Ru	2310	3900
Ge	937.4	2830	S rhom	112.8	444.674
H	-259.14	-252.5	mono	119.0	444.67
He	<-272.2	-278.934	Sb	630.74	1950
Hf	2227	4602	Sc	1541	2831
Hg	-38.842	356.58	Se	217	684.9
Ho	1474	2695	Si	1410	2355
I	113.5	184.35	Sm	1077	1791
In	156.61	2080	Sn	231.9681	2270
Ir	2410	4130	Sr	769	1384

MELTING AND BOILING POINTS OF ELEMENTS (contd)

Element	Melt. Pt., °C	Boil. Pt., °C	Element	Melt. Pt., °C	Boil. Pt., °C
Ta	2996	5425			
Tb	1356	3123			
Tc	2172	4877			
Te	449.5	989.8			
Th	1750	-4790			
Tl	1660	3287			
Tl	303.5	1457			
Tm	1545	1947			
U	1132.3	3818			
V	1890	3380			
W	3410	5660			
Xe	-111.9	-107.1			
Y	1522	3338			
Yb	819	1194			
Zn	419.58	907			
Zr	1852	4377			

VAPOR PRESSURE EQUATIONS FOR ELEMENTS

Source: Smithells Metals Reference Book, 6th ed., E. A. Brandes, ed., Butterworths (1983).

The constants that are listed are for the following equation:

$$\log p \text{ (mm Hg)} = A + B/T + C \log T + 10^{-3} DT$$

where T = temperature in Kelvin

Element	A	B	C	D	Temp. Range (K)
Ag	11.66	-14710	-0.755	-	298 - 1234
Ag	12.23	-14260	-1.055	-	1234 - 2400
Al	12.36	-16450	-1.023	-	1200 - 2800
Am	13.97	-13700	-1.0	-	1103 - 1453
As <sub>4</sub>	9.82	-6160	-	-	600 - 900
Au	10.81	-19820	-0.306	-0.16	298 - 1336
Au	12.38	-19280	-1.01	-	1336 - 3240
B	13.88	-29900	-1.0	-	1000 - mp
Ba	7.83	-9730	-	-	750 - 983
Ba	7.42	-9340	-	-	983 - 1200
Be	9.067	-10734	-	-0.145	900 - 1557
Bi	12.35	-10400	-1.26	-	mp - bp
Bi <sub>2</sub>	18.1	-10730	-3.02	-	mp - bp
Ca	14.97	-10300	-1.76	-	713 - mp
Ca	12.55	-9600	-1.21	-	mp - bp
Ce	8.305	-20305	-	-	1611 - 2038
Cd	9.717	-5908	-0.232	-0.284	450 - 594
Cd	12.286	-5819	-1.257	-	594 - 1050
Co	10.817	-22210	-	-0.223	1000 - 1772
Cr	14.56	-20680	-1.31	-	298 - mp
Cs	11.38	-4075	-1.45	-	280 - 1000
Cu	10.63	-17870	-0.236	-0.16	298 - 1356
Cu	13.39	-17650	-1.273	-	1356 - 2870
Eu	-8.16	-8980	-	-	696 - 900
Fe	16.89	-21080	-2.14	-	900 - 1812
Fe	13.27	-19710	1.27	-	1812 - 3000
Ga	10.07	-14700	-0.5	-	mp - bp
Ge	13.28	-20150	-0.91	-	298 - mp
Ge	12.87	-18700	-1.16	-	mp - bp
Hf(α)	11.81	-32000	-0.5	-	298 - 2023

VAPOR PRESSURE EQUATIONS FOR ELEMENTS (contd)

Element	A	B	C	D	Temp. Range (K)
Hf(β)	11.63	-31630	-0.5	-	2023 - mp
Hf	9.20	-29830	-	-	mp - bp
Hg	10.373	-3308	-0.8	-	298 - 630
I <sub>2</sub>	17.72	-3578	-2.51	-	298 - mp
I <sub>2</sub>	23.65	-3205	-5.18	-	mp - bp
In	9.79	-12580	-0.45	-	mp - bp
Ir	13.18	-35070	-0.7	-	298 - mp
K	11.58	-4770	-1.370	-	350 - 1050
La	10.39	-22120	-0.33	-	298 - mp
La	9.89	-21530	-0.33	-	mp - bp
Li	11.34	-8415	-1.0	-	mp - bp
Mg	11.41	-7780	-0.895	-	298 - mp
Mg	12.79	-7550	-1.41	-	mp - bp
Mn	17.88	-14850	-2.52	-	993 - 1373
Mn	17.27	-13900	-2.52	-	mp - bp
Mo	11.66	-34700	-0.236	-0.145	298 - mp
Na	9.235	-5561	-0.5	-	400 - 1200
Nb	9.94	-37650	+0.715	-0.166	298 - mp
Ni	13.60	-22500	-0.96	-	298 - mp
Ni	15.95	-22400	-2.01	-	mp - bp
P <sub>4</sub> (yell)	19.09	-3530	-3.5	-	298 - 317
P <sub>4</sub>	7.84	-2740	-	-	317 - 553
Pb	11.16	-10130	-0.985	-	600 - 2030
Pd	11.82	-19800	-0.755	-	298 - mp
Pd	4.81	-17500	+1.0	-	mp - bp
Pr	8.10	-17190	-	-	1425 - 1692
Pt	13.24	-29200	-0.855	-	298 - mp
Pt	14.30	-28500	-1.26	-	mp - bp
Pu	7.90	-17590	-	-	1392 - 1793
Rb	12.00	-4560	-1.45	-	312 - 952
Re	14.20	-40800	-1.16	-	298 - 3000
Rh	13.50	-29360	-0.88	-	298 - mp
Ru	10.76	-33550	-	-	2000 - 2500
S <sub>2</sub>	16.22	-6975	-1.53	-1.0	mp - bp
S <sub>x</sub>	23.88	-4380	-5.0	-	mp - bp
Sb <sub>x</sub>	22.40	-11560	-3.52	-	298 - mp
Sb <sub>2</sub>	18.54	-11170	-3.02	-	mp - bp
Se (β)	13.07	-19700	-1.0	-	1607 - mp
Se <sub>x</sub>	8.09	-4990	-	-	493 - 958
Si	10.84	-20900	-0.565	-	mp - bp

VAPOR PRESSURE EQUATIONS FOR ELEMENTS (contd)

Element	A	B	C	D	Temp. Range (K)
Sm	13.76	-11170	-1.56	-	298 - mp
Sn	8.23	-15500	-	-	505 - bp
Sr	13.08	-9450	-1.31	-	813 - mp
Sr	12.63	-9000	-1.31	-	mp - bp
Ta	10.29	-40800	-	-	298 - mp
Te <sub>2</sub>	19.68	-9175	-2.71	-	298 - mp
Te <sub>2</sub>	22.29	-7830	-4.27	-	mp -
Th	12.95	-30200	-1.0	-	298 - mp
Tl (β)	13.18	-24400	-0.91	-	1155 - mp
Tl	11.74	-23200	-0.66	-	mp - bp
Tl	11.10	-9300	-0.892	-	700 - 1800
Tm	9.18	-12550	-	-	807 - 1219
U	18.58	-25580	-2.62	-	298 - mp
U	13.20	-24090	-1.26	-	mp - 4200
V	10.12	-26900	+0.33	-0.265	298 - mp
W	8.76	-44000	+0.50	-	298 - mp
Y	11.835	-22230	-0.66	-	298 - mp
Y	16.13	-22280	-1.97	-	mp - bp
Zn	9.418	-6883	-0.0503	-0.33	473 - 692.5
Zn	12.00	-6670	-1.126	-	692.5 - 1000
Zr	11.78	-31820	-0.50	-	1125 - mp
Zr	9.38	-30300	-	-	mp - bp

**Section A.1**

**General**

## B. THERMODYNAMICS

### B.1 Enthalpy and Heat Capacity\*

#### B.1.1 Uranium-Zirconium Alloys

Measurements of the heat capacity of uranium-zirconium alloys have been reported by Federov and Smirnov [1], who used an electrical-pulse technique for their work. Samples of pure zirconium and uranium were investigated, and also alloys with uranium contents of 11, 27, 39, 59, and 87 at.%. Federov and Smirnov give the following equations for heat capacity  $C_p$  (cal  $K^{-1}$  mol $^{-1}$ ) for the temperature ranges 203-873 K for U( $\alpha$ ) and the alloys and 293-1073 K for Zr( $\alpha$ ).

$$\begin{array}{ll} \text{Zr}(\alpha) & C_p = 6.15 + (1.927 \times 10^{-3} T) - (3.485 \times 10^4 T^{-2}) \\ \text{U}(\alpha) & C_p = 2.69 + (9.698 \times 10^{-3} T) - (1.072 \times 10^5 T^{-2}) \\ 11 \text{ at.\% U} & C_p = 3.89 + (6.48 \times 10^{-3} T) + (7.71 \times 10^4 T^{-2}) \\ 27 \text{ at.\% U} & C_p = 3.08 + (8.43 \times 10^{-3} T) + (9.83 \times 10^4 T^{-2}) \\ 39 \text{ at.\% U} & C_p = 3.47 + (9.32 \times 10^{-3} T) + (7.01 \times 10^4 T^{-2}) \\ 59 \text{ at.\% U} & C_p = 0.265 + (1.32 \times 10^{-2} T) + (2.62 \times 10^5 T^{-2}) \\ 87 \text{ at.\% U} & C_p = 0.356 + (1.425 \times 10^{-2} T) + (2.59 \times 10^5 T^{-2}) \end{array}$$

Heat-capacity data for the alloy of interest, U-10 wt % Zr (U-22.5 at.% Zr) were obtained by linear interpolation. The following equations give heat capacity,  $C_p$  (J  $K^{-1}$ ), and enthalpy,  $H(T) - H(298)$  (J mol $^{-1}$ ), for that alloy.

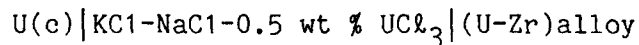
$$C_p(\text{U-10 wt \% Zr}) = 1.359 + 0.05812T + (1.086 \times 10^6 T^{-2})$$

$$\begin{aligned} H(T) - H(298)(\text{U-10 wt \% Zr}) &= 654.0 + 1.359T + 0.02906T^2 \\ &\quad - (1.086 \times 10^6 T^{-1}) \end{aligned}$$

\* The reference list for Section B.1 is on page B.1-27.

The data of Federov and Smirnov for pure uranium and zirconium are high by about 3-4% when compared with the best current values [3,4]. Uncertainties of about  $\pm 5\%$  are reasonable for these estimates for the U-10 wt % Zr alloy.

Obtaining heat-capacity and enthalpy data for the high-temperature body-centered-cubic (bcc) alloy phases is somewhat more difficult. For the heat capacities of U( $\gamma$ ) and Zr( $\beta$ ) and the high-temperature bcc alloy phases, the data of Federov and Smirnov are presented graphically. Values obtained from their plots at 1100 K, in (at. % U) and  $\text{cal K}^{-1} \text{mol}^{-1}$ , given in an IAEA publication [2] are: (0) 7.45, (11) 8.2, (27) 8.9, (39) 9.3, (59) 9.5, and (87) 9.5. These values are constant in the temperature range of the bcc solid solution. At the higher temperatures Federov and Smirnov give only heat capacity. In order to calculate enthalpy of the higher-temperature bcc solid solutions, we need an enthalpy value in the higher-temperature phase. Federov and Smirnov [5] also measured the emf of cells of the type



The temperature range of their measurements was 1033-1183 K. Thermodynamic properties for U-Zr alloys were calculated at 1100 K from the emf data of Federov and Smirnov [5] by Chiotti et al. [2]. Included in the tabulation of Chiotti et al. is the enthalpy of mixing from which the requisite values could be estimated. However, there are significant discrepancies in the U-Zr system [2], and Pelton [6] discounts the data entirely. We have calculated the enthalpy of the U-10 wt % Zr alloy at 1200 K assuming an ideal solution, and have used the heat-capacity data of Federov and Smirnov to calculate enthalpies at other temperatures. The values calculated in this way are about 10% higher than those resulting from using the enthalpy-of-mixing data. Because of the lack of data, the details of the transition region from 890 to about 1000 K are not considered in the present analysis. The transition region is

simply treated as a single phase transition. The enthalpy data resulting from these considerations are shown in Fig. B.1-1 (along with data for U and Zr), and are combined with heat-capacity data in Table B.1-1. Data are given up to the solidus temperature (1487 K). Values at the liquidus (1657 K) and above were estimated using an ideal solution assumption. For values between the solidus and liquidus temperatures, linear interpolation is recommended.

**TABLE B.1-1. Enthalpy and Heat Capacity of Uranium-10 wt % Zirconium**

T (K)	$C_p$ (J K <sup>-1</sup> mol <sup>-1</sup> )	H(T) - H(298) (kJ mol <sup>-1</sup> )
298	30.9	0.0
400	31.4	3.13
500	34.8	6.43
600	39.2	10.1
700	44.3	14.3
800	49.6	18.9
890	54.5	23.7
1000	36.7	31.1
1100	36.7	39.0
1200	36.7	43.0
1400	36.7	46.9
1487(s)	36.7	50.0
1657(l)	45.2	68.5
1700	45.2	70.4
1800	45.2	74.8
1900	45.2	79.4
2000	45.2	84.0

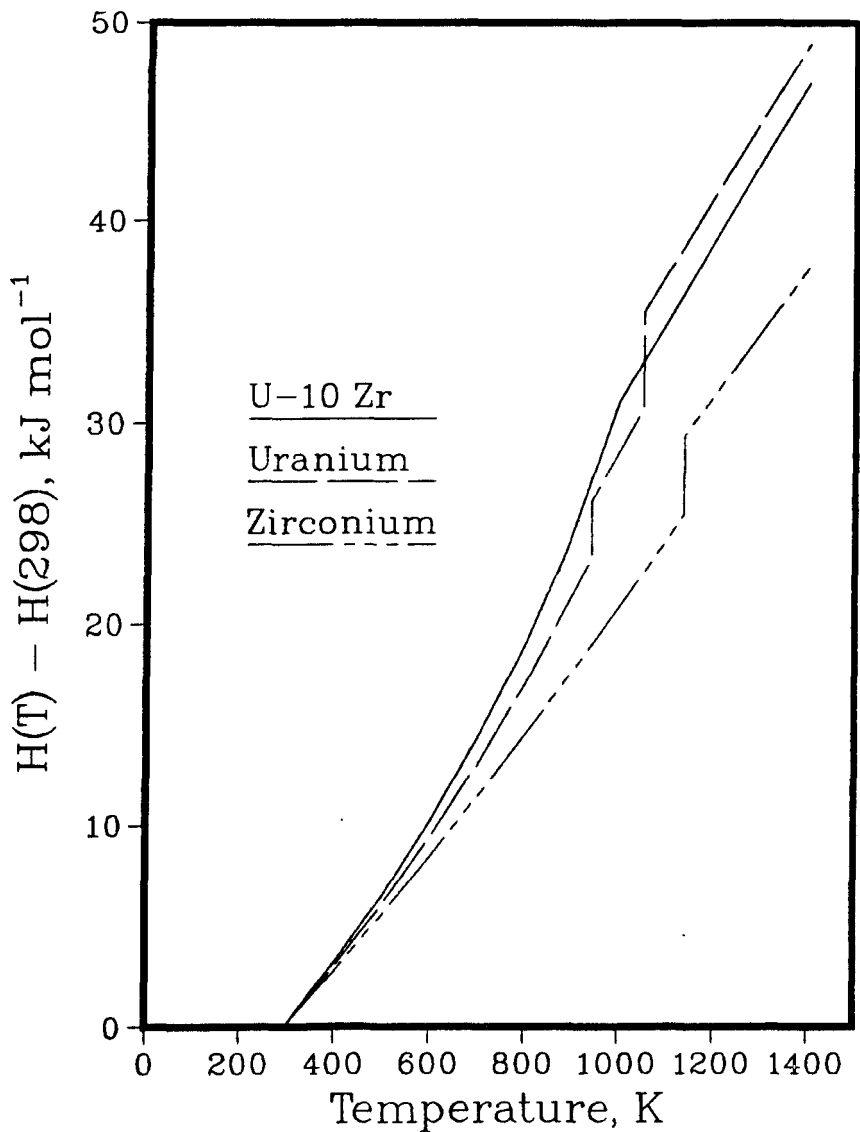


Fig. B.1-1. Enthalpy,  $H(T) - H(298)$ ,  $\text{kJ mol}^{-1}$ , of U-10 wt % Zr

B.1.2 Uranium-Plutonium-Zirconium Alloys

Measurements have been reported of the enthalpy of U-15 wt % Pu-10 wt % Zr (U-12.8 at.% Pu-22.5 at.% Zr) from about 306 to 1140°C [7]. The data appear to be reliable (probably to 1%) [8] and cover most of the solid range of this alloy. The experimental values as given in [7] are presented in Table B.1-2.

TABLE B.1-2. Enthalpy of U-15 wt % Pu-10 wt % Zr

Temperature (°C)	H(T)-H(25°C) (cal/g)
306.5	10.2
402.4	14.1
505.3	18.7
599.6	23.9
696.1	34.7
98.1	38.9
897.0	43.3
997.0	47.4
1097.0	52.4
1140.3	55.1

These data were fit to two quadratic equations in [7] covering the temperature ranges above and below the solid-state phase transitions. These equations are reproduced below (a sign error has been corrected).

$$H(T) - H(25^\circ\text{C}) = -0.9 + 0.0310T + (1.55 \times 10^{-5} T^2) \quad 25\text{-}600^\circ\text{C}$$

$$H(T) - H(25^\circ\text{C}) = 14.2 + 0.0185T + (1.52 \times 10^{-5} T^2) \quad 650\text{-}1150^\circ\text{C}$$

Enthalpies are given in cal/g and temperatures are in °C. Heat capacities may be obtained simply by differentiating the enthalpy equations. The coefficients of the "T" terms given for heat capacity in [7] are too large by a factor of ten. After correction of the coefficients, these enthalpy equations yield the following equations for temperatures in K and enthalpies in J/mol. A small correction was made in the low-temperature equation so that H(T) - H(298) was zero at

T = 298.15. The higher-temperature equation was modified to the current heat estimate of the solidus temperature (1379 K)[6].

$$\begin{aligned} H(T) - H(298) &= -6948 + 19.34T + 0.0133T^2 && 298-873K \\ H(T) - H(298) &= 8772 + 8.752T + 0.01304T^2 && 923-1379K \end{aligned}$$

The enthalpies and heat capacity of the ternary alloy are given in Table B.1-3. Included in the table are values above the liquidus temperature (1588 K) that were calculated assuming an ideal solution. For values between the solidus and liquidus temperature, linear interpolation is recommended. The enthalpies of U-15 wt % Pu-10 wt % Zr, pure uranium, and U-10 wt % Zr are compared in Fig. B.1-2. To assess the possibilities of estimation and extrapolation of enthalpy data, we calculated the mole-average enthalpy for the ternary alloy, using data for U [3], Pu [3], and Zr [4] from standard sources. Because the melting point of Pu of 913 K is well below the solidus temperature of the alloy, we simply extrapolated the data for Pu( $\epsilon$ ) above its melting point, assuming a constant heat capacity. This appeared to be a more reasonable approach than introducing data for liquid Pu. The results of this calculation are compared with the experimental values in Fig. B.1-3. Except for the phase-transition temperatures the agreement is reasonable, and estimates for other compositions and temperatures may be possible.

**TABLE B.1-3. Enthalpy and Heat Capacity of Uranium-15 wt %  
Plutonium-10 wt % Zirconium**

T (K)	$C_p$ (J K <sup>-1</sup> mol <sup>-1</sup> )	H(T) - H(298) (kJ mol <sup>-1</sup> )
298	27.3	0.0
400	30.0	2.92
500	32.6	6.05
600	35.3	9.44
700	38.0	13.1
800	40.6	17.0
873	42.6	20.1
923	32.8	28.0
1000	34.8	30.6
1100	37.4	34.2
1200	40.0	38.1
1300	42.7	42.2
1379(s)	44.7	45.6
1588(l)	44.4	64.4
1600	44.4	64.9
1700	44.4	69.4
1800	44.4	73.8
1900	44.4	78.3
2000	44.4	82.7

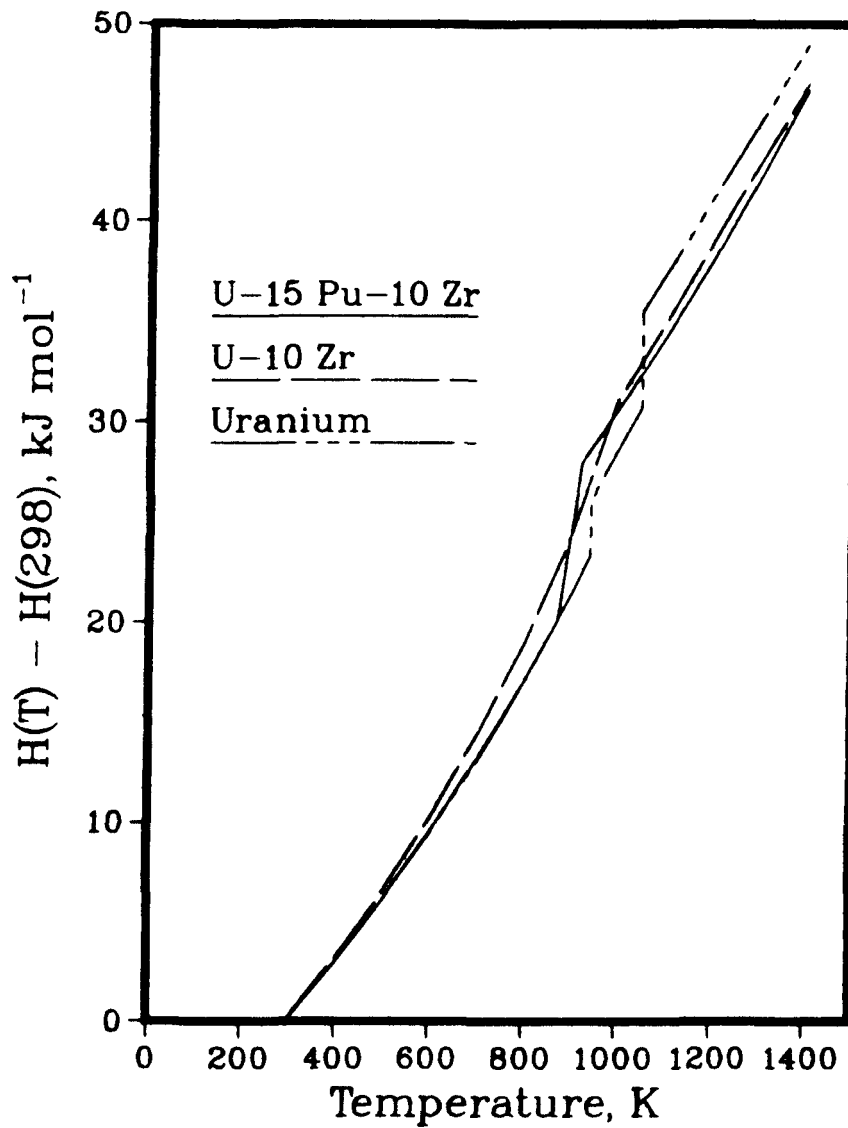


Fig. B.1-2. Enthalpy,  $H(T) - H(298)$   $\text{kJ mol}^{-1}$ , for Uranium, U-10 wt % Zr, and U-15 wt % Pu-10 wt % Zr

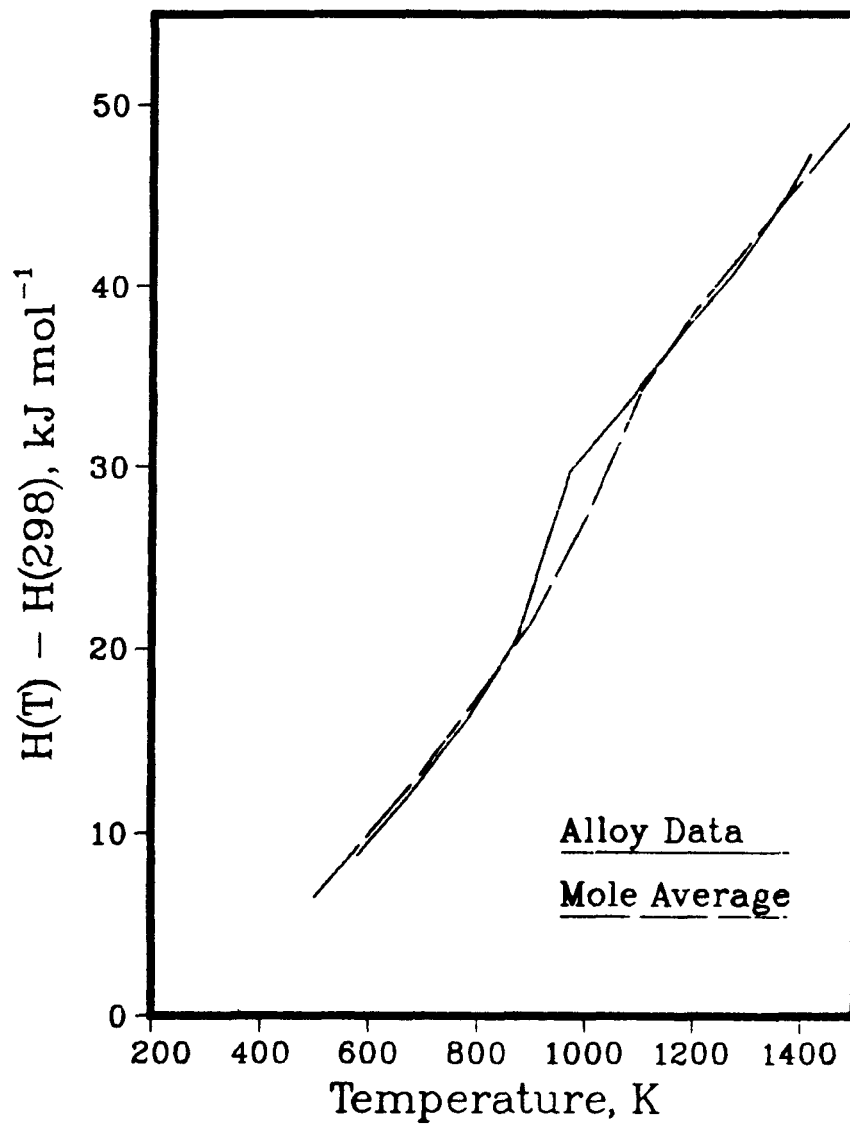


Fig. B.1-3. Enthalpy,  $H(T) - H(298)$   $\text{kJ mol}^{-1}$ , for U-15 wt % Pu-10 wt % Zr Compared with Mole-average Values

B.1.3 Others

TABLE B.1-4. High-temperature Heat Capacity and Enthalpy of Uranium

T (K)	$C_p$ ( $J K^{-1} mol^{-1}$ )	H(T) - H(298) ( $J mol^{-1}$ )
298	27.665	0
300	27.700	51
400	29.684	2919
500	31.997	5999
600	34.762	9333
700	38.021	12968
800	41.791	16955
900	46.081	21344
942( $\alpha$ )	48.038	23320
942( $\beta$ )	42.928	26111
1000	42.928	28600
1049( $\beta$ )	42.928	30704
1049( $\gamma$ )	38.284	35461
1100	38.284	37414
1200	38.284	41242
1300	38.284	45070
1400	38.284	48899
1408( $\gamma$ )	38.284	49205
1408( $\delta$ )	48.660	58347
1500	48.660	62842
1600	48.660	67690
1700	48.660	72556
1800	48.660	77422
1900	48.660	82288
2000	48.660	87154
2100	48.660	92020
2200	48.660	96886
2300	48.660	101752
2400	48.660	106618
2500	48.660	111484

High-temperature Heat Capacity and Enthalpy of Uranium\*

The high-temperature enthalpy and heat capacity of uranium have been determined by several investigators. The more precise

\* This section adopted from Ref. 3.

heat-capacity results are shown in Fig. B.1-4. The early enthalpy measurements of Moore and Kelley [9] and of Ginnings and Corruccini [10] cover the lower temperature range, 298 to 1300 K and 298 to 1173 K, respectively. The two investigations are in good agreement on the enthalpy of the  $\alpha$ -phase of uranium, although Ginnings and Corruccini [10] report a steeper rise in the enthalpy function, indicating a more pronounced pretransition effect. North [11], using an adiabatic method, reported heat-capacity measurements from 373 to 1073 K consistently below the values reported above. Savage and Seibel [12], using a drop calorimeter, determined the enthalpy increment of uranium in the temperature range of 413 to 1454 K. Their results are in agreement with those of Moore and Kelley [9] and Ginnings and Corruccini [10] below 1100 K, but become significantly higher above this temperature. Mit'kina [13] reported the specific heat capacity of uranium from 323 to 873 K. Her results are much lower below 573 K, but above that temperature they are in good agreement with the results of Moore and Kelley [9], and of Ginnings and Corruccini [10]. For this assessment we have adopted the heat-capacity values for  $\alpha$ -phase uranium reported by Ginnings and Corruccini [10], since these data are believed to be the most reliable.

The heat capacities of the  $\beta$ - and  $\gamma$ -phase of uranium metal are constant at 43.43 and 38.07 J K<sup>-1</sup> (as reported by Moore and Kelley [9]), and at 42.47 and 38.28 J K<sup>-1</sup> mol<sup>-1</sup> (as reported by Ginnings and Corruccini [10]). The adopted heat-capacity values for the  $\beta$ - and  $\gamma$ -phase of uranium metal are based on the results of these two investigations: 42.93 J K<sup>-1</sup> mol<sup>-1</sup> for the  $\beta$ -phase and 38.28 J K<sup>-1</sup> mol<sup>-1</sup> for the  $\gamma$ -phase, respectively. Levinson [14] has determined the enthalpy increment of the  $\gamma$ -phase and the liquid. His resulting heat-capacity value for the  $\gamma$ -phase, 40.08 J K<sup>-1</sup> mol<sup>-1</sup> is considerably higher than the values reported earlier by Moore and Kelley [9] and by Ginnings and Corruccini [10].

The enthalpies of transition, as reported by various investigators (Table B-1.5), are in fairly good agreement. However, the

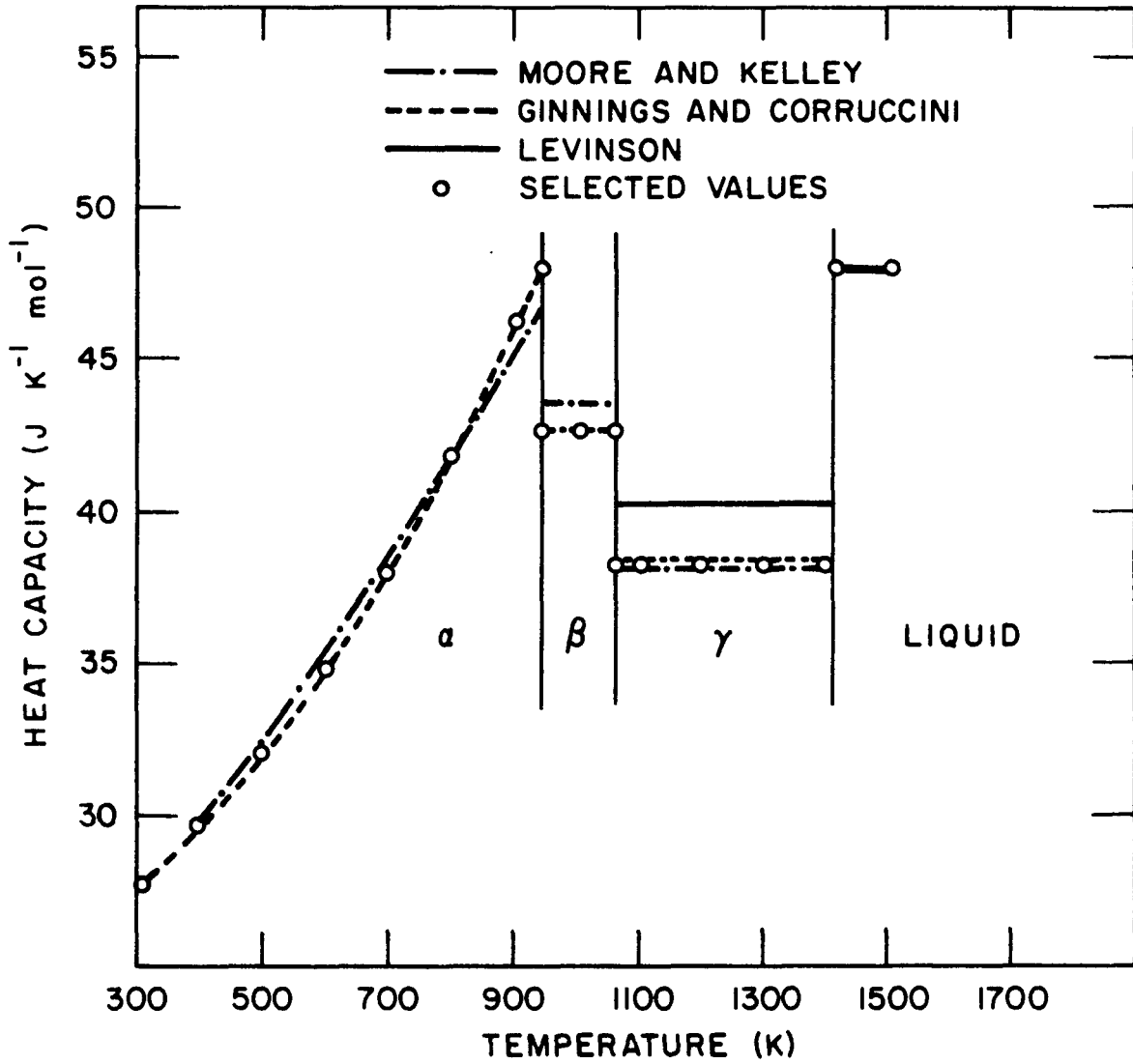


Fig. B.1-4. Heat-capacity Data for Uranium from Various Investigators

values for the enthalpies of transition used in this compilation are chosen so as to reproduce the measured enthalpy increments for the  $\beta$ - and  $\gamma$ -phases.

**TABLE B-1.5. Enthalpies of Transition for Uranium**

Source	$\Delta H_t(\alpha \leftrightarrow \beta)$ (kJ mol <sup>-1</sup> ) (T <sub>t</sub> =942K)	$\Delta H_t(\beta \leftrightarrow \gamma)$ (kJ mol <sup>-1</sup> ) (T <sub>t</sub> =1049K)
Moore and Kelley [9]	2.845	4.874
Ginnings and Corruccini [10]	2.820	4.732
North [11]	2.979	4.782
Savage and Seibel [12]	3.284	4.581
Adopted value	2.791	4.757

The selected values for heat capacity and enthalpy of the solid phases are identical with those tabulated by Hultgren et al. [4], except for minute differences resulting from the use of an equation for the heat capacity for the  $\alpha$ -phase and correction to the International Practical Temperature Scale (IPTS-1968).

#### Melting Point and Enthalpy of Fusion

The melting point of uranium metal has been reported by several investigators: by Blumenthal [15] as (1405 ± 0.8) K, by Buzzard et al. [16] as 2406 K, by Udy and Boulger [17] as (1405 ± 10) K, and by Dahl and Cleaves [18] as (1406 ± 2) K. The agreement is remarkable, and (1406 ± 2) K is selected as the melting point of uranium on IPTS-1948, which becomes (1408 ± 2) K on IPTS-1968. Ackermann and Rauh [19] measured (1408 ± 1) K on the latter scale.

There have been two determinations of the enthalpy of liquid uranium. Levinson [14] measured  $H(T)-H(310)$  for  $U(l)$  contained in tantalum from 1205 to 1579 K, obtaining a value for the enthalpy of fusion of  $(8.326 \pm 0.130)$   $\text{kJ mol}^{-1}$  and a constant value for the heat capacity of  $U(l)$  of  $47.91 \text{ J K}^{-1} \text{ mol}^{-1}$ . When corrected for tantalum solubility (Ackermann and Rauh [20]), this latter value becomes  $44.35 \text{ J K}^{-1} \text{ mol}^{-1}$ .

However, we have preferred the much more extensive enthalpy results of Stephens [21] from 1428 to 2348 K. These results were obtained by levitation calorimetry, which avoids the problems of reactions with containers. His data, which are represented by the equation

$$H(T) - H(298) = 48.66T - 10138 \text{ J mol}^{-1}$$

when combined with the selected data for the solid thus give a value for the enthalpy of fusion of  $9.14 \text{ kJ mol}^{-1}$  at 1408 K and a constant value of  $C_p^0 U(l)$  of  $48.66 \text{ J K}^{-1} \text{ mol}^{-1}$ .

Recently, Thayer and Robbins [22] have determined the heat capacity of  $U(l)$  by using a prompt-burst reactor to heat thin wafers of the metal very rapidly. Their value of  $(37.66 \pm 2.1)$   $\text{J K}^{-1} \text{ mol}^{-1}$  for the heat capacity of  $U(l)$  is appreciably lower than the other two measurements. The uncertainties in this interesting technique at this time lead us to prefer the very extensive measurements of Stephens [21].

The heat capacity of  $U(\alpha)$ ,  $298 \leq T \leq 942$  K, in  $\text{J K}^{-1} \text{ mol}^{-1}$  is given by the following equation:

$$C_p(U\alpha) = 26.92 - (2.502 \times 10^{-3} T) + (26.556 \times 10^{-6} T^2) - (7.7 \times 10^4 T^{-2}).$$

For  $U(\beta)$ ,  $U(\gamma)$ , and  $U(\delta)$ , the heat capacity is constant. The recommended enthalpies are shown in Fig. B.1-5.

#### High-temperature Heat Capacity and Enthalpy of Plutonium\*

The high-temperature heat capacity of plutonium has been reported by two investigators (Engel [23] and Loasby [24]). Their results are plotted in Fig. B.1-6, along with the low-temperature heat-capacity measurements of Sandenaw and Gibney [25], who took measurements up to 370 K, within 25 K of the  $\alpha \leftrightarrow \beta$  transition. Kay and Loasby [24] report high-temperature heat-capacity data (error span  $\pm 5\%$ ) for plutonium metal up to the melting point. However, to allow for unsuspected errors in their chemical and isotopic analyses used in the calculation of the self-heating coefficients (Taylor [26]), they increased the error span to  $\pm 10\%$ . They used an adiabatic calorimeter and utilized the self-heating of the isotopic mixture of plutonium as the heat source in determining the heat-capacity value. Such a method has the advantage of ensuring uniform heating of the specimen; however, it has the disadvantage of errors arising from nonequilibrium conditions, in particular in the transformation regions.

Other sources of error in these heat-capacity measurements lie in assuming an accurate value of each isotopic power output, as well as in making an accurate isotopic analysis of the metal specimen. Recent power-output values for the individual plutonium isotopes (Oetting [27]) differ somewhat from the values cited by Kay and Loasby [24]; however, an error band of  $\pm 10\%$  covers the error involved in the power values.

A comparison of the heat-capacity values of Kay and Loasby [24] and of Sandenaw and Gibney [25], from room temperature to the  $\alpha \leftrightarrow \beta$  transformation (395 K), shows the values of Kay and Loasby to be

---

\* This section adopted from Ref. 3.

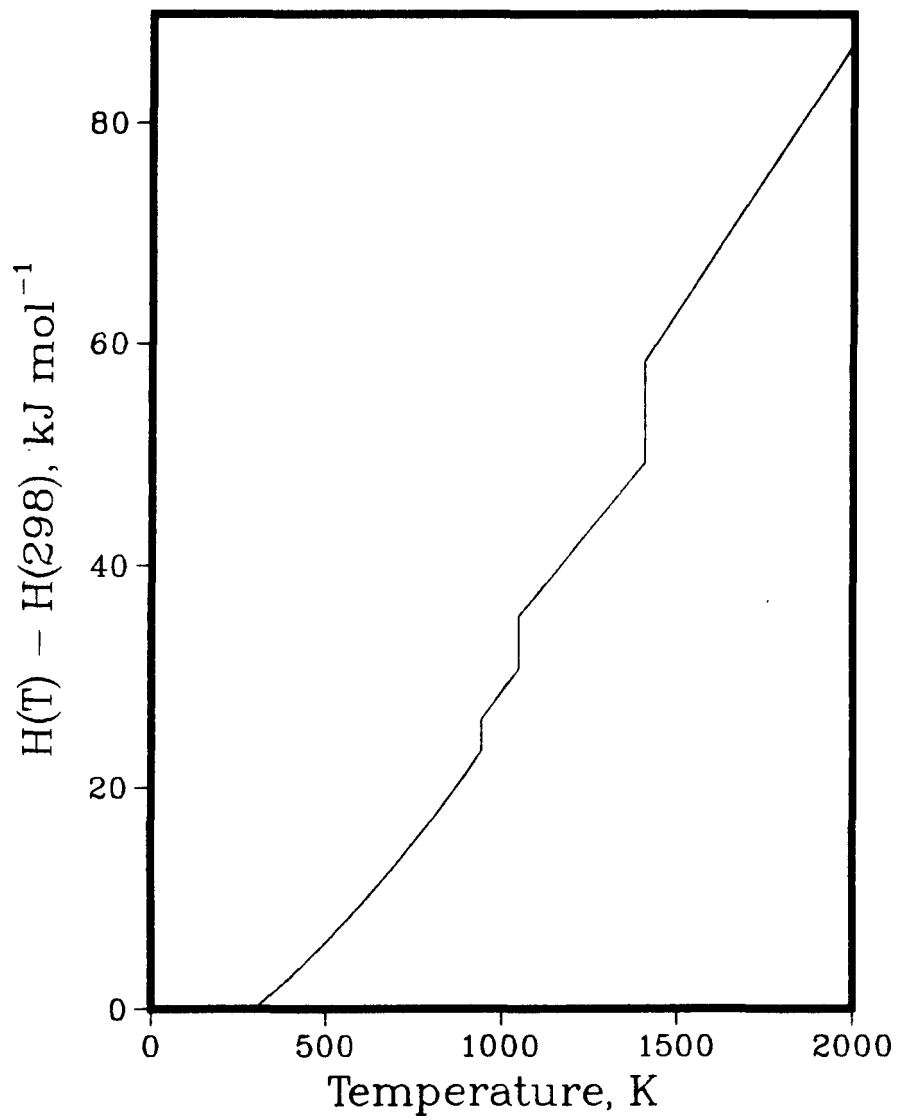


Fig. B-1.5. Enthalpy,  $H(T) - H(298) \text{ kJ mol}^{-1}$  for Uranium

TABLE B.1-6. High-temperature Heat Capacity and Enthalpy of Plutonium

T (K)	$C_p$ (J K <sup>-1</sup> mol <sup>-1</sup> )	H(T) - H(298) (J mol <sup>-1</sup> )
298	32.844	0
300	32.922	61
395(α)	38.715	3436
395(β)	33.882	6867
400	33.991	7036
480(β)	35.731	9825
480(γ)	35.171	10390
500	35.736	11099
588(γ)	38.221	14353
588(δ)	37.154	14939
600	37.154	15385
700	37.154	19100
730(δ)	37.154	20215
730(δ')	35.564	20299
752(δ')	35.564	21081
752(ε)	34.434	22922
800	34.434	24575
900	34.434	28018
913(ε)	34.434	28466
913(λ)	42.258	31290
1000	42.258	34967
1100	42.258	39192
1200	42.258	43418
1300	42.258	47644
1400	42.258	51870
1500	42.258	56096
1600	42.258	60322
1700	42.258	64547
1800	42.258	68733
1900	42.258	72999
2000	42.258	77225
2100	42.258	81451
2200	42.258	85657
2300	42.258	89903
2400	42.258	94128
2500	42.258	98354

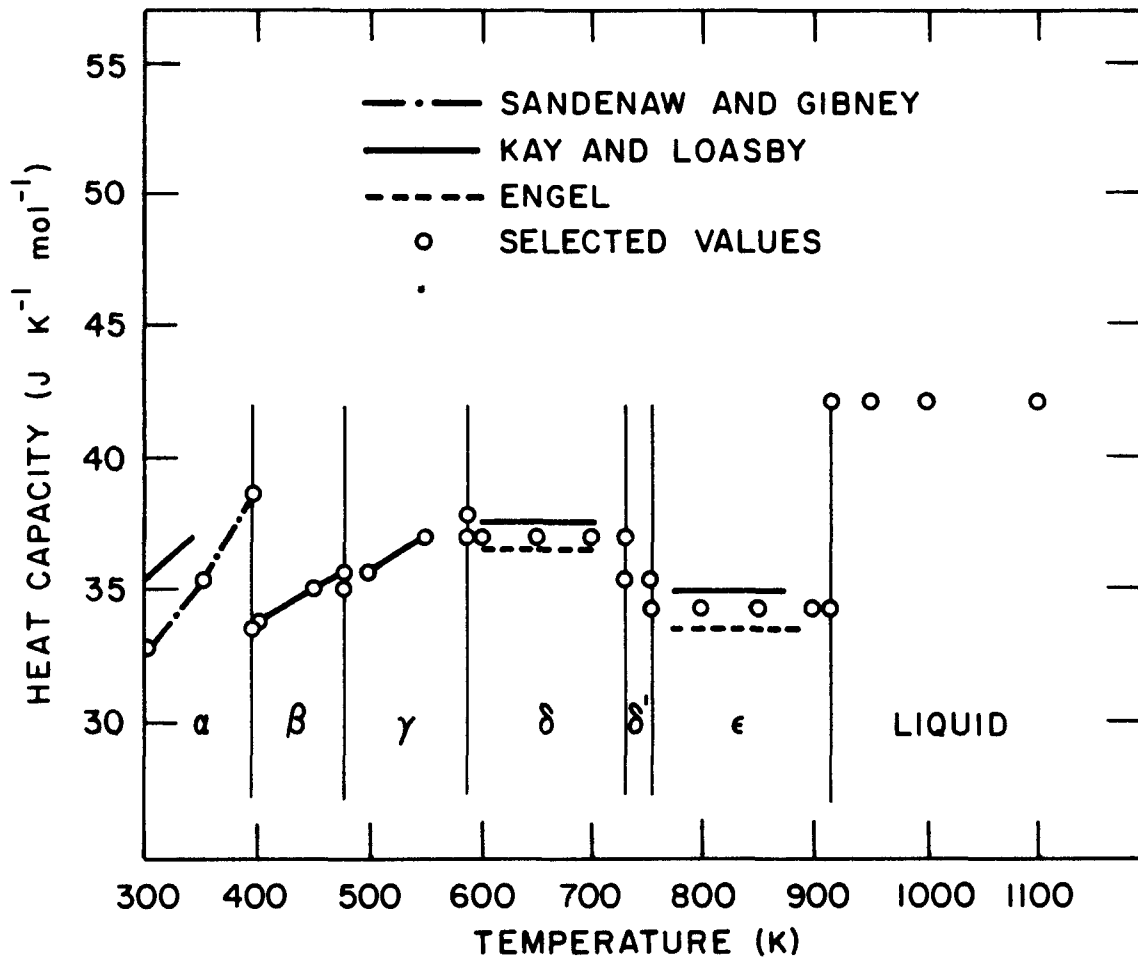


Fig. B.1-6. Heat-capacity Data for Plutonium from Various Investigators

higher by about 7%. As it is believed that the low-temperature data of Sandenaw and Gibney are more accurate, their values were adopted for the heat capacity of the  $\alpha$ -phase of plutonium above room temperature.

Kay and Loasby [24] indicate a slight temperature dependence for the heat capacity of the  $\beta$ - and  $\gamma$ -phases but no temperature dependence for the  $\delta$ - and  $\epsilon$ -phases. Engel [23] also found no temperature dependence for the heat capacity of the  $\delta$ -,  $\delta'$ - and  $\epsilon$ -phases of plutonium. The agreement between the heat capacity values for the  $\delta$ - and  $\epsilon$ -phases of Engel and Kay and of Loasby is quite good, i.e., 2.6% and 4.0% respectively. The averages of the two values are taken for this compilation. The value of  $35.56 \text{ J K}^{-1} \text{ mol}^{-1}$  given by Engel for the heat capacity of the  $\delta'$ -phase is also used.

The consistency of the thermodynamic data for the plutonium allotropes can be checked by a consideration of the thermal properties of a Pu-Ga alloy with ~3.3 at.% Ga, which stabilizes the  $\delta$ -phase at low temperatures. Taylor et al. [28] have measured the low-temperature heat capacities. The specific power for the sample used was consistent with the latest specific powers for the plutonium isotopes given by Oetting [27]. Integration of the  $C_p$  values gives

$$\text{Pu}_{0.968}\text{Ga}_{0.032}(\delta - \text{phase})S^0(298) = 67.82 \text{ J K}^{-1} \text{ mol}^{-1}$$

Rose et al., [29] have measured the enthalpy increments of an alloy of very similar composition. Their data give a smooth continuation of the heat-capacity values of Taylor et al., [28] as follows:

$$\text{Pu}_{0.967}\text{Ga}_{0.033}(\delta - \text{phase})S(588) - S(298) = 22.59 \text{ J K}^{-1} \text{ mol}^{-1}$$

and hence  $S(588) = 90.41 \text{ cal K}^{-1} \text{ mol}^{-1}$ .

Since  $S^0(588) - S^0(298)$  for Ga(c) can be estimated from the values for the neighbouring elements (Hultgren et al.[4]) to be  $-17.32 \text{ J K}^{-1} \text{ mol}^{-1}$ , we have:

<u>Phase</u>	<u>S(588)(J K<sup>-1</sup> mol<sup>-1</sup>)</u>
Ga(c)	58.16
Pu <sub>0.967</sub> Ga <sub>0.033</sub> ( $\delta$ )	90.42
Pu( $\delta$ )	91.50

This is in excellent agreement with the value obtained by integration through the  $\alpha$ -,  $\beta$ - and  $\gamma$ -phases, namely 91.17 J K<sup>-1</sup> mol<sup>-1</sup>.

#### Melting Point and Enthalpy of Fusion

Table B.1-7 includes a survey of the reported values for the melting point and enthalpy of fusion of plutonium metal. Again, more weight is given to the more recent data, and the suggested values are (913  $\pm$  2) K for the melting point, and (2824  $\pm$  105) J mol<sup>-1</sup> for the enthalpy of fusion. The heat capacity of the liquid plutonium, measured just above the melting point, has been reported informally by two investigators (Loasby [30] and Engel [23]), with good agreement (41.84 and 42.68 J K<sup>-1</sup> mol<sup>-1</sup>, respectively). The average value of (42.4  $\pm$  0.8) J K<sup>-1</sup> mol<sup>-1</sup> used in this assessment is in good agreement with the recent value of 42.7 J K<sup>-1</sup> mol<sup>-1</sup> (Thayer and Robbins, [22]).

The heat capacity of Pu( $\alpha$ ), 298  $\leq$  T  $\leq$  395 K, in J K<sup>-1</sup> mol<sup>-1</sup> is given in the following equation:

$$C_{p,Pu(\alpha)} = 37.610 - (7.380 \times 10^{-2} T) + (1.939 \times 10^{-4} T^2).$$

The heat capacity of Pu( $\beta$ ), 395  $\leq$  T  $\leq$  480 K, in J K<sup>-1</sup> mol<sup>-1</sup> is given by the following equation:

$$C_{p,Pu(\beta)} = 25.288 + (2.176 \times 10^{-2} T)$$

The heat capacity of Pu( $\gamma$ ), 480  $\leq$  T  $\leq$  588 K, in J K<sup>-1</sup> mol<sup>-1</sup> is given by the following equation:

$$C_{p,Pu(\gamma)} = 21.615 + (2.824 \times 10^{-2} T)$$

TABLE B.1-7. Temperature and Enthalpy of Plutonium Transitions

Ref.	Method <sup>a</sup>	$\alpha+\beta$		$\beta+\gamma$		$\gamma+\delta$		$\delta+\delta'$		$\delta+\epsilon$		$\epsilon+liq$	
		T (K)	$\Delta H_t$ (J mol <sup>-1</sup> )	T (K)	$\Delta H_t$ (J mol <sup>-1</sup> )	T (K)	$\Delta H_t$ (J mol <sup>-1</sup> )	T (K)	$\Delta H_t$ (J mol <sup>-1</sup> )	T (K)	$\Delta H_t$ (J mol <sup>-1</sup> )	T (K)	$\Delta H_t$ (J mol <sup>-1</sup> )
31	Dil	388		458		583		725		753			
32	TA	392 ± 2	3531 ± 42	477 ± 6	515 ± 25	588 ± 2	653 ± 63	730 ± 2	79 ± 25	752 ± 4	1724 ± 105		
23	Cal							741 ± 2	29 ± 13	754	1925 ± 33		
33		390 ± 0.5											
24	Cal	392	3360 ± 42	477	636 ± 63	584	523 ± 21	731	84 ± 42	753	1858 ± 42	911	2900 ± 42
34	Cal	400	3389 ± 21	480	519 ± 50	593	569 ± 29	733	105 ± 33	754	1845 ± 33	913	2741 ± 25
35	Dil	385 ± 1		457 ± 2									
36		395 ± 2		479 ± 3		592 ± 6		724 ± 4		749 ± 4		913	
37	Dil	383 ± 4		476 ± 6		586 ± 7		733 ± 5		749 ± 4			
38	TA	399 ± 2		482 ± 3		589 ± 2		729		757 ± 2		914 ± 2	
38	Dil	406		481		579		733		749		907	
39		396 ± 6	5021	488 ± 3	586	588 ± 2	544		<167	752 ± 7	1590	914 ± 2	2218
40	Res	396.7 ± 0.3	3925 ± 42	475 ± 2		591 ± 2		729 ± 2		757 ± 3			
41	Dil, TA	395	3201 ± 502	484	699 ± 105	588	799 ± 105	713	-0	733	1598 ± 293	908	3301 ± 502
42	Cal	394	4008 ± 42	481	586 ± 63	589	653 ± 63	728	71 ± 42	752	1966 ± 42		
43	Dil, TA	395 ± 2		478 ± 3		593 ± 5		725 ± 4		749 ± 5		913 ± 2	
*		395 ± 4	3431 ± 84	480 ± 5	565 ± 63	588 ± 3	586 ± 63	730 ± 2	84 ± 42	752 ± 4	1841 ± 84	913 ± 2	2824 ± 105

<sup>a</sup> Cal = calorimetric, Dil = dilatometric, Res = resistivity, TA = thermal analysis

\* Suggested values

For Pu( $\delta$ ), Pu( $\delta'$ ), Pu( $\epsilon$ ), and Pu( $\lambda$ ), the heat capacity is constant. Recommended enthalpy data for plutonium are given in Fig. B.1-7.

#### High-temperature Heat Capacity and Enthalpy of Zirconium\*

The selected values agree with the heat-content measurements of Douglas and Victor for 373-1173 K [44]; and with Jaeger and Veenstra for 505-1074 K [45]; except that the latter's data show more scatter and are about 3% lower below 600 K. The heat-content data of Fieldhouse and Lange for 472-1807 K [46] are 2% lower below 900 K, trending to 5% higher at 1100 K and averaging about 2.5% higher in the  $\beta$  range. Those of Redmond and Lones for 404-1309 K [47] are highly scattered, averaging about 7% higher in  $\alpha$  and varying from 8% to 0.4% lower in  $\beta$ . The heat-content data of Skinner for 1102-1798 K [48] are about 2% lower. Those of Coughlin and King for 390-1371 K [49] are about 3% higher in  $\alpha$  and only about 1% higher in  $\beta$ . The  $C_p$  values of Klein and Danielson for 298-2118 K [50], obtained by a pulse heating method, are 10% lower in  $\alpha$  and trend from 15% lower to 7% higher in  $\beta$ . Those of Scott for 333-1233 K [51] are 7% lower than the selected values.

Hertzricken and Slyuser [52], using a differential calorimeter, found  $\Delta H(\alpha \leftrightarrow \beta) = 2979 \pm 250 \text{ J mol}^{-1}$ , considerably lower than the selected value; while Scott [8], from adiabatic calorimetry, found  $\Delta H(\alpha \leftrightarrow \beta) = 4155 \pm 105 \text{ J mol}^{-1}$ , only slightly higher than the value chosen.  $C_p(\beta) = 31.4 \text{ J K}^{-1} \text{ mol}^{-1}$  was assumed to remain constant to the melting point.  $\Delta S_m = 7.9 \text{ J K}^{-1} \text{ mol}^{-1}$  was estimated.

The heat capacity of Zr( $\alpha$ ),  $298 \leq T \leq 1136 \text{ K}$ , in  $\text{J K}^{-1} \text{ mol}^{-1}$  is given by the following equation:

\* This section adopted from Ref. 4.

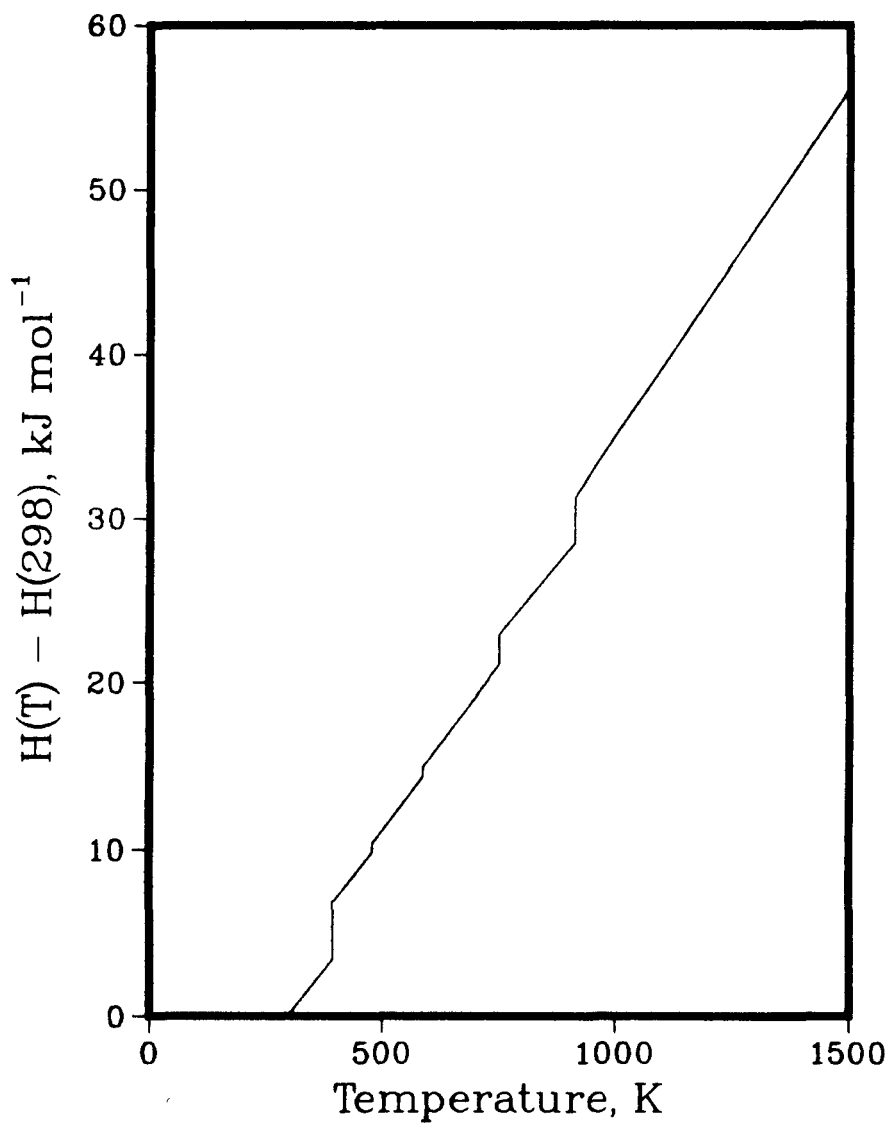


Fig. B.1-7. Enthalpy,  $H(T) - H(298)$   $\text{kJ mol}^{-1}$ , for Plutonium

TABLE B.1-8. High-temperature Heat Capacity and Enthalpy of Zirconium

T (K)	$C_p$ (J K <sup>-1</sup> mol <sup>-1</sup> )	H(T) - H(298) (J mol <sup>-1</sup> )
298	25.36	0
400	27.36	2703
500	28.37	5494
600	29.33	8381
700	30.25	11355
800	31.17	14431
900	32.13	17594
1000	33.05	20853
1100	34.02	24204
1136(α)	34.31	25434
1136(β)	31.4	29372
1200	31.4	31380
1300	31.4	34518
1400	31.4	37656
1500	31.4	40794
1600	31.4	43932
1700	31.4	47070
1800	31.4	50208
1900	31.4	53346
2000	31.4	56484
2100	31.4	59622
2125(β)	31.4	60409
2125(λ)	33.5	77304
2200	33.5	79814
2400	33.5	86508
2600	33.5	93203

$$C_p, \text{Zr}(\alpha) = 27.186 + (3.092 \times 10^{-3} T) \\ + (3.002 \times 10^{-6} T^2) \\ - (2.651 \times 10^5 T^{-2}).$$

The heat capacities of  $\text{Zr}(\beta)$  and  $\text{Zr}(\ell)$  are constant.  
Recommended enthalpy values are shown in Fig. B.1-8.

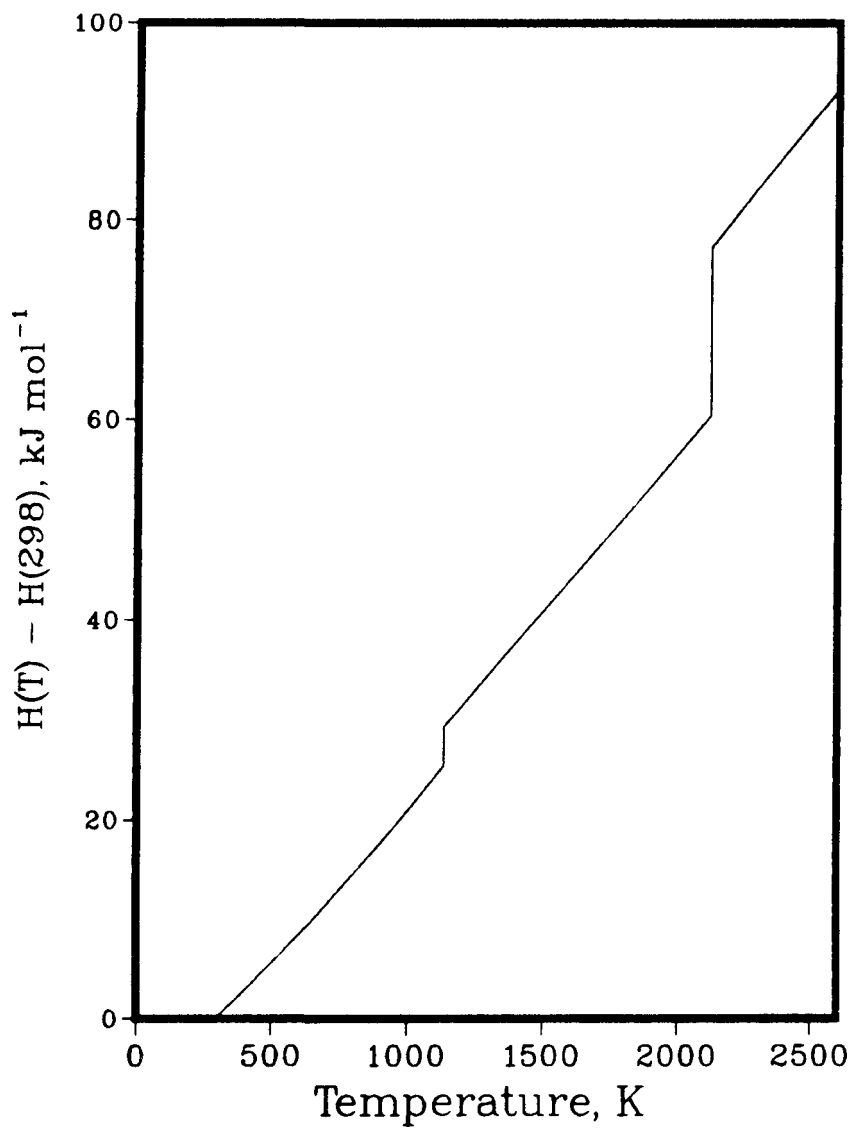


Fig. B.1-8. Enthalpy,  $H(T) - H(298)$   $\text{kJ mol}^{-1}$ , for Zirconium

References for Section B.1

1. G. B. Fedorov and E. A. Smirnov, Thermodynamic Properties of Uranium-Zirconium Alloys, At. Ehnerg. 25, 54 (1968); English translation: Sov. J. At. Energy 25, 795 (1968).
2. P. Chiotti, V. Akhachinskij, I. Ansara, and M. H. Rand, The Chemical Thermodynamics of Actinide Elements and Compounds, Part 5, The Actinide Binary Alloys, International Atomic Energy Agency, Vienna (1981).
3. F. K. Oetting, M. H. Rand, and R. J. Ackermann, The Chemical Thermodynamics of Actinide Elements and Compounds, Part 1, The Actinide Elements, International Atomic Energy Agency, Vienna (1976).
4. R. Hultgren, P. D. Desai, D. T. Hawkins, M. Gleiser, K. K. Kelley, and D. D. Wagman, Selected Values of the Thermodynamic Properties of the Elements, Wiley, New York (1973).
5. G. B. Federov, E. A. Smirnov, N. A. Makhlin, and P. I. Kalinin, Moscow Engineering-Physics Institute, Thermodynamic Properties of Alloys of the Zirconium-Niobium System, At. Ehnerg. 21, 189 (1966), English translation: Sov. J. At. Energy 21, 837 (1966).
6. A. D. Pelton, Calculations of the Liquidus in the Plutonium-Uranium-Zirconium System, Argonne National Laboratory Report ANL-IFR-12 (1985).
7. H. Savage, Heat Content and Heat Capacity of U-15w/oPu-10w/oZr and U-15w/oPu-6w/oTi Alloys, Annual Progress Report for 1966, Metallurgy Division, Argonne National Laboratory Report, ANL-7299, 21-22 (1967).
8. R. J. Dunworth, B. Blumenthal, and O. L. Kruger, Plutonium Physical Properties Laboratory - DL208, Annual Progress Report for 1961, Metallurgy Division, Argonne National Laboratory Report, ANL-6516, 403-407 (1962).
9. G. E. Moore and K. K. Kelley, High Temperature Heat Content of Uranium, Uranium Oxide and Uranium Trioxide, J. Am. Chem. Soc. 69, 2105-7 (1947).
10. D. C. Ginnings and R. J. Corruccini, Enthalpy, Specific Heat and Entropy of Aluminum Oxide from 0° to 900°C, J. Research Nat'l. Bur. Standards 39, 309 (1946).
11. J. M. North, Skull Melting and Centrifugal Casting Experiments on Monocarbide Produced by the Carbothermic Reduction of Uranium Oxide, Carbides in Nuclear Energy 2, Atomic Energy Research Establishment Report, Harwell, Eng., M/R 1016 (1956).

12. H. Savage and R. D. Seibel, Heat Capacity Studies of Uranium and Uranium-Fissium Alloys, Argonne National Laboratory Report, ANL-6702, 27 (1963).
13. E.A. Mit'kina, Experimental Determination of True Specific Heats of Uranium, Thorium, and of Other Metals, Atomnaya Energy 7.5, 163 (1959).
14. L. S. Levinson, Heat Content of Molten Uranium, J. Chem. Phys. 40, 3584 (1964).
15. B. J. Blumenthal, The Transformation Temperatures of High Purity Uranium, J. Nucl. Mat. 2, 23-30 (1960).
16. R. W. Buzzard, R. B. Liss, and D. P. Fickle, Titanium-Uranium System in the Region 0 to 30 Atomic Percent of Titanium, J. Research Nat'l Bur. Standards 50, 209 (1953).
17. M. C. Udy and F. W. Boulger, Uranium-Titanium Alloy System, J. Met. 6, 207-210 (1954).
18. A. I. Dahl and H. E. Cleaves, The Freezing Point of Uranium, J. Research Nat'l. Bur. Standards 43, 513 (1949).
19. R. J. Ackermann and E. G. Rauh, Determination of Liquidus Curves for the Th--W, Th--Ta, Zr--W, and Hf--W Systems: The Anomalous Behavior of Metallic Thorium, High Temp. Sci. 4, 272 (1972).
20. R. J. Ackermann and E. G. Rauh, Measurements of the Solubilities and Derived Thermodynamic Properties of Tungsten and Tantalum in Liquid Thorium and Uranium, High Temp. Sci. 4, 496 (1972).
21. H. P. Stephens, Determination of the Enthalpy of Liquid Copper and Uranium with a Liquid Argon Calorimeter, High Temp. Sci. 6, 156 (1974).
22. W. L. Thayer and J. L. Robbins, Enthalpy and Heat Capacity of Liquid Plutonium and Uranium, Proc. 5th Int. Conf. on Plutonium and Other Actinides, Baden-Baden, Karlsruhe, Germany, (1975).
23. T. K. Engel, Reactor Fuels and Materials Development Plutonium Research, Mound Laboratory Report MLM01347, Miamisburg, Ohio (1967).
24. A. E. Kay and R. G. Loasby, The Specific Heat of Plutonium at High Temperatures, Phil. Mag. 9, 37-49 (1964).
25. T. A. Sandenaw and R. B. Gibney, Heat Capacity and Derived Thermodynamic Functions of  $^{242}\text{Pu}$ , J. Chemical Thermodynamics 3, 85 (1971).
26. J. C. Taylor, Atomic Weapons Research Establishment (British), Aldermaston, private communication to F. L. Oetting, M. H. Rand, and R. J. Ackermann (1966).

27. F. L. Oetting, Half-life of  $^{239}\text{Pu}$  by Calorimetry, Proc. 4th Int. Conf. on Plutonium and Other Actinides, Sante Fe, NM, Met. Soc., New York, 154, (1970).
28. J. C. Taylor, P. F. T. Linford, and D. J. Dean, Low-temperature Elastic Constants and Specific Heats of Some Delta-Phase Plutonium-Gallium Alloys, J. Inst. Metals 96, 178-82 (1968).
29. R. L. Rose, J. L. Robbins, and T. B. Massalski, Heat Content and Heat Capacity of a Pu/1 wt Percent Ga Delta-stabilized Alloy at Elevated Temperatures, J. Nucl. Mater. 36, 99-107 (1970).
30. R. G. Loasby, Discussion of Papers, Proc. 2nd Int. Conf. Plutonium Metallurgy, Grenoble, 97 (1960).
31. A. Goldberg and T. B. Massalski, Phase Transformation in the Actinides, Proc. 4th Int. Conf. Plutonium and Other Actinides, Sante Fe, NM, Metallurgical Society, 875 (1970).
32. C. Prunier, C. Roux, and M. Rapin, Compared Study of the Plutonium Transformation Heats as Determined by Enthalpic Analysis and by the Use of High Pressure, Proc. 4th Int. Conf. Plutonium and Other Actinides, Santa Fe, NM, Met. Soc., New York, 1001 (1970).
33. J. W. Anderson, Studies on the Equilibrium of Temperature for the Alpha-Beta Transformation, 3rd Int. Conf. on Plutonium, London, Institute of Metals, (1967).
34. T. K. Engel, K.C. Jordan, D. M. Scott, and G. W. Otto, A High Temperature Calorimeter for Thermal Property Measurements of Plutonium Metal, US Atomic Energy Commission Report, TID-7641 (1962).
35. J. D. Hill, Exploring the Transformation Behaviour of the Allotropes of Plutonium, J. Less-Common Metals 4, 376 (1962).
36. E. M. Cramer, L. L. Hawes, W. N. Miner, and F. W. Schonfeld, The Dilatometry and Thermal Analysis of Plutonium Metal, The Metal Plutonium, A.S. Coffinberry and W. N. Miner, eds., University of Chicago Press, Chicago, IL, 112 (1961).
37. R. Abramson, A Dilatometric Study of Plutonium, The Metal Plutonium, A. S. Coffinberry and W. N. Miner, eds., University of Chicago Press, Chicago, IL, 123 (1961).
38. J. A. Lee and P. G. Mardon, Some Physical Properties of Plutonium Metal Studied at Harwell, The Metal Plutonium, A. S. Coffinberry and W. N. Miner, eds, University of Chicago Press, Chicago, IL, 133 (1961).

39. R. Pascard, Study by Thermal Analysis of Allotropic Transformations of Plutonium, Acta Metallurgica 7, 305 (1959).
40. T.A. Sandenaw and R. B. Gibney, The Electrical Resistivity and Thermal Conductivity of Plutonium Metal, J. Phys. Chem. Solids 6, 81 (1958).
41. S. T. Konobeevsky, et al., Some Physical Properties of Uranium, Plutonium and Their Alloys, Peaceful Uses of Atomic Energy, Proc. 2nd Int. Conf., Geneva, United Nations, 6 194-203, (1958).
42. D. J. Dean, A. E. Kay, and R.G. Loasby, Note on the Specific Heat of Plutonium Metal, J. Inst. Metals 86, 464 (1958)
43. E. R. Jette, Some Physical Properties of Plutonium Metal, J. Chem. Phys. 23, 365 (1955).
44. T. B. Douglas and A. C. Victor, Heat Content of Zirconium and of Five Compositions of Zirconium Hydride from 0 to 900°C, J. Research Nat'l Bur. Standards 61, 13 (1958).
45. F. M. Jaeger and W. A. Veenstra, Rec. Trav. Chim. 53, 13 (1958).
46. I. B. Fieldhouse and J. I. Lang, Measurement of Thermal Properties, WADD Technical Report 60-904, Armour Research Foundation (1961).
47. R. F. Redmond and J. Lones, Enthalpies and Heat Capacities of Stainless Steel (316), Zirconium, and Lithium at Elevated Temperatures, Oak Ridge National Laboratory Report ORNL-1342 (1952).
48. G. B. Skinner, Thermodynamic and Structural Properties of Zirconium Ph. D. Thesis, Dissertation Abstracts International Chemistry, Physical, 18/05, Ohio State University, 1646 (1951).
49. J. P. Coughlin and E. G. King, High-temperature Heat Contents of Some Zirconium-containing Substances, J. Am. Chem. Society 72, 2262 (1950).
50. A. H. Klein and G. C. Danielson, Specific Heat of Zirconium by a Pulse Heating Method, Proc. Black Hills Summer Conf. on Transport Phenom., South Dakota School of Mines and Tech., Rapid City, A4, 47 (1962).
51. J. L. Scott, A Calorimetric Investigation of Zirconium, Titanium, and Zirconium Alloys from 60 to 960°C, Oak Ridge National Laboratory Report ORNL-2328, (1957).
52. S. D. Gertsriken and B. P. Ukrain, Fiz. Zhur. 7, 439 (1962).

**Section B.1**

**Enthalpy and Heat Capacity**

**Section B.2**

**Phase Equilibria**

## B. THERMODYNAMICS

### B.2 Phase Equilibria\*

#### B.2.1 Uranium-Zirconium Alloys (and Other Binary Systems)

U-Zr: The uranium-zirconium phase diagram, as shown in Fig. B.2-1, was taken from [9]. Only one intermediate phase,  $\delta$ , exists in this system. It is unstable above 890 K. The body-centered cubic forms of uranium ( $\gamma$ ) and zirconium ( $\beta$ ) are completely miscible. The  $\alpha$ -phase has a composition range of 67-73 at.% Zr. Its crystal structure appears to be uncertain and has been described as simple hexagonal, body-centered cubic, or hexagonal--isotypic with  $\text{InNi}_2$  [10].

U-Pu: Figure B.2-2 shows the U-Pu phase diagram, taken from Ref. 9. The diagram indicates that although there is agreement on its general form, precise values for the phase limits as a function of temperature are still not well established. There are two phases in addition to the nine allotropes of the end members: a  $\zeta$ -phase, extending from about 25 to 70 at.% U, and a tetragonal  $\eta$ -phase which is stable only between 551 and 978 K, from about 5 to 70 at.% U. The  $\zeta$ -phase is described as "cubic (at 300 K)" in Ref. 9 and as tetragonal in Ref. 10. Note that Pu( $\epsilon$ ) and U( $\gamma$ ) form a continuous solid-solution region although this solid solution is stable over a range of only about 20 K between 25 and 45 at.% U.

Pu-Zr: The Pu-Zr phase diagram, shown in Fig. B.2-3, was taken from Elliot [11]. Note that in this diagram temperatures are given in  $^{\circ}\text{C}$  rather than in K as in the other two binary diagrams. Elliot describes the Pu-Zr system as having the following features: continuous solid solubility between Pu ( $\epsilon$ ) and Zr ( $\beta$ ), with a constantly

---

\* The reference list for Section B.2 is on page B.2-36.

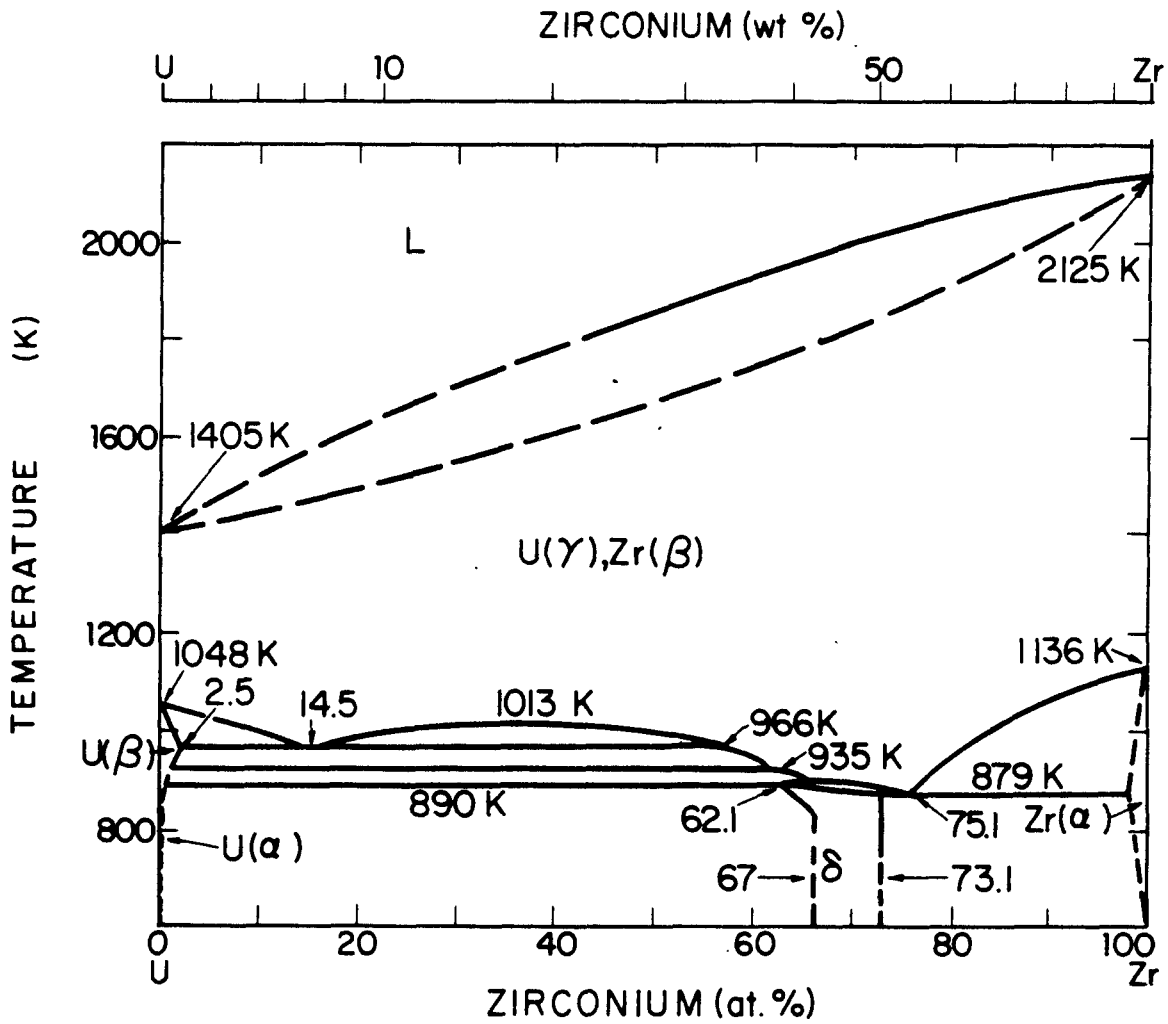


Fig. B.2-1. Phase Diagram of the System Uranium-Zirconium

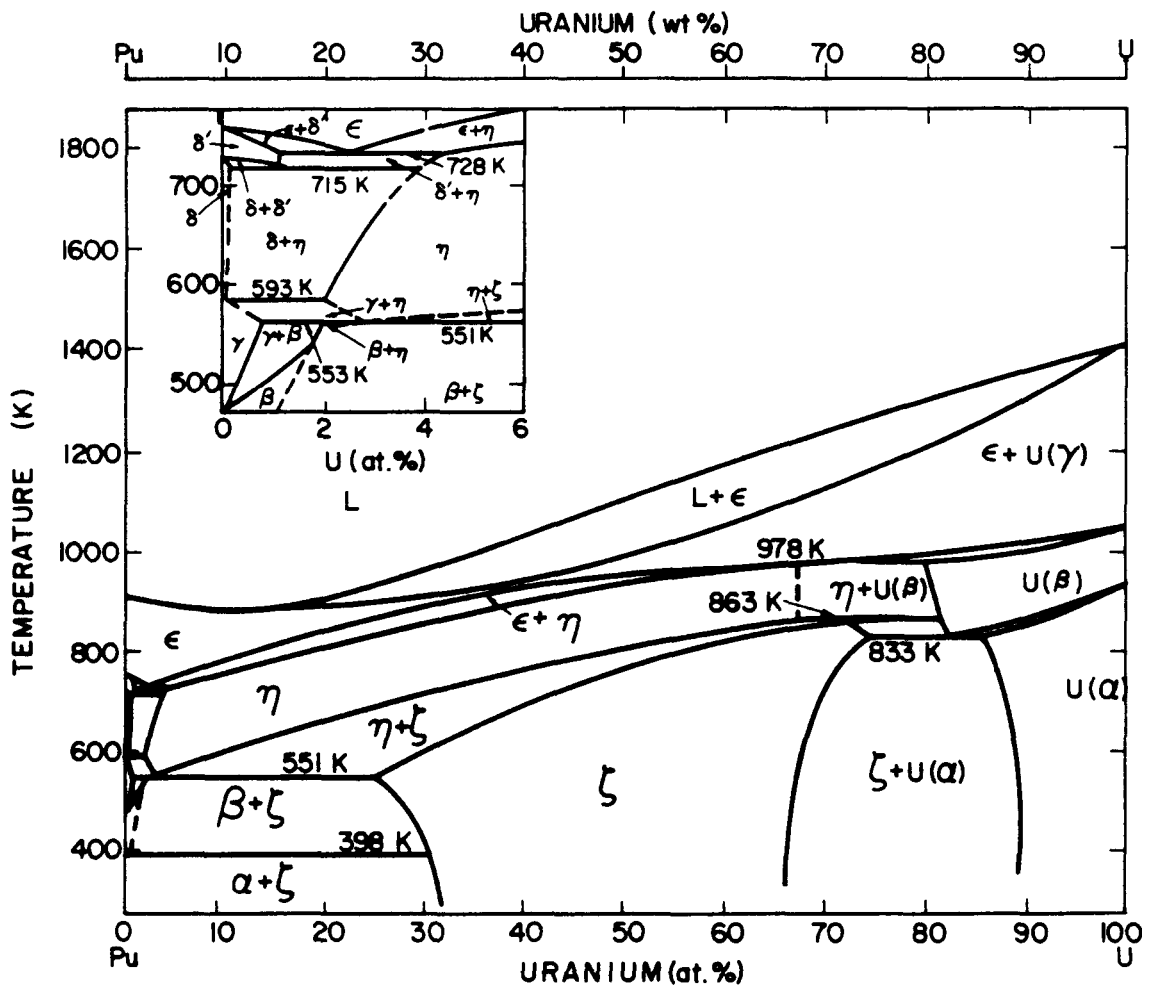


Fig. B.2-2. Phase Diagram of the System Plutonium-Uranium

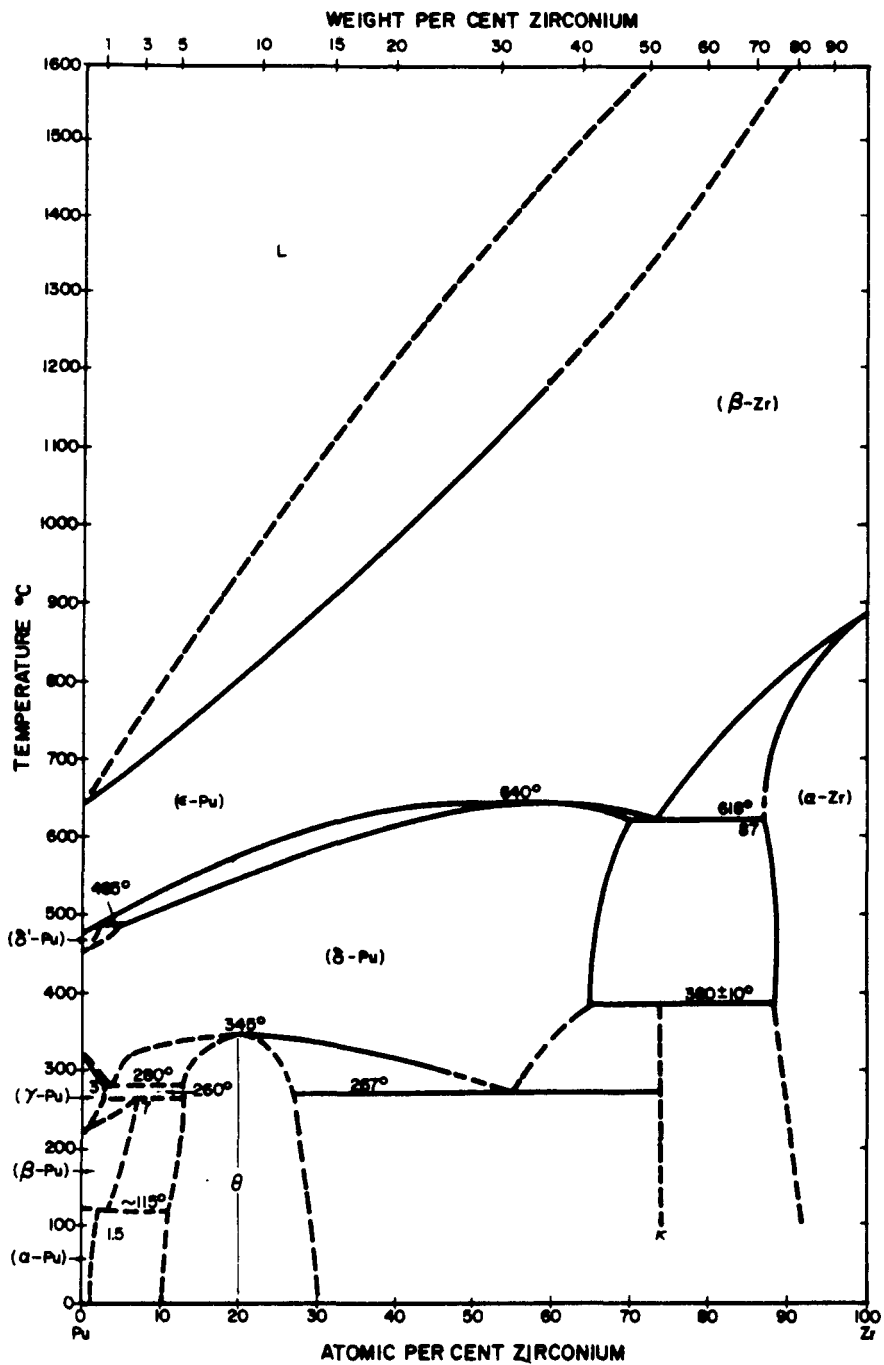


Fig. B.2-3. Phase Diagram of the Plutonium-Zirconium System

rising solidus from Pu to Zr; two intermediate phases; an extended Pu ( $\delta$ ) solid-solution field (to about 70 at.% Zr) which gives rise to two eutectoids; and a rather large Zr ( $\alpha$ ) solid-solution field (13-15 at.% Pu). The two intermediate phases are  $\text{Pu}_6\text{Zr}$  and  $\text{PuZr}_2$ . These are believed to be, respectively, orthorhombic and hexagonal.

## B.2.2 Uranium-Plutonium-Zirconium Alloys

Solid-state Transitions: A detailed study of solid-state transitions in the ternary system performed at Argonne National Laboratory was reported by O'Boyle and Dwight [1]. A study of the system was performed by the Mound Laboratory [3] with emphasis on melting in the plutonium corner of the phase diagram. Some early measurements on phase transitions in the solid state were reported by CEA [12] and by Argonne [13].

The following description of the phases in the ternary system is taken from [1]. The same nomenclature is used to identify both the binary and the ternary phases. The following are the phases existing in the ternary alloy.

- $\gamma$ : Body-centered cubic phase showing complete miscibility for U( $\gamma$ ), Pu( $\epsilon$ ), and Zr( $\beta$ ). The designations  $\gamma_1$  and  $\gamma_2$  are used in [1] for uranium-rich and zirconium-rich modifications of the  $\gamma$  phase.
- $\alpha, \beta$ : Orthorhombic and tetragonal uranium allotropes dissolving up to 15 and 20 at.% Pu respectively, but little Zr.
- $\eta$ : Tetragonal intermediate phase in the U-Pu binary with limited solubility for Zr.
- $\zeta$ : Tetragonal intermediate phase in the U-Pu system with up to 5 at.% solubility for Zr. This is referred to in [1] as a cubic phase but is likely tetragonal [7].
- $\delta$ : Hexagonal phase in the U-Zr system with extensive solid solubility for Pu.

Pu ( $\delta$ ): Face-centered cubic Pu phase with extensive solid solubility for Zr but very limited solubility for U.

The phase relations given in [1] are shown in Figs. B.2-4a through -4i, in which isothermal sections are shown ranging from 700 down to 500°C. Below the solidus temperature the three elements show complete miscibility of the body-centered cubic high-temperature allotropes U ( $\gamma$ ), Pu ( $\epsilon$ ), Zr ( $\beta$ ). The body-centered cubic  $\gamma$ -phase is stabilized by additions of zirconium and plutonium. With decreasing temperatures from 700 to 600°C, the gamma single-phase boundary sweeps rapidly from the U-Zr and U-Pu binary sides of the system toward the Zr-Pu side of the system. The major four-phase reactions in the uranium corner of the system are  $\gamma + \beta \rightarrow \alpha + \zeta$  at 650°C and  $\gamma + \alpha \rightarrow \delta + \zeta$  at 595°C. These reactions may be involved in the zone formation observed on heating the ternary alloy in thermal gradients [14,15].

Solidus-Liquidus: Calculations of the solidus and liquidus surfaces for the ternary U-Pu-Zr system have been performed by Dr. Arthur D. Pelton, McGill University, Ecole Polytechnique, using the system "Facility for the Analysis of Chemical Thermodynamics" (F\*A\*C\*T) [8]. These calculations were performed using the best available data and models but are estimates and should be used with due caution. Data for the three binary systems were critically evaluated and used to calculate thermodynamic properties for the ternary system. From these data ternary phase diagrams were calculated. Error limits on the binary and ternary solidus and liquidus curves were estimated. Activity coefficients for all three components of the ternary system were calculated for solutions near the melting region. In the figures that follow (B.2-5 through -18) isothermal sections are presented showing solidus and liquidus curves from 700-1700°C. Near the median of the composition triangle, error limits are estimated as  $\pm 75^\circ$  for the liquidus and  $\pm 125^\circ$  for the solidus.

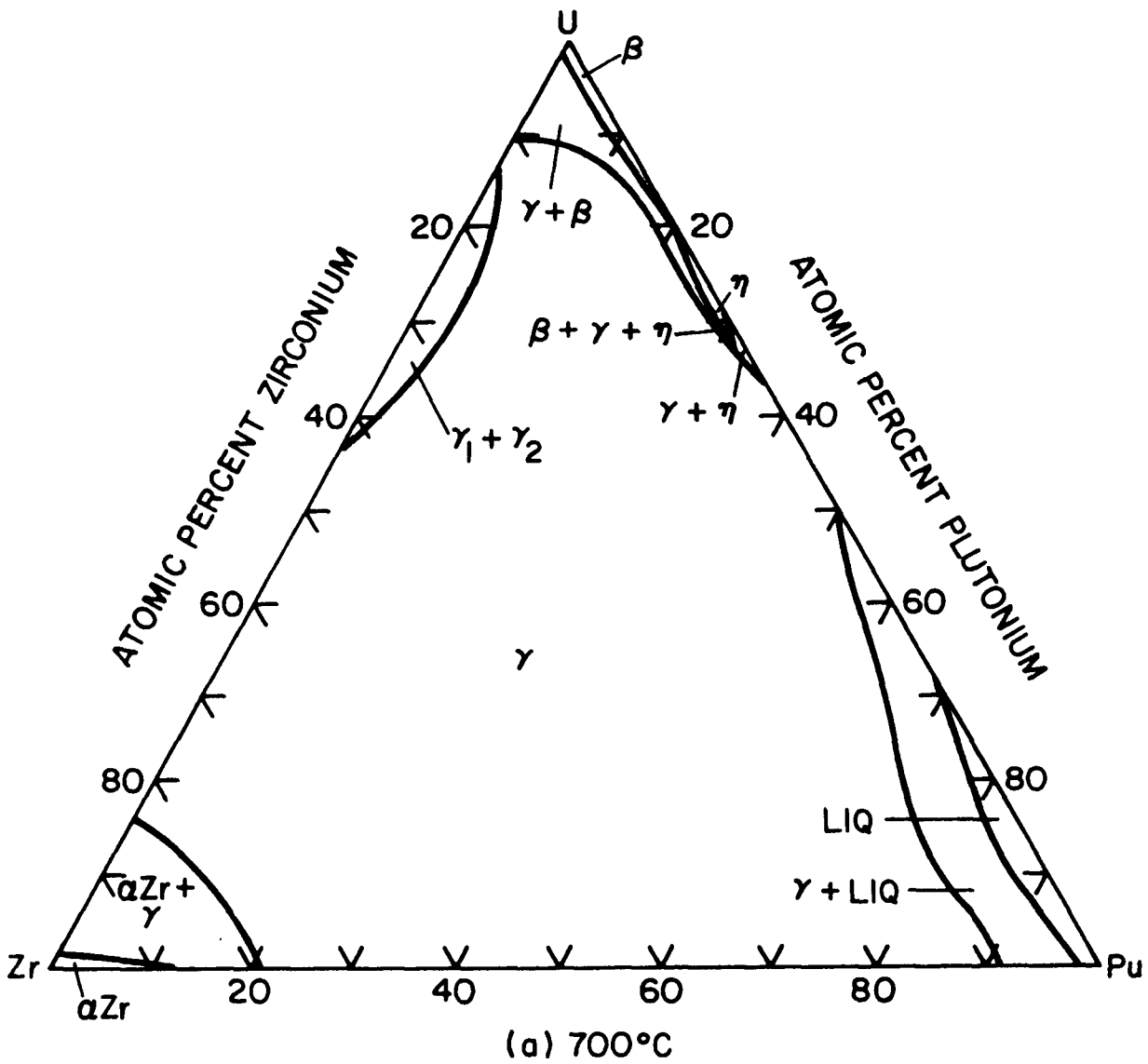


Fig. B.2-4a. Uranium-Plutonium-Zirconium Phase Diagram

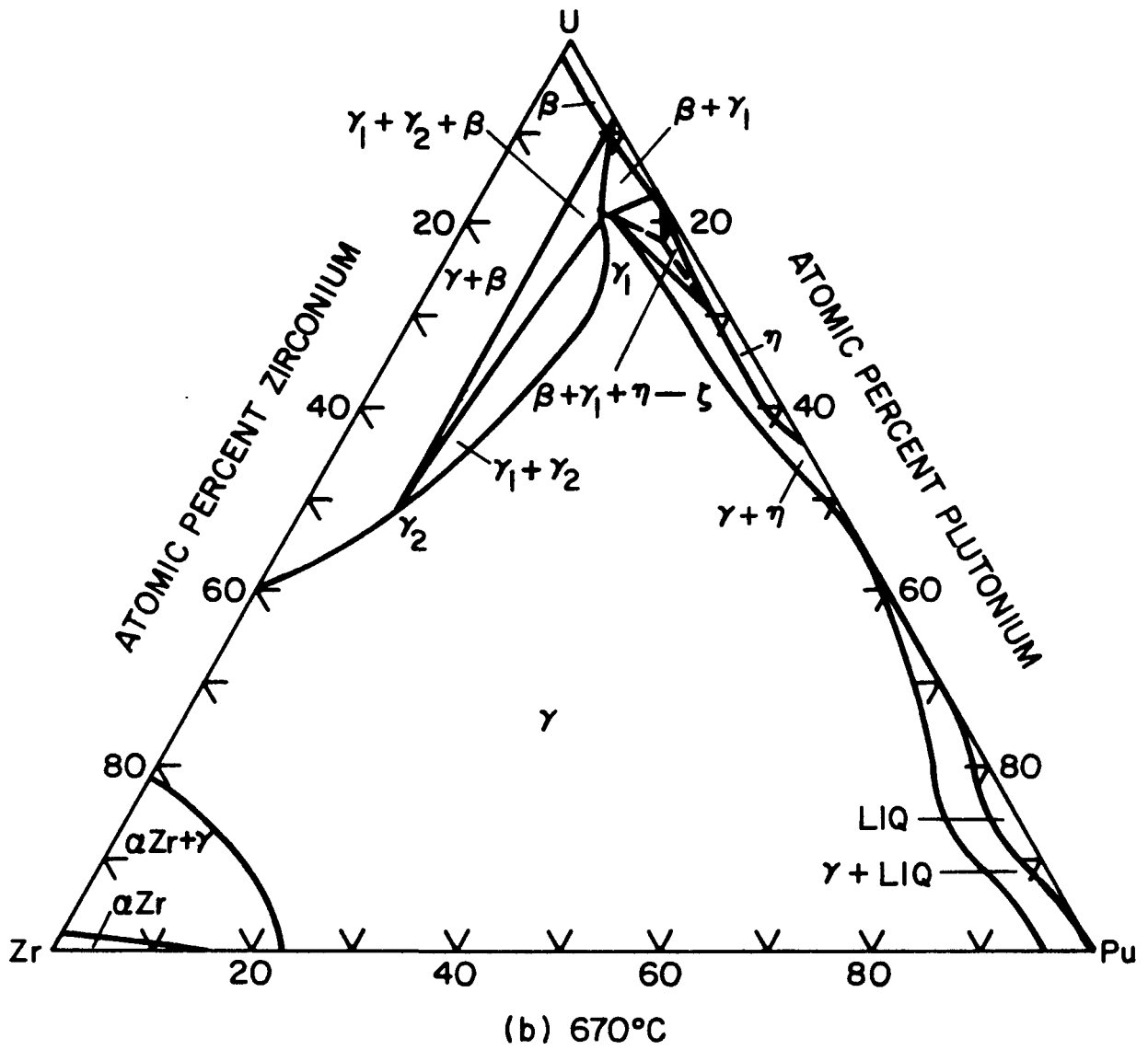


Fig. B.2-4b. Uranium-Plutonium-Zirconium Phase Diagram



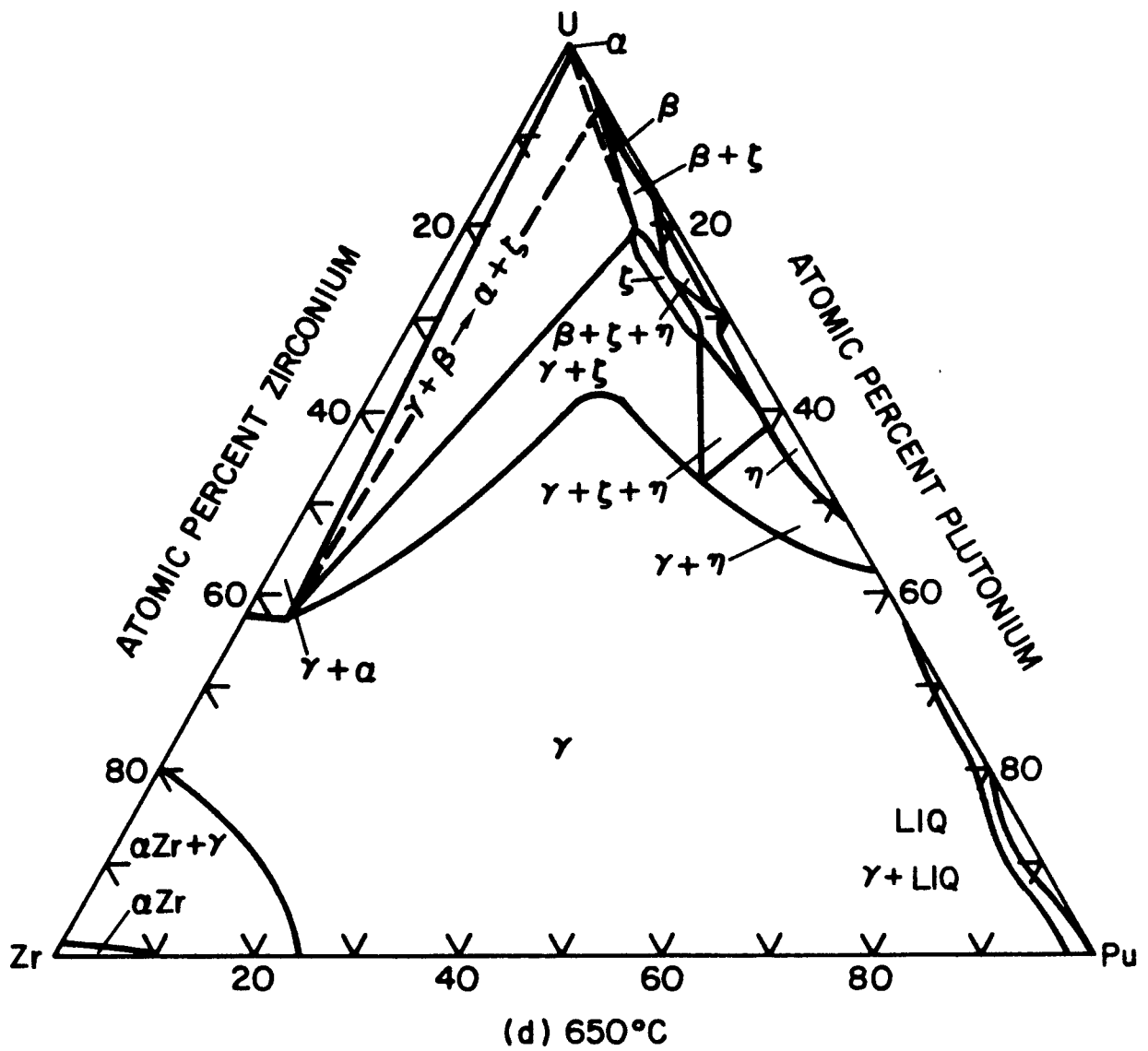


Fig. B.2-4d. Uranium-Plutonium-Zirconium Phase Diagram

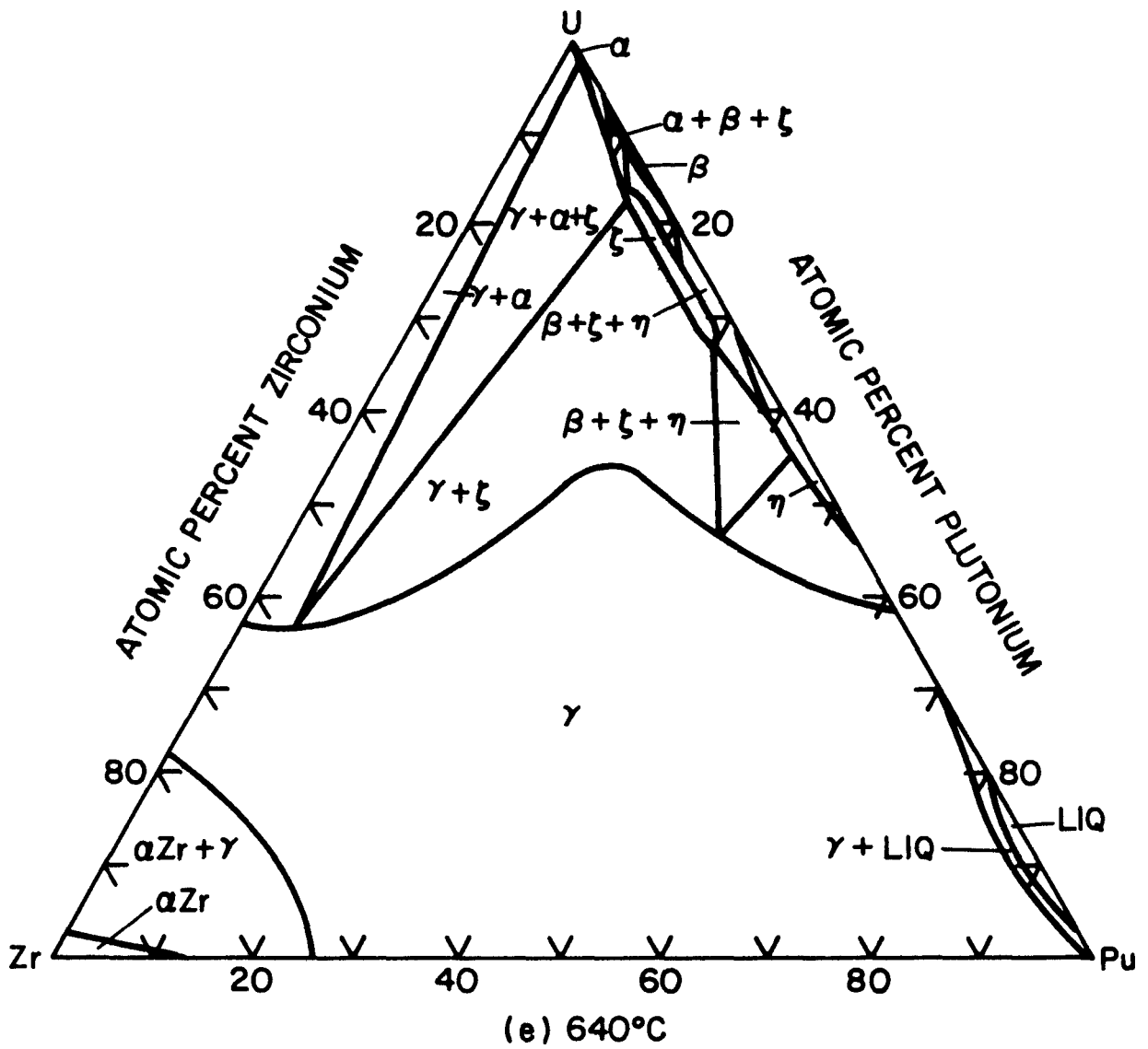


Fig. B.2-4e. Uranium-Plutonium-Zirconium Phase Diagram

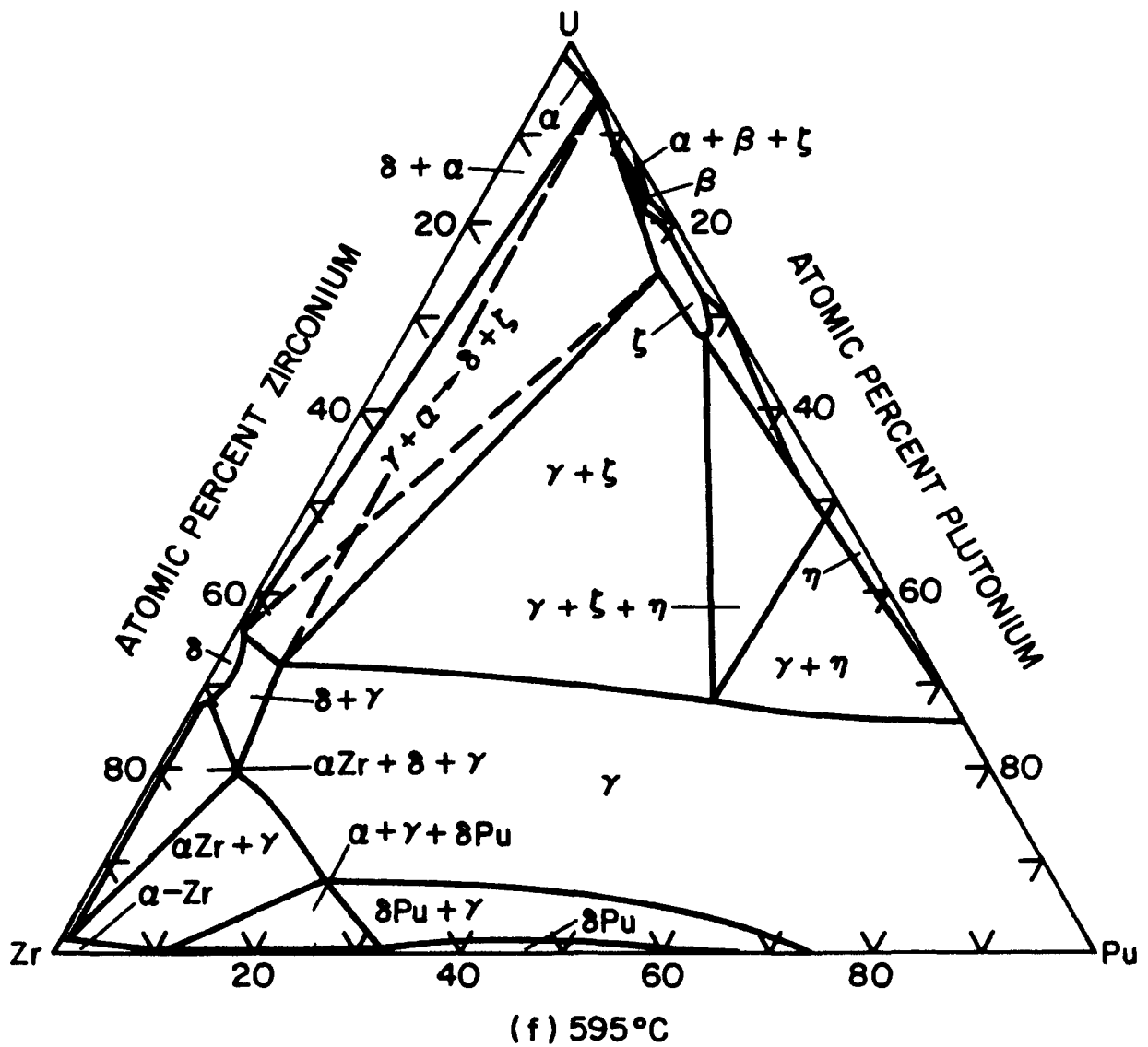


Fig. B.2-4f. Uranium-Plutonium-Zirconium Phase Diagram

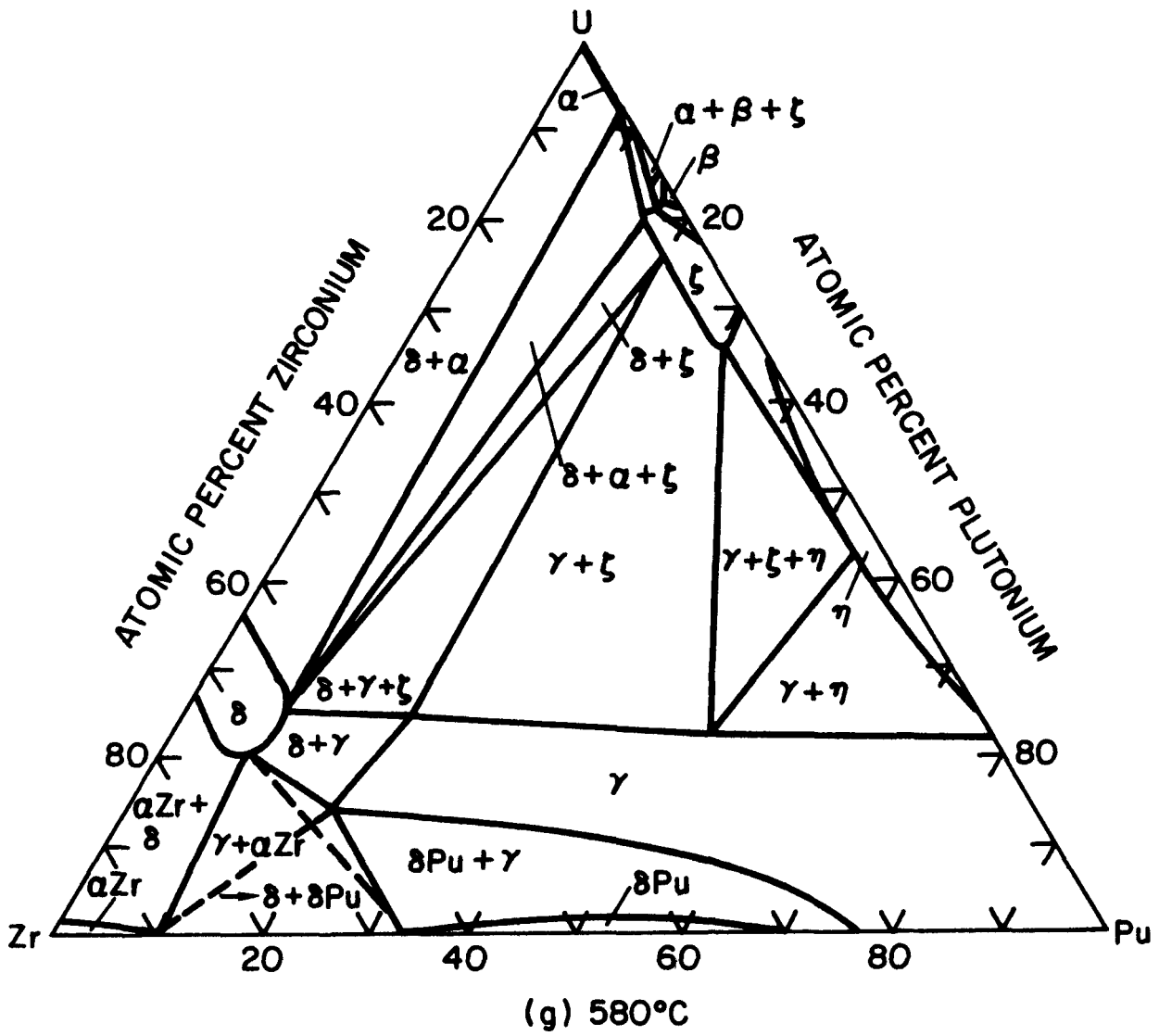


Fig. B.2-4g. Uranium-Plutonium-Zirconium Phase Diagram

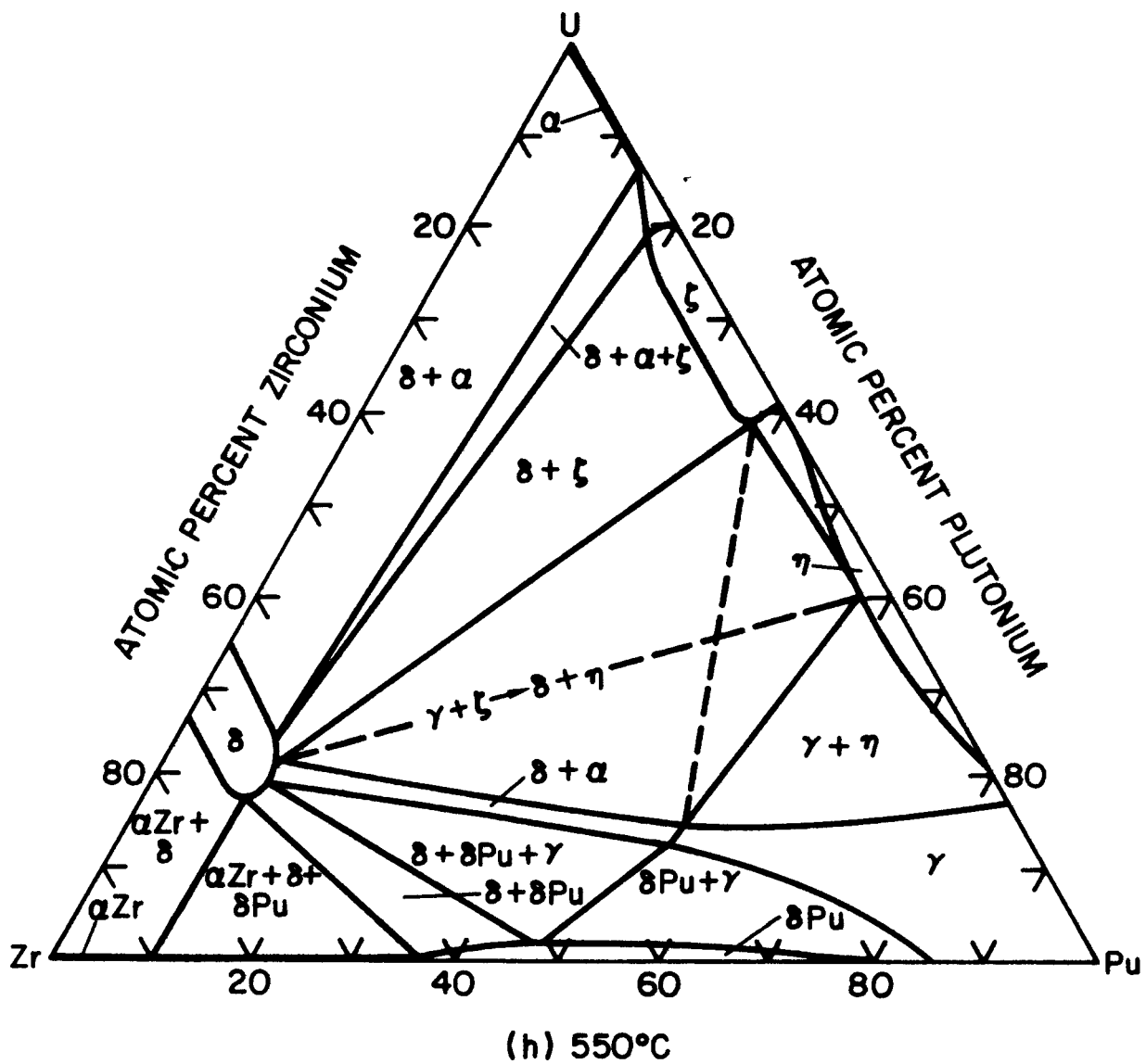


Fig. B.2-4h. Uranium-Plutonium-Zirconium Phase Diagram

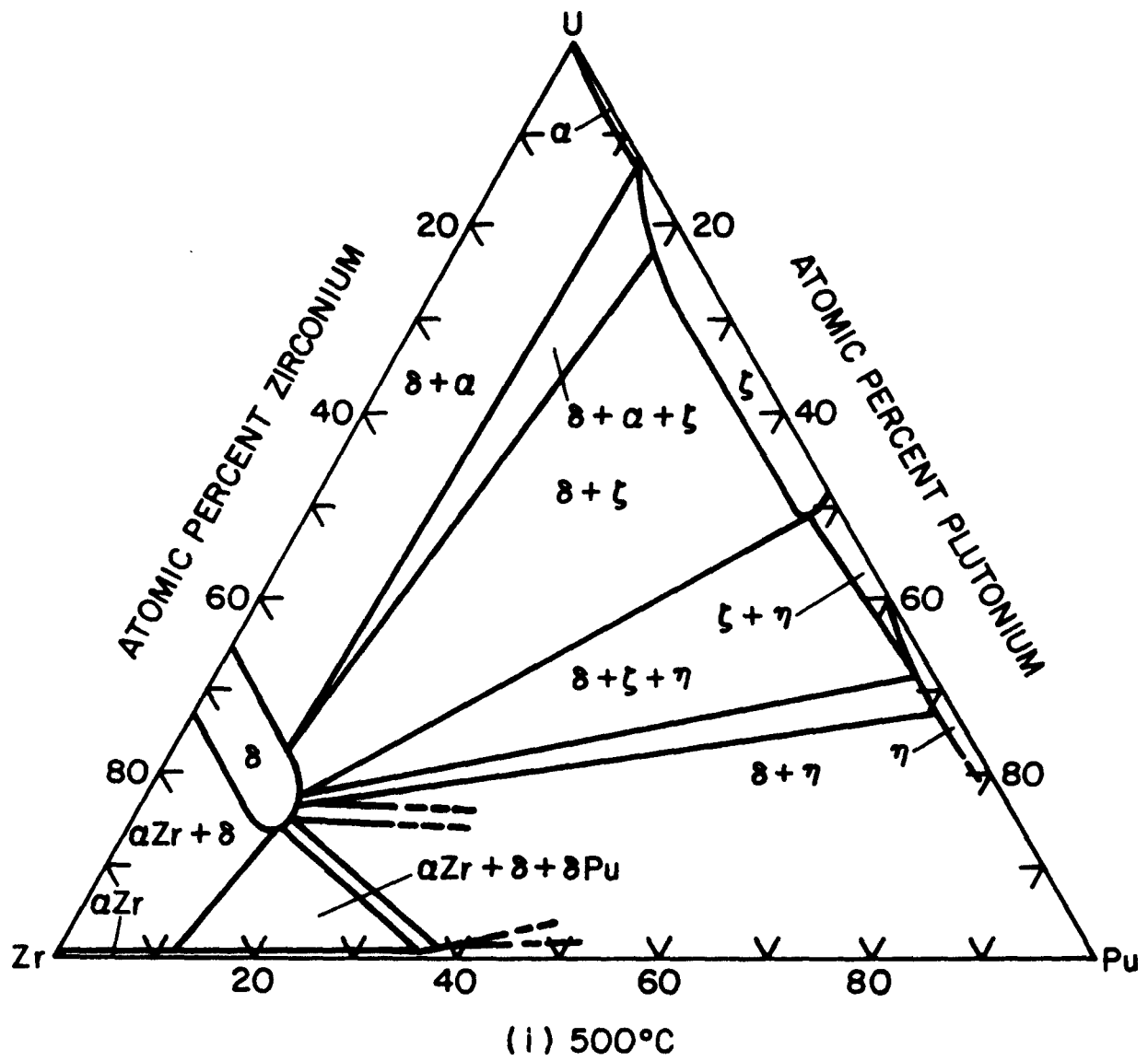


Fig. B.2-4i. Uranium-Plutonium-Zirconium Phase Diagram

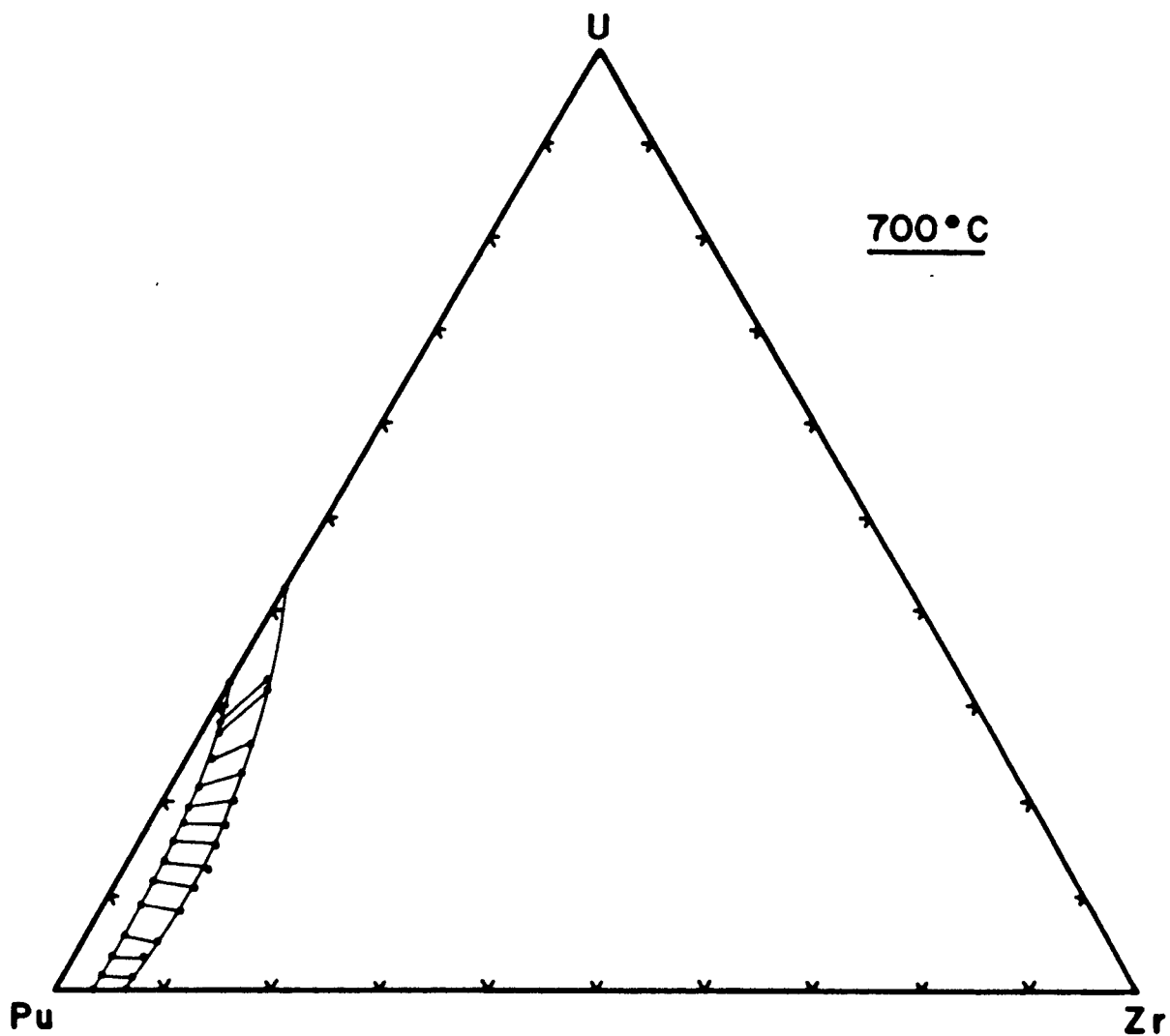


Fig. B.2-5. Calculated Section of the Pu-U-Zr  
Phase Diagram (mol %); 700°C

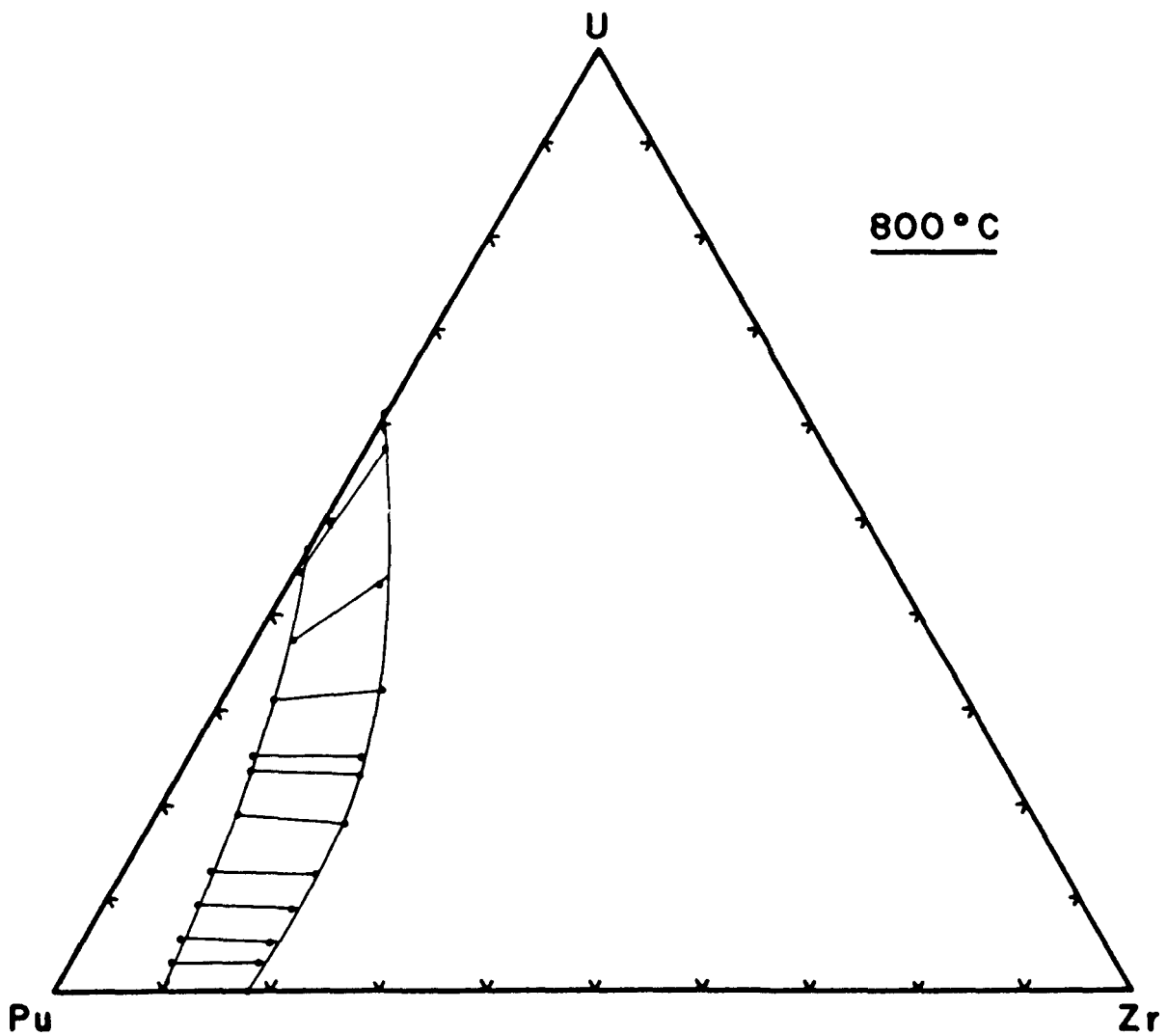


Fig. B.2-6. Calculated Section of the Pu-U-Zr  
Phase Diagram (mol %); 800°C

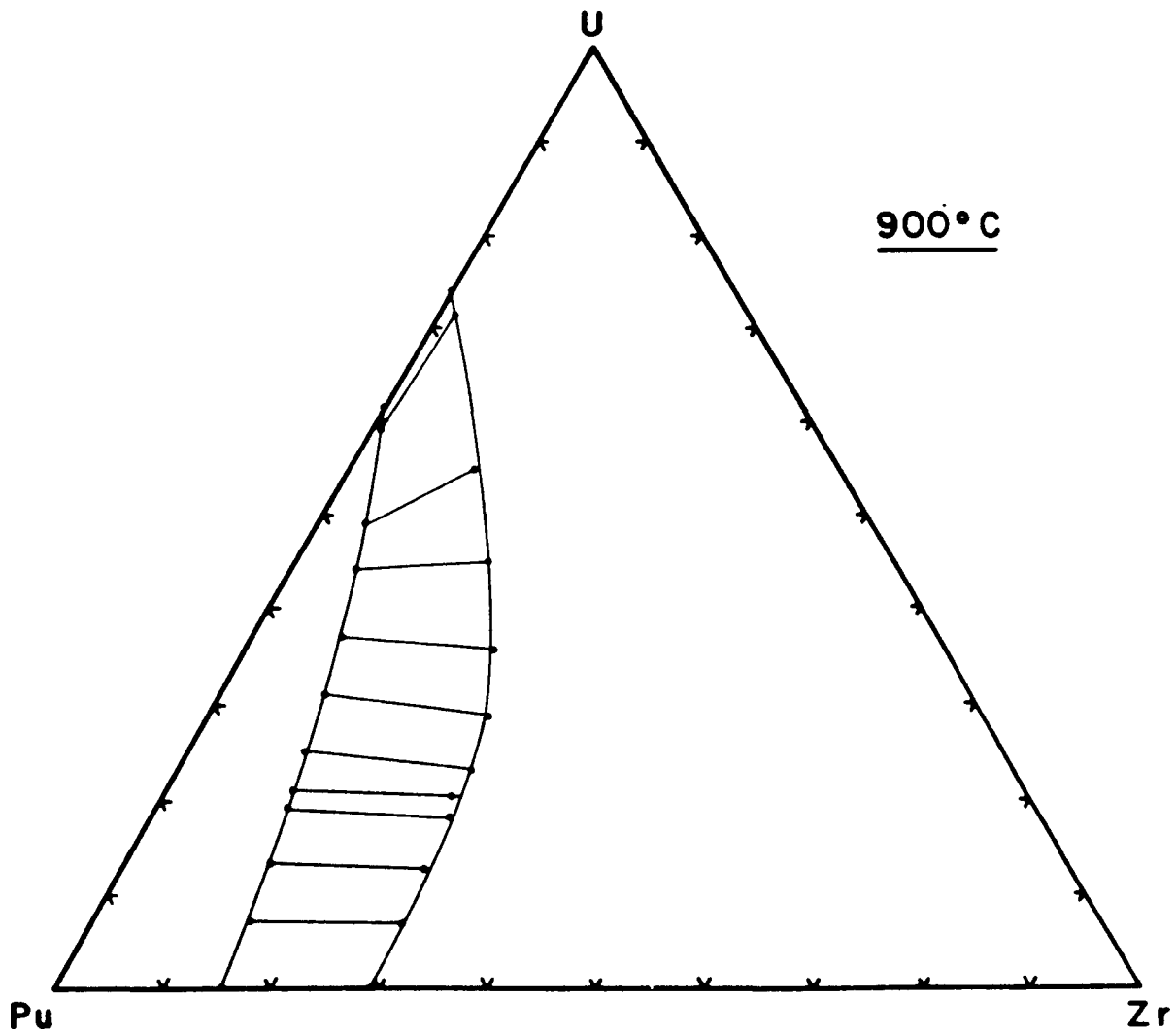


Fig. B.2-7. Calculated Section of the Pu-U-Zr  
Phase Diagram (mol %); 900°C

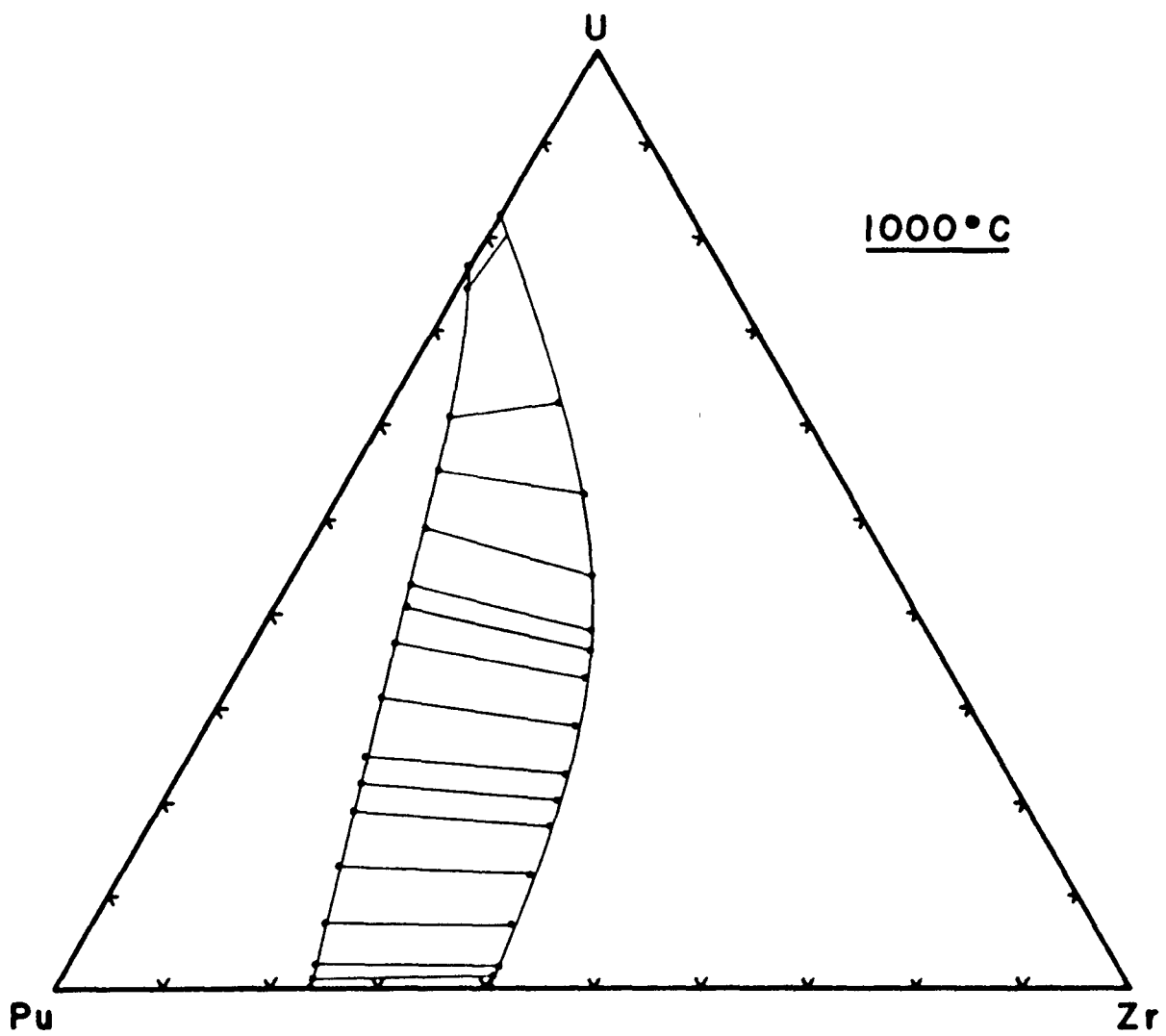


Fig. B.2-8. Calculated Section of the Pu-U-Zr  
Phase Diagram (mol %); 1000°C

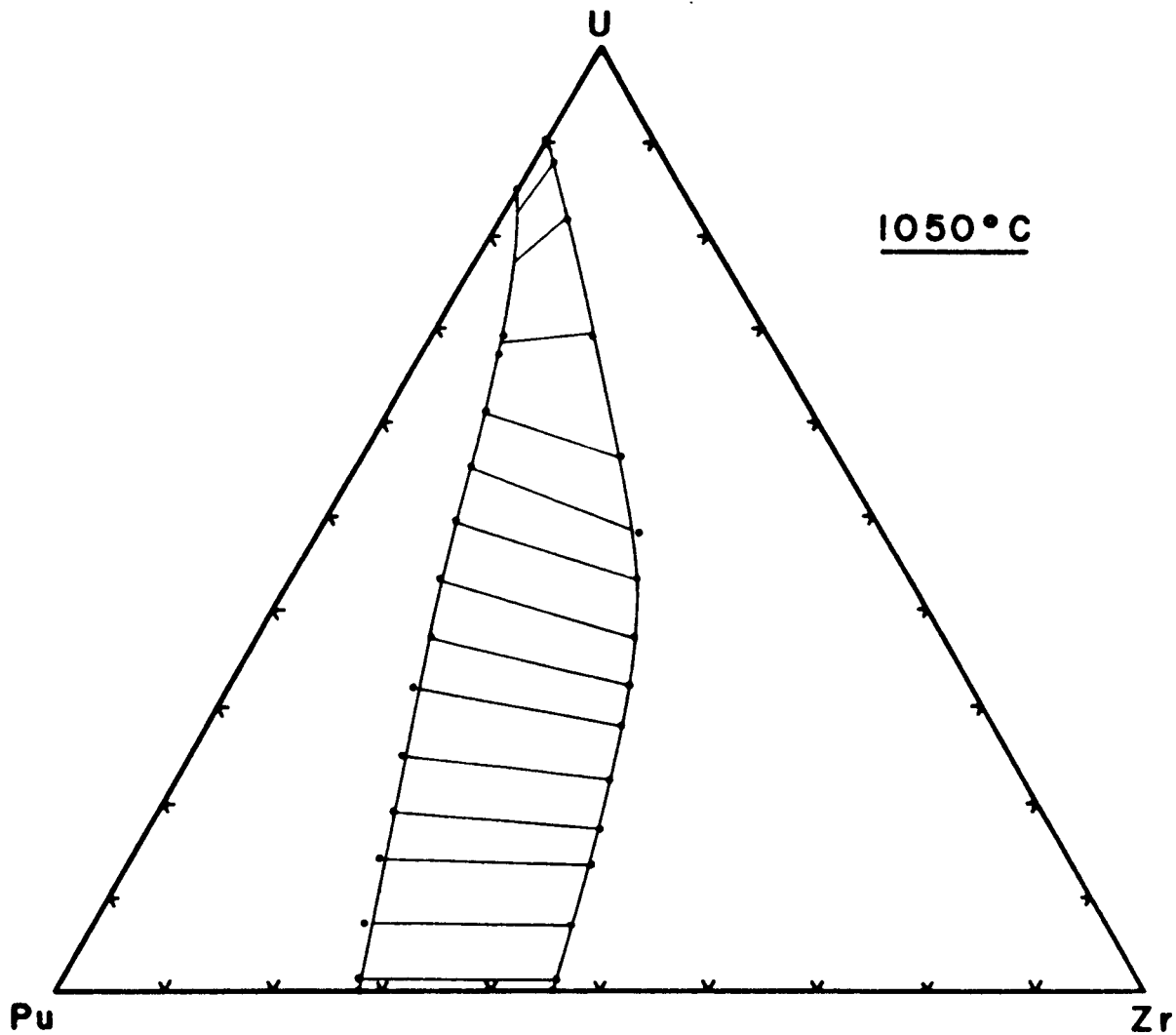


Fig. B.2-9. Calculated Section of the Pu-U-Zr  
Phase Diagram (mol %); 1050°C

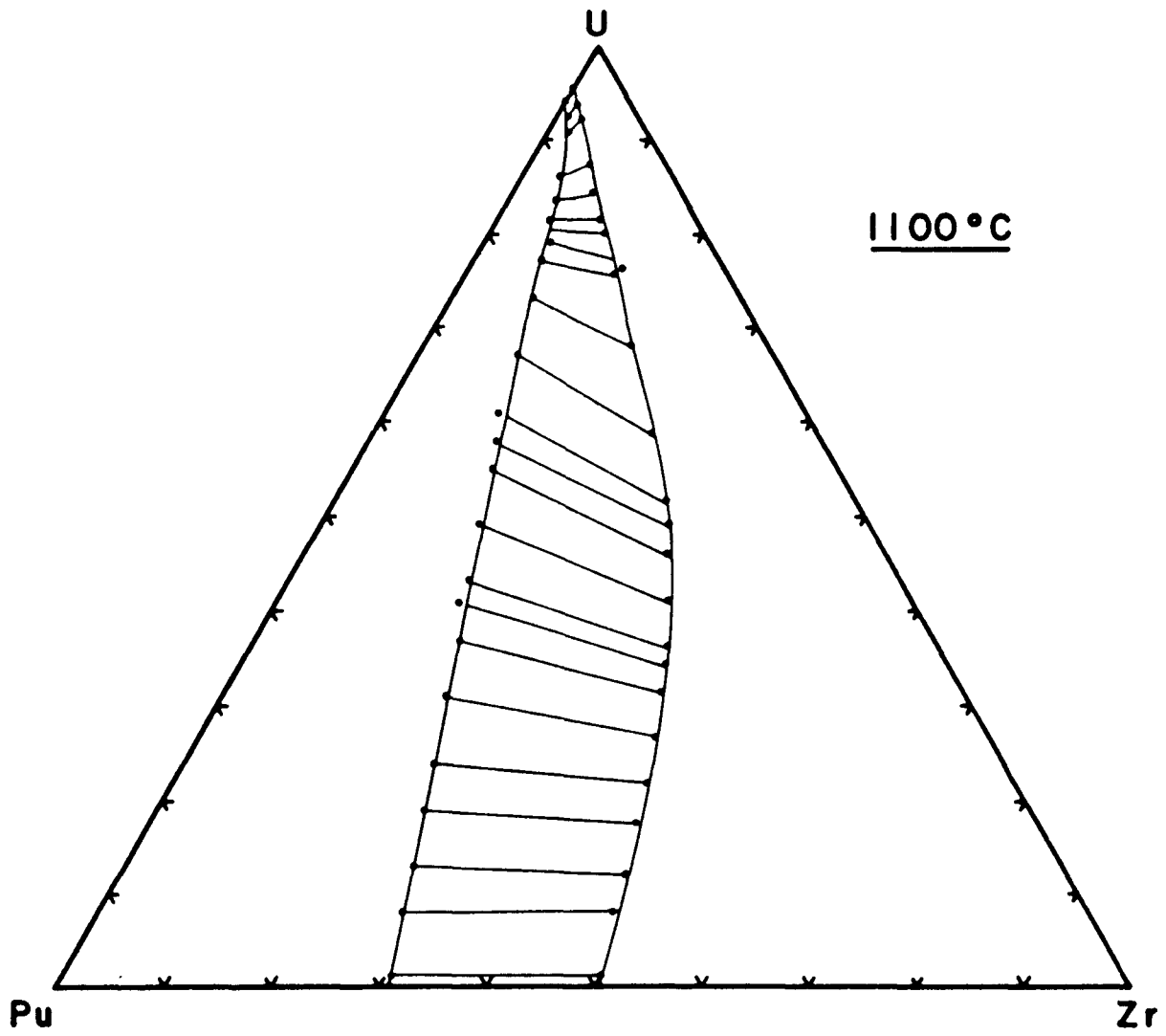


Fig. B.2-10. Calculated Section of the Pu-U-Zr Phase Diagram (mol %); 1100°C

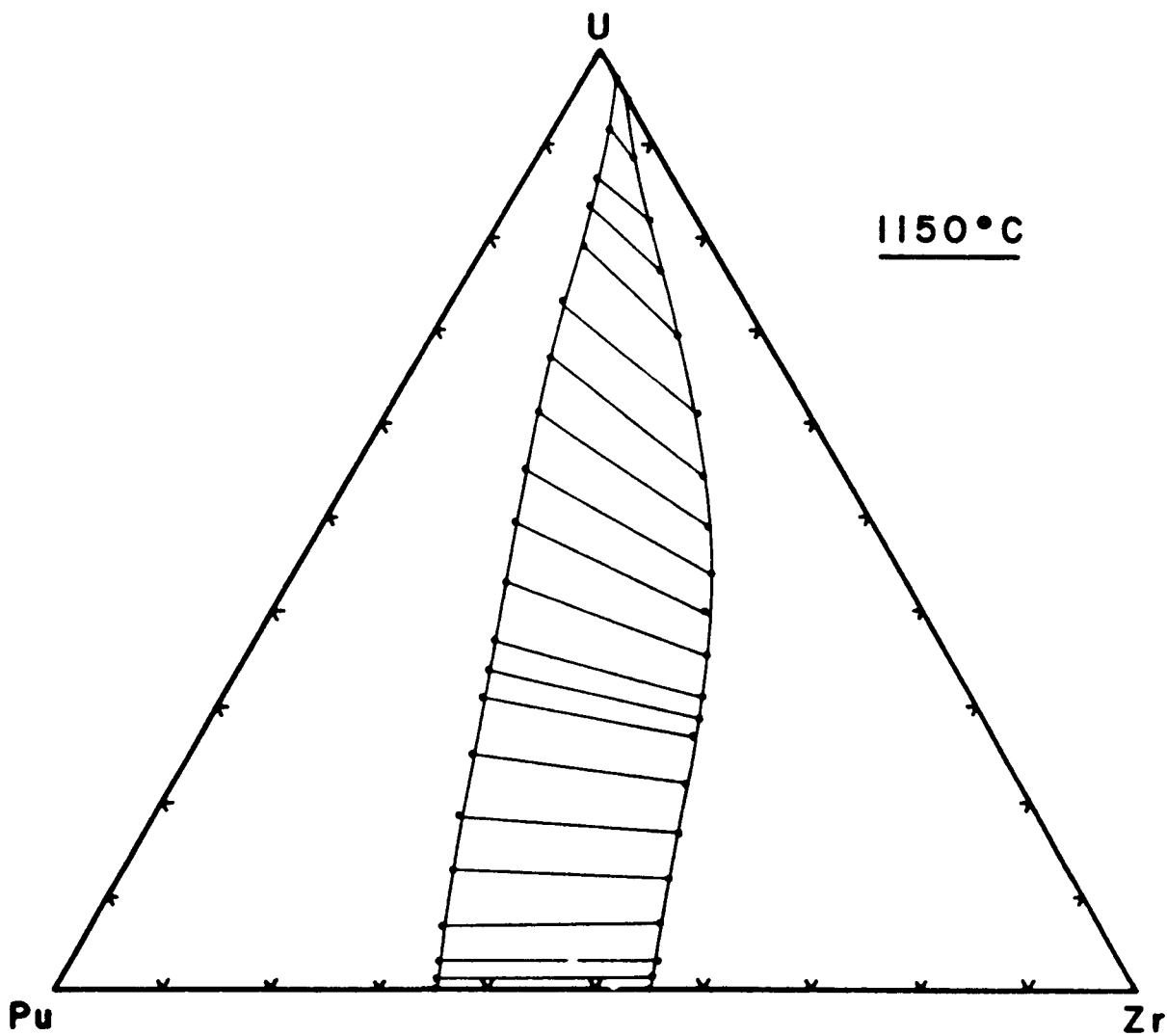


Fig. B.2-11. Calculated Section of the Pu-U-Zr Phase Diagram (mol %); 1150°C

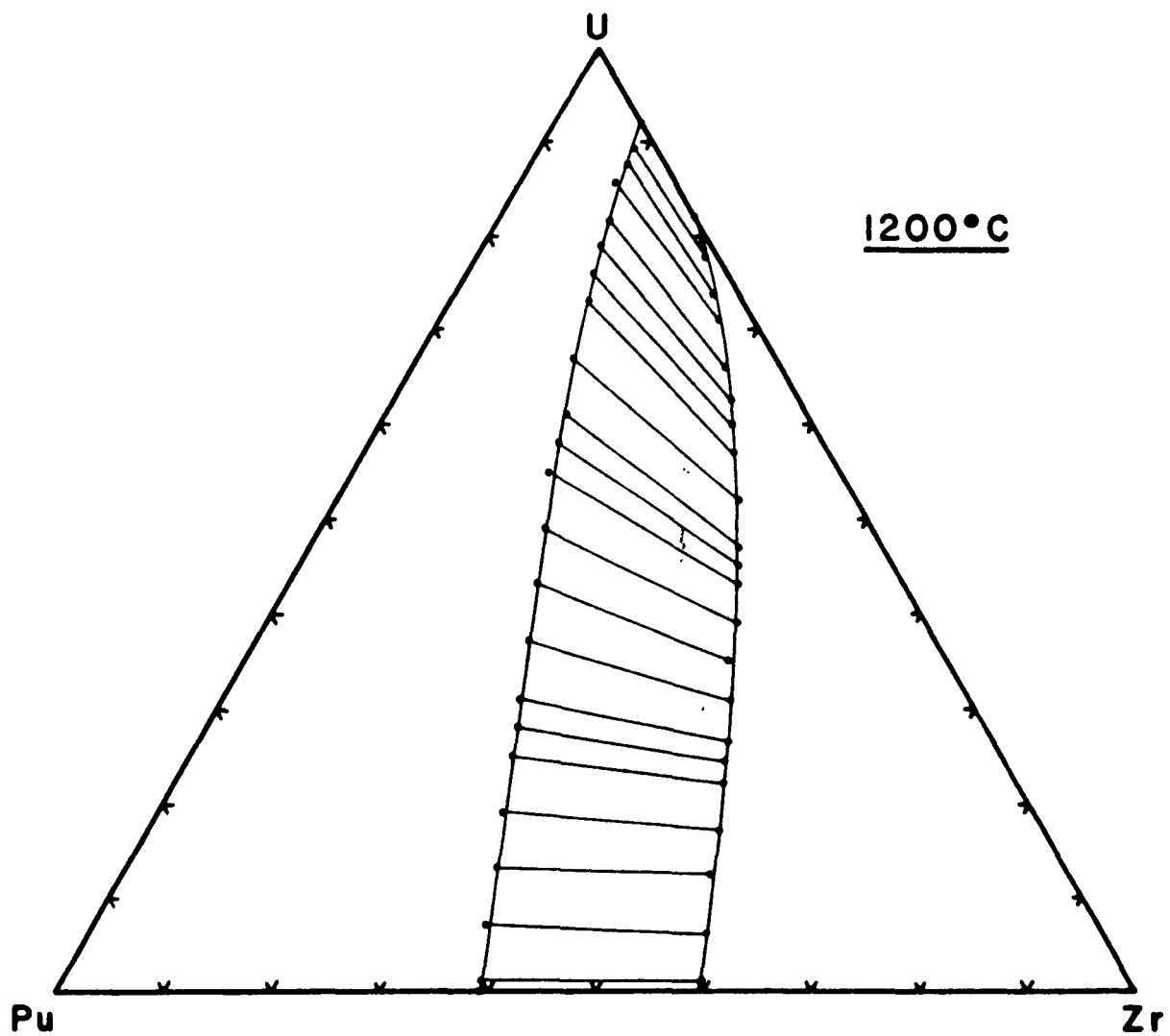


Fig. B.2-12. Calculated Section of the Pu-U-Zr  
Phase Diagram (mol %); 1200°C

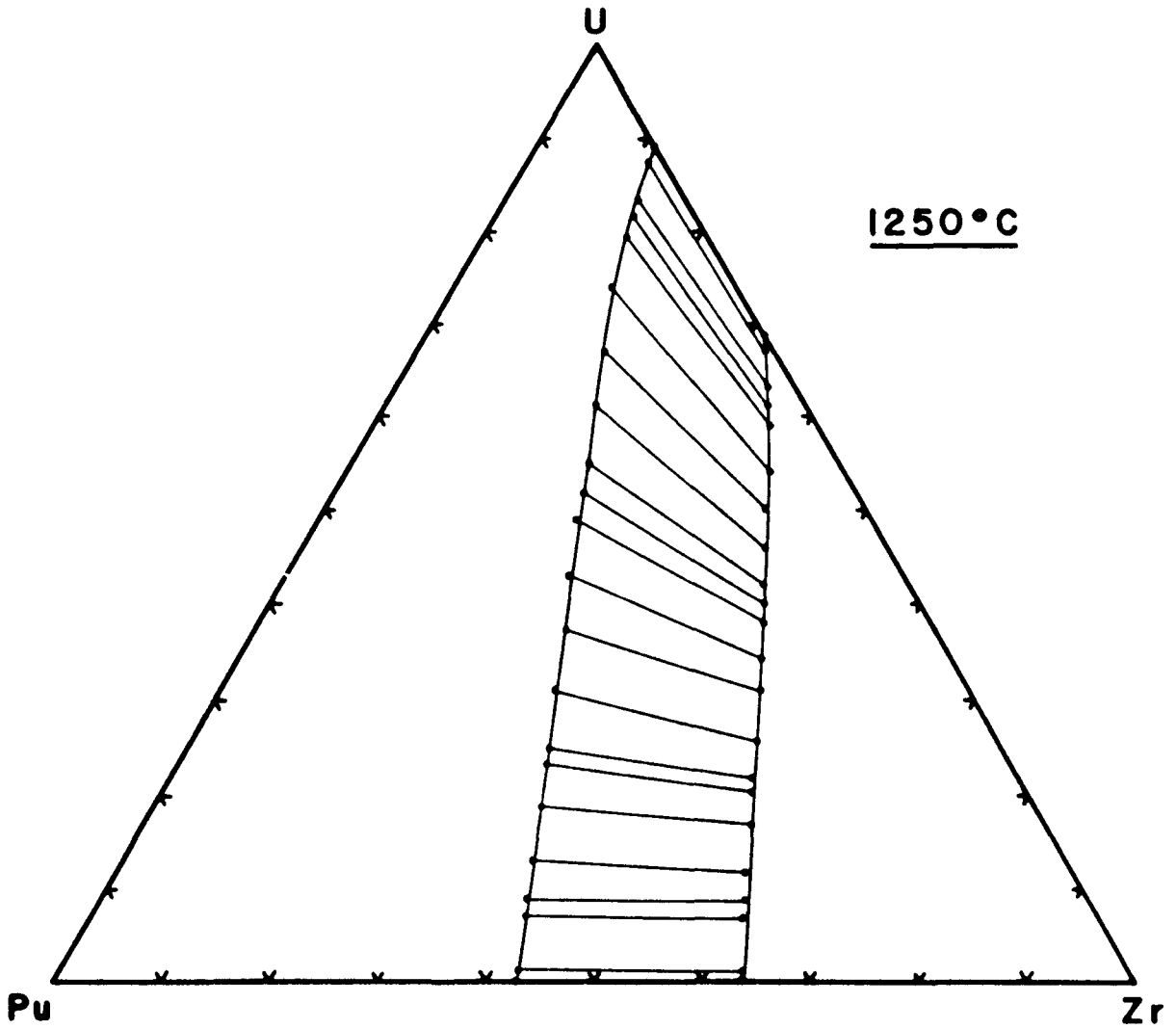


Fig. B.2-13. Calculated Section of the Pu-U-Zr  
Phase Diagram (mol %); 1250°C

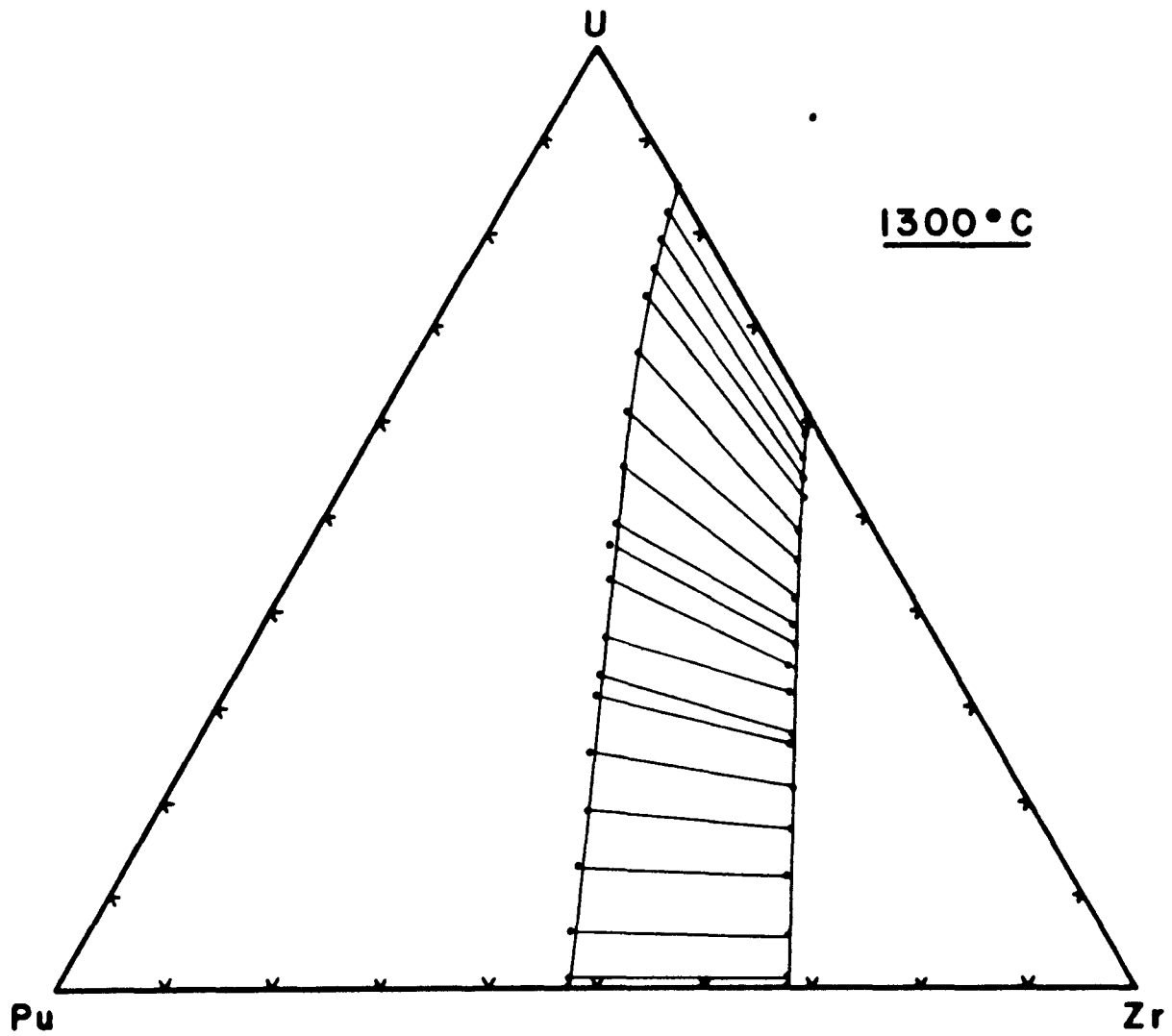


Fig. B.2-14. Calculated Section of the Pu-U-Zr  
Phase Diagram (mol %); 1300°C

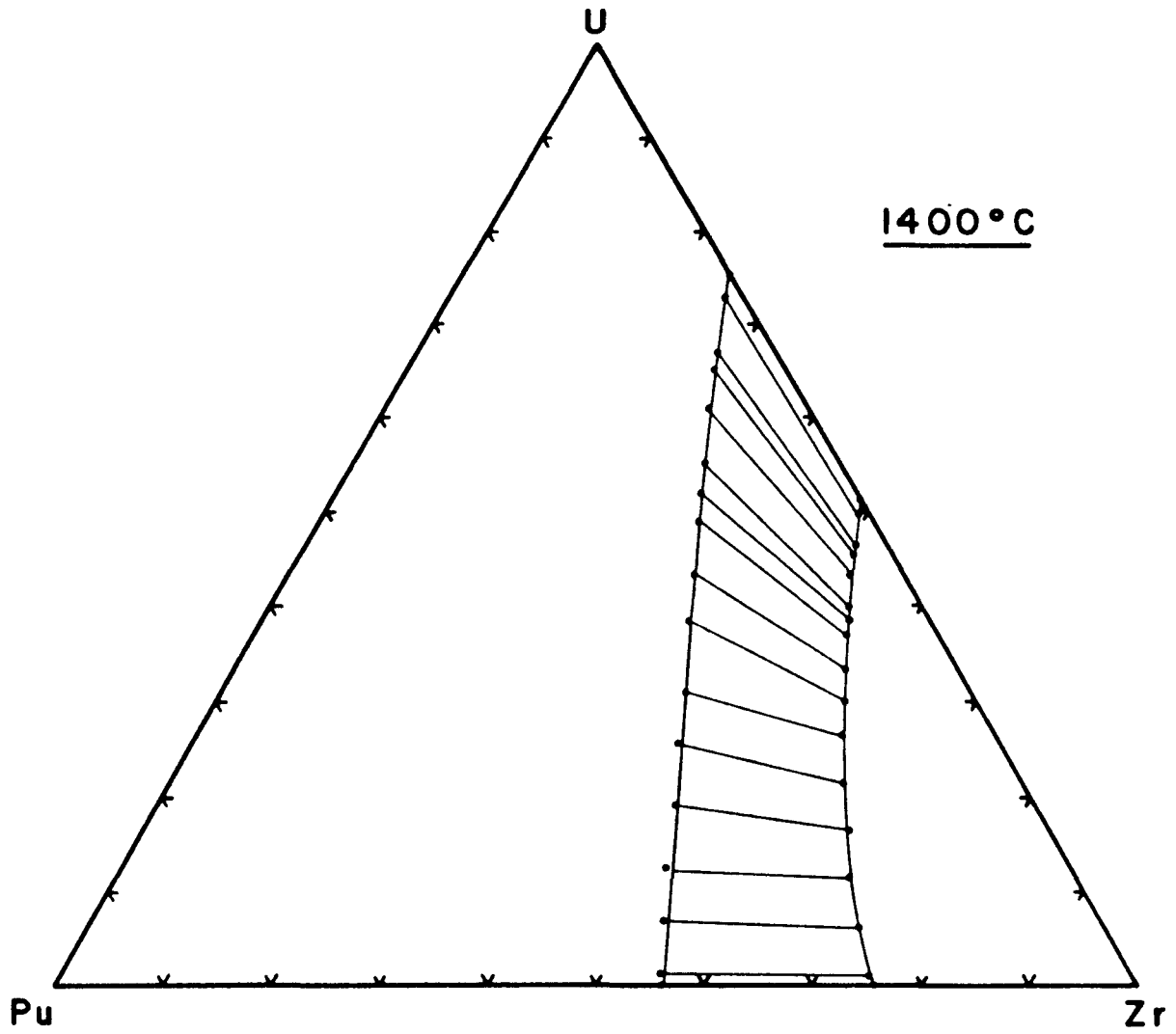


Fig. B.2-15. Calculated Section of the U-Pu-Zr Phase Diagram (mol %); 1400°C

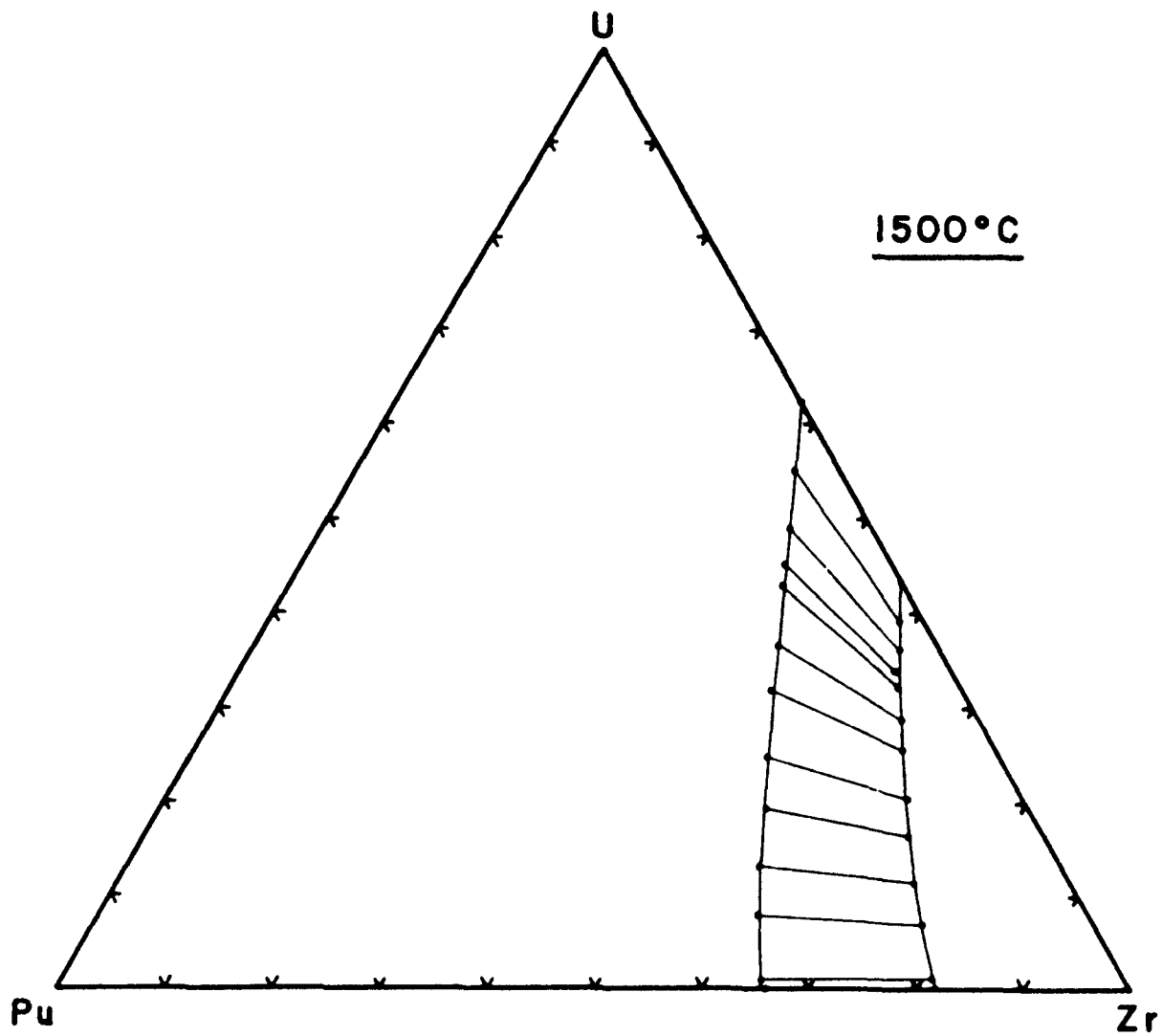


Fig. B.2-16. Calculated Section of the Pu-U-Zr  
Phase Diagram (mol %); 1500°C

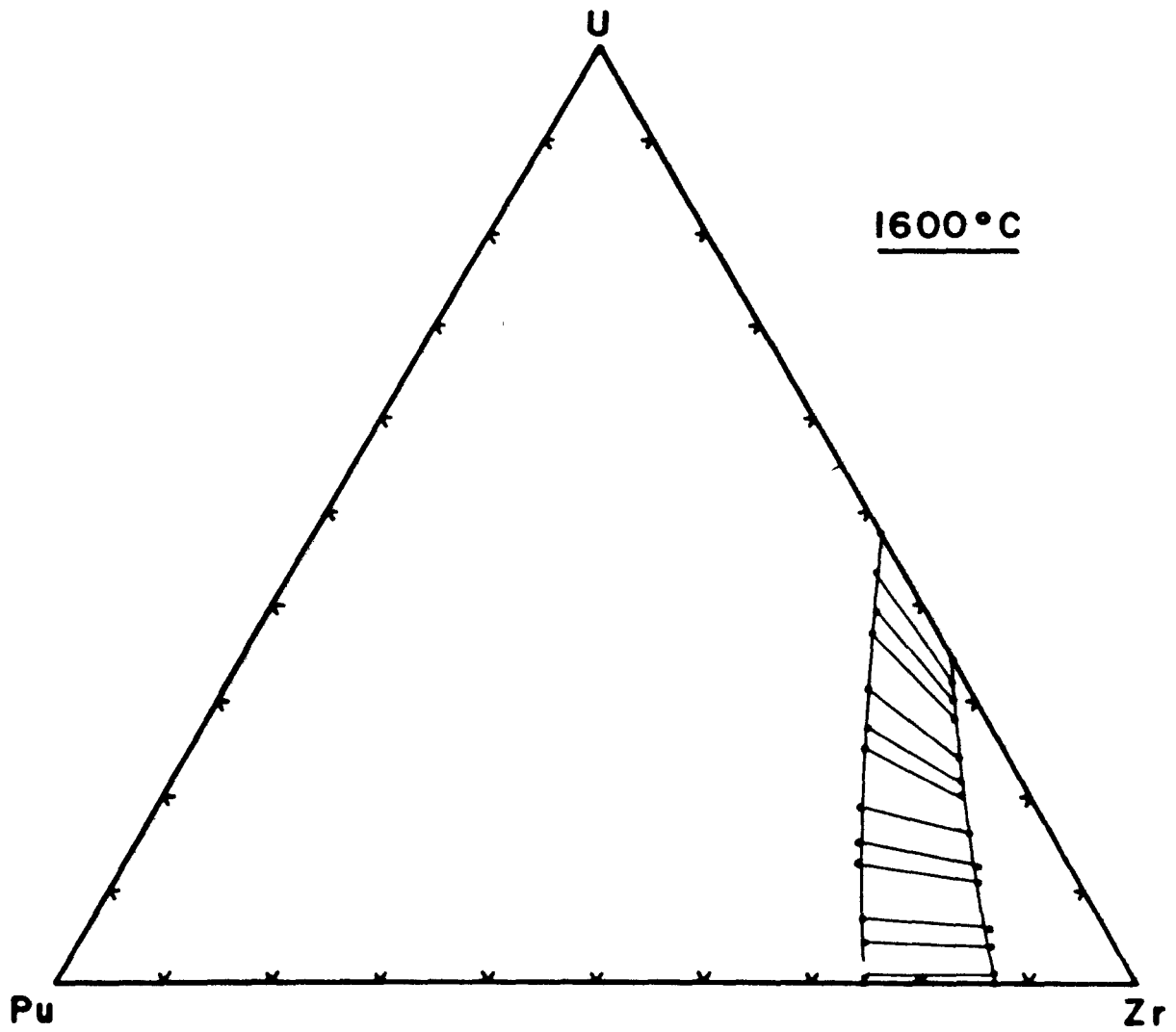


Fig. B.2-17. Calculated Section of the Pu-U-Zr Phase Diagram (mol %); 1600°C

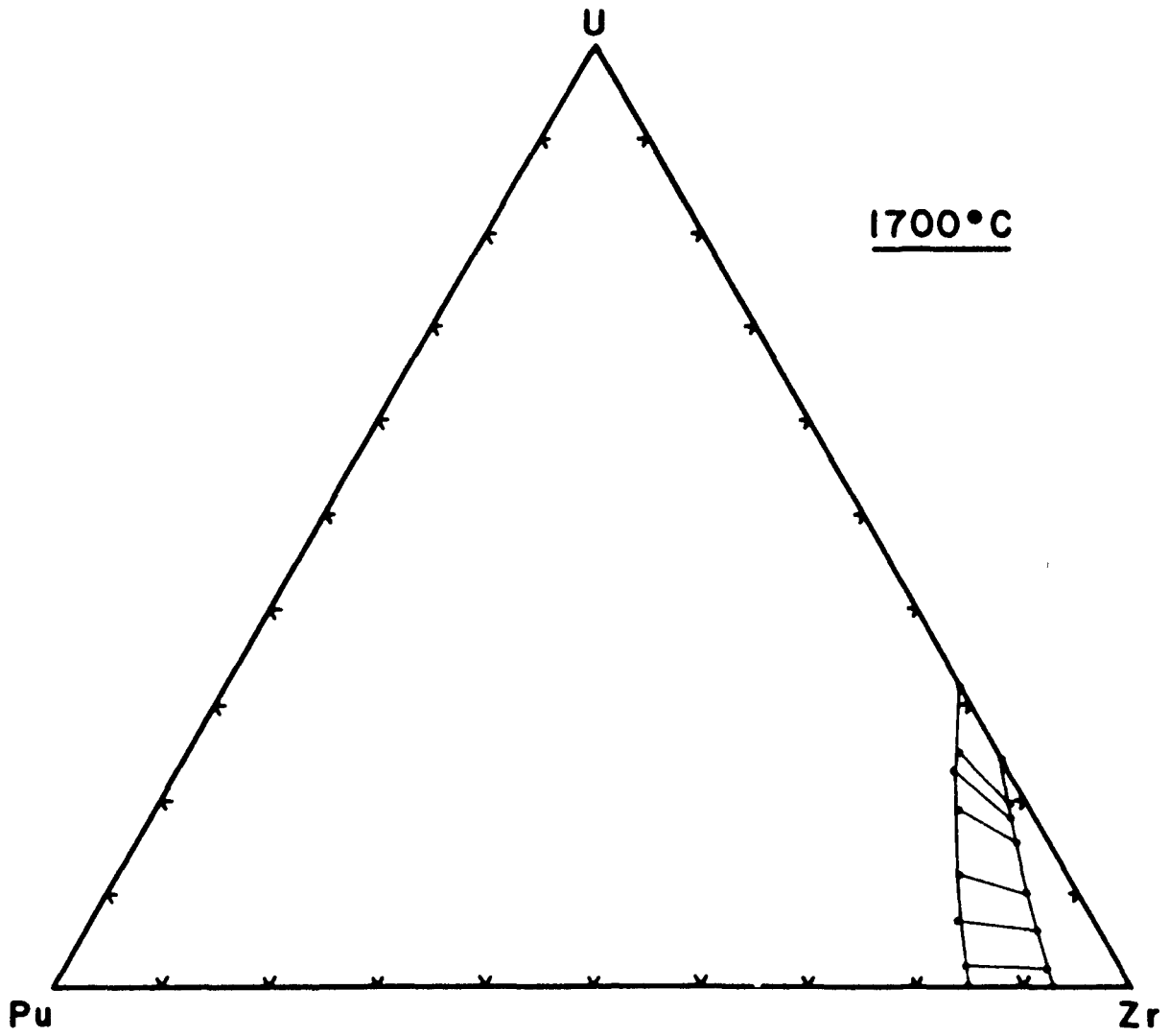


Fig. B.2-18. Calculated Section of the Pu-U-Zr  
Phase Diagram (mol %); 1700°C

Curves giving solidus temperatures for this system have been published previously [16] but no detail has been given on the source of the data. These calculations are in good agreement with measured solidus and liquidus temperatures reported in [17]. Ternary isotherms in the Pu corner of the diagram reported by Mound [3] give liquidus temperatures in the Pu-Zr binary much higher than any other reported values and have been discounted by Pelton.

### B.2.3 Others

The phase-transition temperatures, heats of transition, and crystal structures for the allotropic forms of uranium, plutonium, and zirconium are summarized in Table B.2-1. Data for uranium and plutonium have been taken from an IAEA assessment [4], while data for zirconium have been taken from the compilation of Hultgren and coworkers [5]. For the convenience of the readers, Fig. B.2-19 and Table B.2-2, adapted from [6], have been included. These show the differences among the crystal systems discussed, in terms of the axes a, b, and c and the angles  $\alpha$ ,  $\beta$ , and  $\gamma$ .

The IAEA [4] in its assessment relied heavily on the data of Blumenthal [7] for transition temperatures of uranium because of the high purity of his uranium and his avoidance of effects of hysteresis, superheating, and undercooling. The IAEA [4] converted Blumenthal's temperatures from the 1948 International Practical Temperature Scale (IPTS-1948) to IPTS-1968, which raised his values by about 2 K at the melting point. For this reason there are slight differences between [4], which uses IPTS-1968, and [5], which uses IPTS-1948, even though the same data are recommended. Pelton [8] questions the value chosen by the IAEA [4] for the enthalpy of fusion of uranium (9.142 kJ/mol) on the basis that it gives poor agreement with the Pu-U binary phase diagram, and recommends 12.134 kJ/mol. It seems unlikely that the IAEA value, obtained calorimetrically, is in error by such a large amount, and we have retained the IAEA value. There is clearly an inconsistency, however, which at present remains unresolved.

Plutonium is unique in having six allotropes stable at atmospheric pressure. Extensive studies have been made on the crystalline forms of plutonium but there is comparatively wide scatter in the results. This is probably due to the presence of impurities, hysteresis, sluggish transformations, and self-heating of the sample material. In its assessment the IAEA [4] heavily weighted the more recent data.

**TABLE B.2-1. Phase Transitions and Structures in U, Pu, and Zr**

Phase	Structure <sup>a</sup>	Transition <sup>b</sup>	T (K)	$\Delta H_t$ (kJ mol <sup>-1</sup> )
U( $\alpha$ )	orthorhombic	$\alpha \rightarrow \beta$	942	2.791
U( $\beta$ )	tetragonal	$\beta \rightarrow \gamma$	1049	4.757
U( $\gamma$ )	b.c. cubic	$\gamma \rightarrow \text{liq}$	1408	9.142
Pu( $\alpha$ )	monoclinic	$\alpha \rightarrow \beta$	395	3.431
Pu( $\beta$ )	b.c. monoclinic	$\beta \rightarrow \gamma$	480	0.565
Pu( $\gamma$ )	f.c. orthorhombic	$\gamma \rightarrow \delta$	588	0.586
Pu( $\delta$ )	f.c. cubic	$\delta \rightarrow \delta'$	730	0.084
Pu( $\delta'$ )	b.c. tetragonal	$\delta' \rightarrow \epsilon$	752	1.841
Pu( $\epsilon$ )	b.c. cubic	$\epsilon \rightarrow \text{liq}$	913	2.824
Zr( $\alpha$ )	h.c.p.	$\alpha \rightarrow \beta$	1136	3.937
Zr( $\beta$ )	b.c. cubic	$\beta \rightarrow \text{liq}$	2125	16.895

<sup>a</sup> b.c = body-centered; f.c = face centered; h.c.p = hexagonal close packed

<sup>b</sup> liq = liquid

**TABLE B.2-2. The Crystal System [6]**

System	Axes and Interaxial Angles
Triclinic	$a \neq b \neq c; \alpha \neq \beta \neq \gamma \neq 90^\circ$
Monoclinic	$a \neq b \neq c; \alpha = \gamma = 90^\circ \neq \beta$
Orthorhombic	$a \neq b \neq c; \alpha = \beta = \gamma = 90^\circ$
Tetragonal	$a = b \neq c; \alpha = \beta = \gamma = 90^\circ$
Cubic	$a = b = c; \alpha = \beta = \gamma = 90^\circ$
Hexagonal	$a = b \neq c; \alpha = \beta = 90^\circ; \gamma = 120^\circ$
Trigonal	$a = b = c; \alpha = \beta = \gamma \neq 90^\circ$

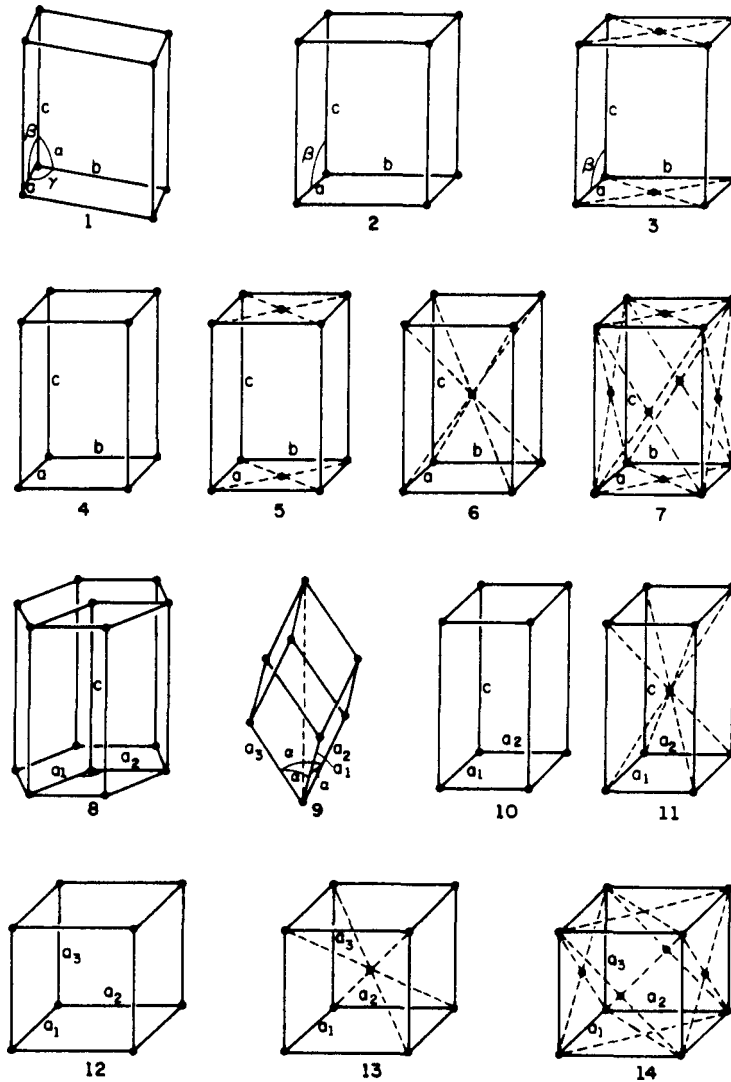


Fig. B.2-19. The 14 Space Lattices Illustrated by a Unit Cell of Each: (1) triclinic, simple, (2) monoclinic, simple, (3) monoclinic, base-centered, (4) orthorhombic, simple, (5) orthorhombic, base-centered, (6) orthorhombic, body-centered, (7) orthorhombic, face-centered, (8) hexagonal, (9) rhombohedral, (10) tetragonal, simple, (11) tetragonal, body-centered, (12) cubic, simple, (13) cubic-body-centered, (14) cubic, face-centered. [6]

Of particular importance is the fact that the high-temperature phases for all three metals, U( $\gamma$ ), Pu( $\epsilon$ ), and Zr( $\beta$ ) have the same structure, namely body-centered cubic. As will be seen later in the binary and ternary systems, continuous solid solution exists for the high-temperature solids.

References for for Section B.2

1. D. R. O'Boyle and A. E. Wright, The Uranium-Plutonium-Zirconium Alloy System, Proc. 4th Int. Conf. on Plutonium and Other Actinides, Santa Fe, NM 970, Met. Soc., New York, 720 (1970).
2. D. R. O'Boyle, H. V. Rhude, and B. Blumenthal, Progress in the Development of Fast-Reactor Fuels, Trans. Am. Nuc. Soc. 9, 1 (1966).
3. (a) Mound Laboratory, Reactor Fuels and Materials Development, Plutonium Research: January-March 1966, MLM-1346 (1967).  
(b) Mound Laboratory, Reactor Fuels and Materials Development, Plutonium Research: 1966 Annual Report MLM-1402 (1967).  
(c) Mound Laboratory, Reactor Fuels and Materials Development, Plutonium Research: January-June 1967, MLM-1445 (1968).  
(d) P. O. Tucker, D. E. Etter, and J. M. Gebhart, Phase Study of Uranium-Plutonium-Zirconium Alloys, Trans. Am. Nuc. Soc. 11, 99 (1968).
4. F. L. Oetting, M. H. Rand, and R. J. Ackermann, The Chemical Thermodynamics of Actinide Elements and Compounds, Part 1, The Actinide Elements, International Atomic Energy Agency, Vienna (1976).
5. R. Hultgren, P. D. Desai, D. T. Hawkins, M. Gleiser, K. K. Kelley, and D. D. Wagman, Selected Values of the Thermodynamic Properties of the Elements, Am. Soc. Met., Metals Park, Ohio (1973).
6. C. S. Barrett and T. B. Massalski, Structure of Metals, Third Ed., McGraw-Hill, New York (1966).
7. B. J. Blumenthal, Transformation Temperatures of High Purity Uranium, J. Nucl. Mat. 2, 23 (1960).
8. A. D. Pelton, Calculation of the Liquidus and Solidus in the Plutonium-Uranium-Zirconium System, Argonne National Laboratory Report ANL-IFR-12 (1985).
9. P. Chiotti, V. Akhachinskij, I. Ansara, and M. H. Rand, The Chemical Thermodynamics of Actinide Elements and Compounds, Part 5, The Actinide Binary Alloys, International Atomic Energy Agency, Vienna (1976).
10. R. Hultgren, P. D. Desai, D. T. Hawkins, M. Gleiser, K. K. Kelley, and D. D. Wagman, Selected Values of the Thermodynamic Properties of Binary Alloys, Am. Soc. Met., Metals Park, Ohio (1973).
11. R. P. Elliot, Constitution of Binary Alloys, First Supplement, McGraw-Hill, New York (1965).

12. R. Boucher and P. Barthelemy, Comparison of the Alloys U-Pu-Mo, U-Pu-Nb, Ti, U-Pu, Zr, Argonne National Laboratory ANL-Trans-138 (1964), translation by B. Blumenthal of CEA-R-2531 (1964).
13. (a) L. R. Kelman et al., Annual Progress Report for 1965, Metallurgy Division, Argonne National Laboratory ANL-7155, 14-25 (1965).  
(b) L. R. Kelman et al., Status of Metallic Plutonium Fast Power-Breeder Fuels, Int. Conf. on Plutonium 1965, A. E. Kay and M. B. Waldron, eds., Chapman and Hall, London, 458 (1967).
14. D. R. Harbur, J. W. Anderson, and W. J. Maraman, Studies on the U-Pu-Zr Alloy System for Fast Breeder Reactor Applications, University of California, LA-4512 (1970).
15. W. F. Murphy, W. N. Beck, F. L. Brown, B. J. Koprowski, and L. A. Neimark, Postirradiation Examination of U-Pu-Zr Fuel Elements Irradiated in EBR-II to 4.5 Atomic Percent Burnup, Argonne National Laboratory ANL-7602 (1970).
16. F. H. Ellinger, W. N. Miner, D. R. O'Boyle, and F. W. Schonfeld, Constitution of Plutonium Alloys, Los Alamos Scientific Laboratory LA-3870 (1968).
17. Reactor Development Program Progress Report, September 1965, Argonne National Laboratory Report ANL-7105, 23 (1965).

**Section B.3**

**Density and Thermal Expansion**

## B. THERMODYNAMICS

### B.3 Density and Thermal Expansion\*

#### General Relations

The thermal-expansion coefficient ( $\alpha_P$ ), is a thermodynamic quantity defined as

$$\alpha_P = \frac{1}{V} \left( \frac{\partial V}{\partial T} \right)_P$$

where  $P$ ,  $V$ , and  $T$  are respectively pressure, volume, and temperature. We will refer to ( $\alpha_P$ ) as the instantaneous volumetric thermal-expansion coefficient. For simplicity we will eliminate the subscript  $P$  from the coefficients in the following discussion and understand that constant pressure is implied in all the equations following. The mean volumetric thermal-expansion coefficient is defined as

$$\bar{\alpha} = \frac{1}{V_0} \left( \frac{V - V_0}{T - T_0} \right)$$

where  $V$  and  $V_0$  are the volumes at temperatures  $T$  and  $T_0$  respectively. Because many measurements of thermal expansion involve measurement of a length change, it is common to find tabulations of the fractional (or percent) change in length,

$$\frac{\Delta L}{L_0} = \left( \frac{L - L_0}{L_0} \right)$$

where  $L$  and  $L_0$  are respectively the sample lengths at temperatures  $T$  and  $T_0$ . The instantaneous and mean linear thermal-expansion coefficients are thus respectively

---

\* The reference list for Section B.3 is on page B.3-17.

$$\alpha_l = \frac{1}{L} \left( \frac{\partial L}{\partial T} \right)$$

and

$$\bar{\alpha}_l = \frac{1}{L_0} \left( \frac{L - L_0}{T - T_0} \right)$$

The instantaneous volumetric thermal-expansion coefficient is just three times the instantaneous linear thermal-expansion coefficient; i.e.,  $\alpha = 3\alpha_l$ . The same relation does not hold exactly for the mean coefficient, as the following considerations show. We write the mean volumetric coefficient as:

$$\bar{\alpha} = \frac{1}{\Delta T} \left( \frac{V}{V_0} - 1 \right)$$

Since  $V = L^3$  we find from the definition of the mean linear coefficient

$$\frac{V}{V_0} = (1 + \bar{\alpha}_l \Delta T)^3$$

whence

$$\bar{\alpha} = 3\bar{\alpha}_l + 3\Delta T \bar{\alpha}_l^2 + \Delta T^2 \bar{\alpha}_l^3$$

The error introduced by taking only the first term in this equation will generally be small in many applications. For example if we take  $\Delta T = 1000$  and  $\bar{\alpha}_l = 1 \times 10^{-5}$ , only a 1% error will be introduced by ignoring the last two terms. The relation between linear thermal expansion and density ( $\rho$ ) is given by

$$\frac{\Delta \rho}{\rho_0} = \frac{1 - (1 + \Delta L/L_0)^3}{(1 + \Delta L/L_0)^3}$$

where  $\Delta \rho = \rho - \rho_0$  is the difference between densities at temperatures  $T$  and  $T_0$ .

### B.3.1 Uranium-Zirconium Alloys

Data for the thermal expansion of U-10 wt % Zr and U-20 wt % Zr are given in [1], which cites Saller et al. [9] as the source. The tabulated values for density were calculated by us, using  $\rho_0$  values obtained assuming an ideal solution [10]. These data are plotted in Fig. B.3-1 along with data for uranium [1]. The tabulated values of  $\Delta L/L_0$  for well-annealed alloys are considered accurate to within  $\pm 7\%$  over the entire temperature range [1]. The tabulated values for the 10% and 20% alloys are represented by the following equations given in Ref. 1:

$$\frac{\Delta L}{L_0}(\%) (\text{U-10 Zr}) = -0.424 + (1.658 \times 10^{-3} T) - (1.052 \times 10^{-6}) T^2 + (1.115 \times 10^{-9} T^3) \quad (293 \leq T \leq 900\text{K})$$

$$\frac{\Delta L}{L_0}(\%) (\text{U-20 Zr}) = -0.301 + (1.160 \times 10^{-3} T) - (7.790 \times 10^{-7}) T^2 + (1.080 \times 10^{-9} T^3) \quad (293 \leq T \leq 900\text{K})$$

From the linear thermal-expansion data and the above equation, the following equations were derived for  $\rho/\rho_0$  for U-10 wt % Zr.

$$\rho/\rho_0 = 1.0122 - (4.629 \times 10^{-5} T) + (2.438 \times 10^{-8} T^2) - (2.805 \times 10^{-11} T^3) \quad (293 \leq T \leq 900\text{K})$$

$$\rho/\rho_0 = 1.0125 - (6.25 \times 10^{-5} T) \quad (1000 \leq T \leq 1200\text{K})$$

For compositions for which data are not available, an ideal-solution approximation should provide reasonable estimates. Values for density as well as mean and instantaneous linear thermal-expansion coefficients are given in Tables B.3-1 and B.3-2.

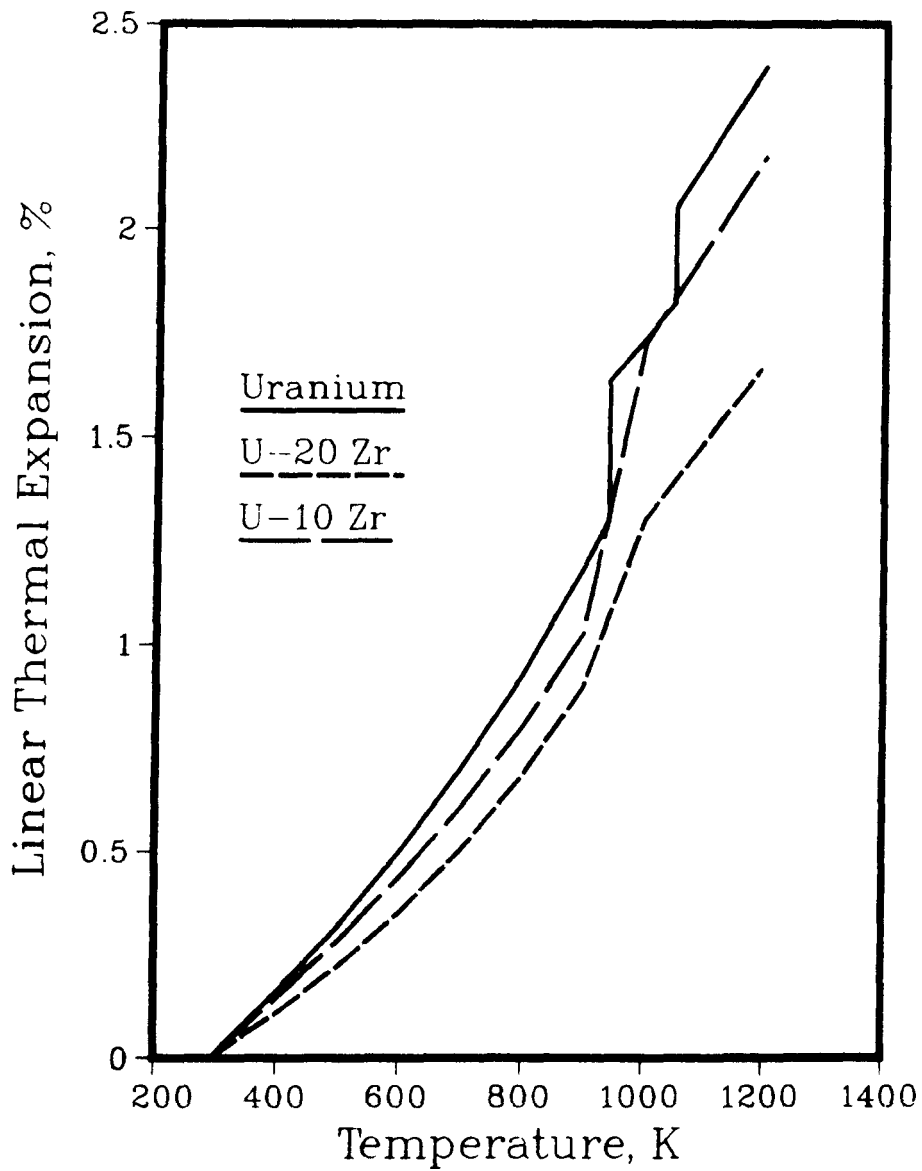


Fig. B.3-1. Mean Linear Thermal Expansion ( $\Delta L/L_0, \%$ ) for Uranium, U-10 wt % Zr, and U-20 wt % Zr.

**TABLE B.3-1. Density and Linear Thermal Expansion of U-10 wt % Zr**

T (K)	$\rho$ (g cm <sup>-3</sup> )	$\Delta L/L_0$ (%)	$\alpha_L \times 10^6$ (K <sup>-1</sup> )
293	16.02	0.000	13.2
400	15.95	0.142	13.5
500	15.89	0.281	14.2
600	15.81	0.433	16.0
700	15.73	0.603	18.2
800	15.64	0.799	21.1
900	15.54	1.027	24.7
1000	15.22	1.725	22.5
1100	15.12	1.950	22.5
1200	15.02	2.175	22.5

**TABLE B.3-2. Density and Linear Thermal Expansion of U-20 wt % Zr**

T (K)	$\rho$ (g cm <sup>-3</sup> )	$\Delta L/L_0$ (%)	$\alpha_L \times 10^6$ (K <sup>-1</sup> )
293	13.81	0.000	9.8
400	13.77	0.107	10.5
500	13.72	0.219	11.9
600	13.67	0.348	13.9
700	13.60	0.500	16.6
800	13.53	0.681	19.9
900	13.44	0.899	24.1
1000	13.29	1.300	18.7
1100	13.21	1.487	18.7
1200	13.14	1.674	18.7

### B.3.2 Uranium-Plutonium-Zirconium Alloys

Data on density and thermal expansion coefficients for some ternary alloys have been reported by CEA [11], ANL [12], and LASL [13]. The available density (for "as-cast" alloys) and thermal-expansion data are summarized in Table B.3-3.

In this table  $\bar{\alpha}_1$  and  $\bar{\alpha}_2$  are the mean thermal-expansion coefficients below and above the solid state-phase-transition region, between about 600 and 700°C, and  $\Delta L/L_0$  is the expansion within the transition region. The densities given in Ref. 11 are at 20°C; those in [12] are at 25°C; and no temperature is given in [13] but "room temperature may be assumed." The transition ranges tabulated are those reported in each reference. For Ref. 13, for which heating and cooling ranges are reported, the temperatures tabulated were those for the start of the transition on heating. In calculating expansion of these alloys  $\bar{\alpha}_2$  should be applied up to the start of the transition,  $\Delta L/L_0$  through the transition, and  $\bar{\alpha}_1$  above the transition region to the solidus temperatures. For the alloy U-15 wt % Pu-10 wt % Zr, we have chosen the data of [12b]. For calculations of densities for compositions or temperatures where there are no data, an ideal-solution approximation is recommended for the present. Thermal-expansion data for the U-15 wt % Pu-10 wt % Zr alloy are shown in Fig. B.3-2 and Table B.3-4.

TABLE B.3-3. Density and Thermal-expansion Coefficients of U-Pu-Zr Alloys

Composition (Pu-Zr wt %)	Ref.	Density (g/cm <sup>3</sup> )	$\bar{\alpha}_1 \times 10^6$ (K <sup>-1</sup> )	$\Delta L/L_0 \times 10^3$ (K <sup>-1</sup> )	$\bar{\alpha}_2 \times 10^6$ (K <sup>-1</sup> )	Transition Range (°C)
15-10	11	15.67	16.3	-	-	600-645
20-10	11	15.73	17.3	-	-	586-650
11.1-6.3	12b	16.8	18.3	5.1	18.1	595-680
15-10	12b	15.8	17.6	5.2	20.1	595-665
18.5-14.1	12b	14.8	17.5	5.0	20.0	595-660
15-6.8	13	16.6	-	-	-	588-643
15-13.5	13	15.0	-	-	-	588-638

TABLE B.3-4. Density and Linear Thermal Expansion of U-15 wt % Pu-10 wt % Zr

T (K)	$\rho$ (g cm <sup>-3</sup> )	$\Delta L/L_0$ (%)	$\alpha_L \times 10^6$ (K <sup>-1</sup> )
298	15.80	0.000	17.6
400	15.72	0.180	17.6
500	15.63	0.356	17.6
600	15.55	0.532	17.6
700	15.47	0.708	17.6
800	15.39	0.884	17.6
868	15.33	1.004	17.6
938	15.17	1.368	20.1
1000	15.11	1.493	20.1
1100	15.02	1.694	20.1
1200	14.93	1.895	20.1
1300	14.85	2.096	20.1
1378	14.78	2.253	20.1

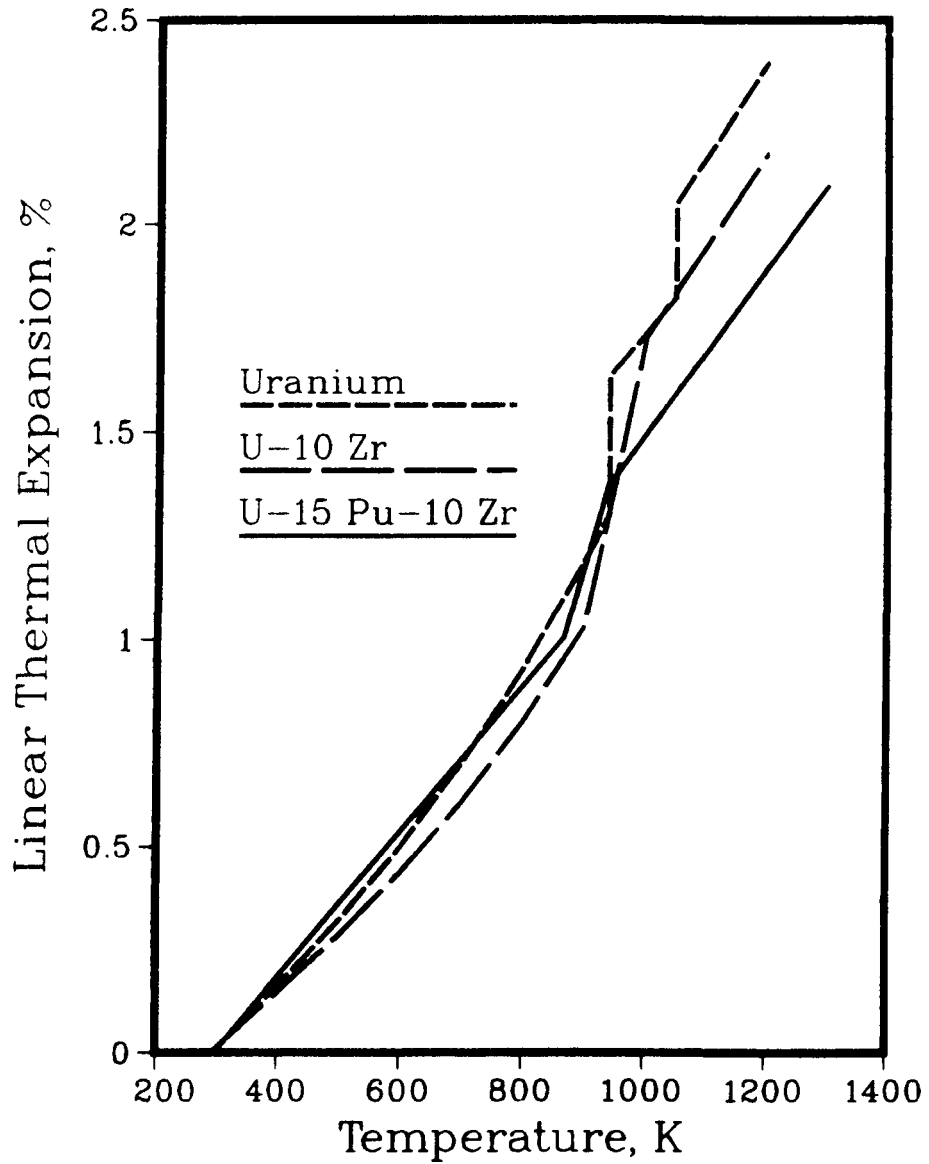


Fig. B.3-2. Mean Linear Thermal-expansion Coefficients ( $\Delta L/L_0, \%$ ) for Uranium, U-10 wt % Zr, and U-15 wt % Pu-10 wt % Zr.

### B.3.3 Others

#### Uranium, Zirconium, Plutonium

The data for the elements were taken from the compilation of the Thermophysical Properties Research Center (Purdue) [1]. The thermal-expansion data are shown in Fig. B.3-3, and Tables B.3-5 through -7. Density values given in the tables were calculated by us, using  $\rho_0$  values from Ref. 1. For uranium the tabulated values for  $\Delta L/L_0$  are considered accurate to within  $\pm 5\%$  below 941 K and  $\pm 7\%$  above. They are represented approximately by the following equations given in Ref. 1.

$$\frac{\Delta L}{L_0}(\%) = -0.379 + (1.264 \times 10^{-3} T) - (8.982 \times 10^{-8} T^2) \\ + (6.844 \times 10^{-10} T^3) \quad (293 \leq T \leq 941\text{K})$$

$$\frac{\Delta L}{L_0}(\%) = -0.149 + (1.775 \times 10^{-3} T) + (4.382 \times 10^{-7} T^2) \\ - (1.239 \times 10^{-10} T^3) \quad (1048 \leq T \leq 1400\text{K})$$

For zirconium the tabulated values for  $\Delta L/L_0$  are considered accurate to within  $\pm 3\%$  below 1137 K and  $\pm 10\%$  above. They are represented approximately by the following equations:

$$\frac{\Delta L}{L_0}(\%) = -0.111 + (2.325 \times 10^{-4} T) + (5.595 \times 10^{-7} T^2) \\ - (1.768 \times 10^{-10} T^3) \quad (293 \leq T \leq 1137\text{K})$$

$$\frac{\Delta L}{L_0}(\%) = -0.759 + (1.474 \times 10^{-3} T) - (5.140 \times 10^{-7} T^2) \\ + (1.559 \times 10^{-10} T^3) \quad (1137 \leq T \leq 1800\text{K})$$

Note that there are very large differences in thermal expansion behavior among these three metals, with plutonium being particularly irregular. This will pose some problems, as we shall see later in understanding the alloys. Data for liquid uranium are not given in Ref. 1 and require some additional discussion.

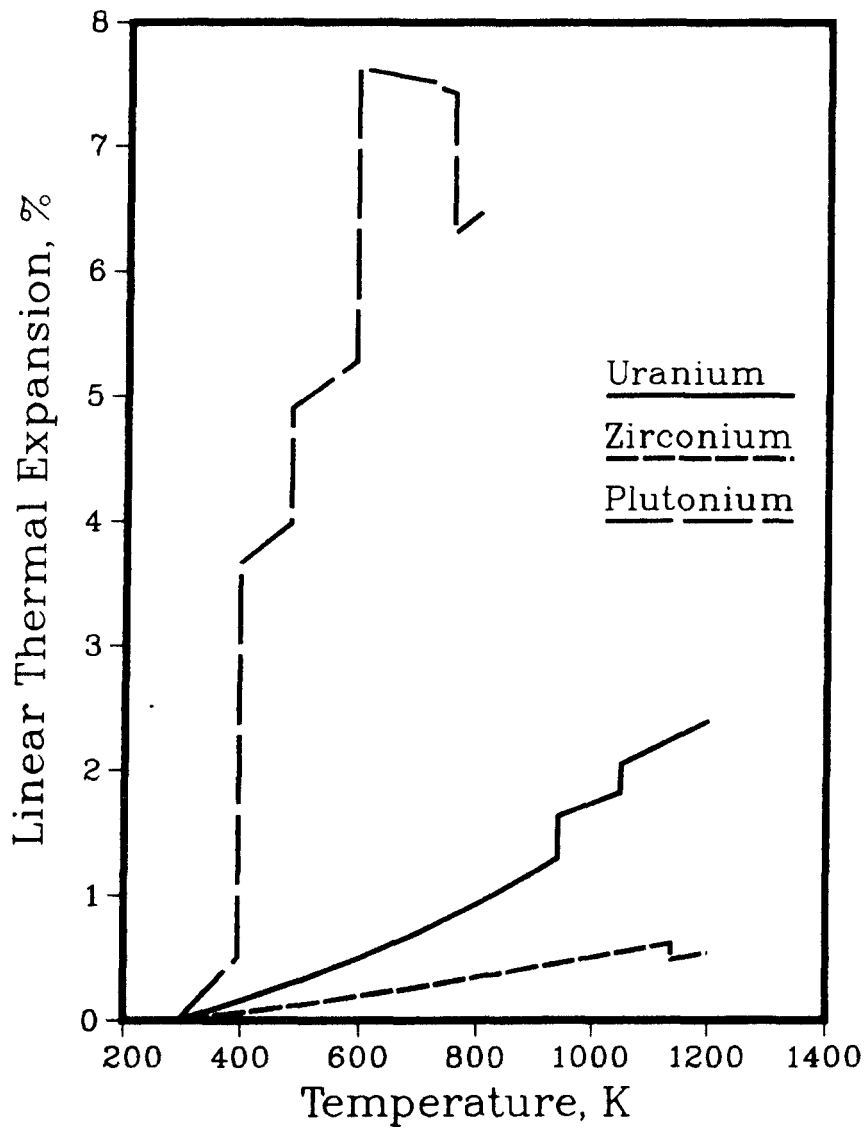


Fig. B.3-3. Mean Linear Thermal Expansion ( $\Delta L/L_0, \%$ ) of Uranium, Plutonium, and Zirconium.

**TABLE B.3-5. Density and Linear Expansion of Uranium**

T (K)	$\rho$ (g cm <sup>-3</sup> )	$\Delta L/L_0$ (%)	$\alpha l \times 10^6$ (K <sup>-1</sup> )
293	19.07	0.000	13.9
400	18.98	0.157	15.2
500	18.89	0.315	16.9
600	18.79	0.494	19.0
700	18.68	0.697	21.4
800	18.55	0.924	24.3
900	18.41	1.186	27.7
941( $\alpha$ )	18.39	1.300	29.1
941( $\beta$ )	18.16	1.635	17.3
1000	18.11	1.737	17.3
1048( $\beta$ )	18.07	1.820	17.3
1048( $\gamma$ )	17.94	2.050	22.9
1100	17.88	2.168	22.9
1200	17.76	2.398	22.9
1400	17.53	2.855	22.9
1408( $\gamma$ )	17.52	2.866	22.9
1408( $\delta$ )	16.95	4.006	25.5
1500	16.84	4.232	25.5
1600	16.71	4.502	25.5

TABLE B.3-6. Density and Linear Thermal Expansion of Zirconium

T (K)	$\rho$ (g cm <sup>-3</sup> )	$\Delta L/L_0$ (%)	$\alpha l \times 10^6$ (K <sup>-1</sup> )
293	6.57	0.000	5.7
400	6.56	0.060	5.9
500	6.55	0.123	6.6
600	6.53	0.192	7.1
700	6.52	0.265	7.6
800	6.50	0.343	7.9
900	6.49	0.442	8.0
1000	6.47	0.505	8.2
1100	6.46	0.586	8.2
1137( $\alpha$ )	6.45	0.617	8.2
1137( $\beta$ )	6.48	0.482	9.0
1200	6.46	0.539	9.1
1400	6.43	0.725	9.5

**TABLE B.3-7. Density and Linear Thermal Expansion of Plutonium**

T (K)	$\rho$ (g cm <sup>-3</sup> )	$\Delta L/L_0$ (%)	$\alpha_l \times 10^6$ (K <sup>-1</sup> )
293	19.75	0.000	46.7
350	19.59	0.279	49.4
395( $\alpha$ )	19.46	0.502	51.0
395( $\beta$ )	17.73	3.663	37.3
450	17.62	3.868	37.3
480( $\beta$ )	17.57	3.980	37.3
480( $\gamma$ )	17.11	4.901	34.6
550	16.99	5.144	34.6
588( $\gamma$ )	16.93	5.275	34.6
588( $\delta$ )	15.84	7.628	-8.6
600	15.85	7.618	-8.6
700	15.88	7.532	-8.6
730( $\delta$ )	15.90	7.506	-8.6
730( $\delta'$ )	15.92	7.458	-16.1
753( $\delta'$ )	15.93	7.421	-16.1
753( $\epsilon$ )	16.45	6.287	36.6
800	16.37	6.459	36.6

For liquid uranium four sets of density measurements have been reported. The earliest of these was published by Grosse and coworkers [2] in 1961. An Archimedean method was used to determine densities from the melting point to about 1900 K. Several years later workers at Mound Laboratory [3] reported data on the density of liquid uranium which disagreed with the Grosse data. A pycnometric technique was used by the Mound group and data were obtained from 1410 to 1518 K. Measurements of the density of liquid uranium were subsequently reported by Shaner [4] (to about 5000 K) using a unique isobaric-expression method (IEX) and by Drotning [5] (1419-1567 K), who used gamma densitometry. The four sets of measurements, which do not agree very well, are compared with solid density data in Fig. B.3-4, and some of the essential aspects of the experiments are summarized in Table B.3-8.

**TABLE B.3-8. Measurements of Density of Liquid Uranium,  $\rho(\text{g/cm}^3) = \alpha - bT(\text{K})$**

Reference	Method	$\alpha$	$b \times 10^4$
TPRC [1]	(Solid)	19.22	11.4
Grosse et al. [2]	Archimedean	19.36	10.33
Rohr & Wittenberg [3]	Pycnometry	19.52	16.01
Shaner [4]	Isobaric Expansion	20.00	17.
Drotning [5]	Gamma Densitometry	18.77	12.9

As is clear from Fig. B.3-4, two of the measurements indicate a density increase on melting while two show the more usual density decrease on melting. There is, fortunately, some additional information that can help to make a reasonable decision among these conflicting values. First, in conjunction with sessile-drop measurements of interfacial tension of uranium [6], observations were made of the volume change on melting. It was estimated that about a 3% expansion occurred on melting. Second, measurements were made of the pressure-temperature phase diagram of uranium [7]. From the slope of the  $\gamma$ -liquid phase

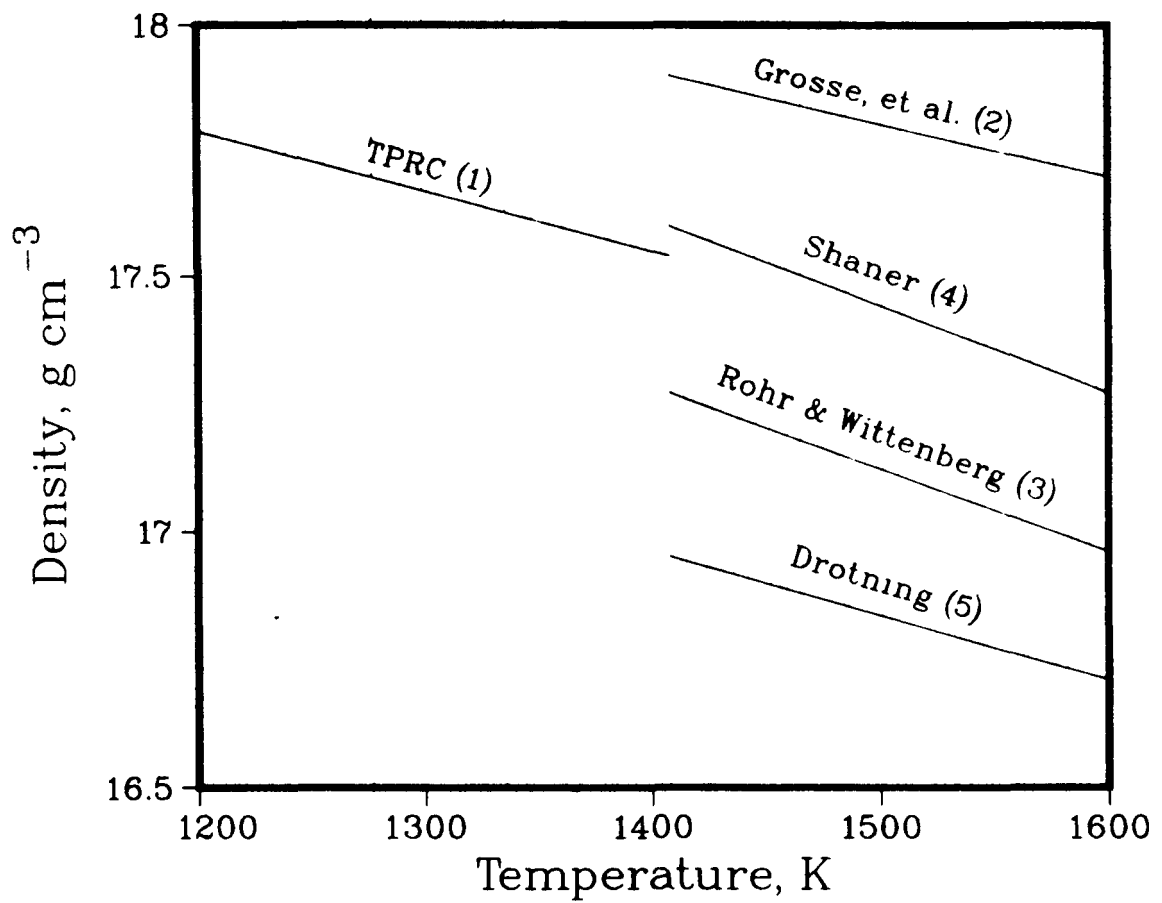


Fig. B.3-4. Density of Solid and Liquid Uranium.

boundary the volume change on melting was calculated to be 0.49 cm<sup>3</sup>/mol. Finally, observations made during casting operations [8] clearly indicate that the liquid shrinks on freezing.

Based on these facts it seems clear that the density data of Grosse et al. are incorrect. The values of Shaner, which show a very small density increase on melting, are also suspect. In fact Shaner, in commenting on his technique, points out that because of basic experimental difficulties the IEX technique is less accurate than other standard methods. Its chief value is in allowing measurements over a very wide temperature range, not of principal concern here. Of the remaining two sets of measurements we recommend the Drotning data for general use. His work is recent, and most importantly he made measurements on solid uranium, which was not done by the Mound workers, which agree very well with the TPRC data. The resulting volume change on melting is 0.46 cm<sup>3</sup>/mol, which agrees well with the value reported from the uranium phase diagram [7]. Table B.3-9 gives a summary of some pertinent values at the melting point of uranium (1408 K).

**TABLE B.3-9. Density and Volume of Solid and Liquid Uranium (T=T<sub>m</sub>)**

Phase	Density (g/cm <sup>3</sup> )	Volume (cm <sup>3</sup> /mol)
liquid	16.95	14.04
gamma	17.52	13.58
Δ	-0.57	0.46

References for Section B-3

1. Y. S. Touloukian, R. K. Kirby, R. E. Taylor, and P. D. Desai, **Thermophysical Properties Matter 12**, Thermal Expansion, Metallic Elements and Alloys, Plenum, New York (1965).
2. A. V. Grosse, J. A. Cahill, and A. D. Kirshenbaum, **Density of Liquid Uranium**, J. Am. Chem. Society 83, 4665-6 (1961).
3. W. G. Rohr and L. J. Wittenberg, **Reactor Fuels and Materials Development Plutonium Research, January--June 1967**, MLM-1445, 2-13, Mound Lab., Miamisburg, Ohio (1968).
4. J. W. Shaner, **Thermal Expansion of Metals Over the Entire Liquid Range**, Thermal Expansion 6 69, Proc. 6th Int. Symposium on Thermal Expansion, I. D. Peggs, ed., 69, August 29-31, 1977 (1977).
5. W. D. Drotning, **Density and Thermal Expansion of Liquid U-Nb Alloys**, High Temperatures - High Pressures, (England), 14, No. 3, 253-258 (1982).
6. C. L. Rosen, N. R. Chellew, and H. M. Feder, **The Melt Refining of Irradiated Uranium: Application to EBR-II Fast Reactor Fuel. IV.** Interaction of Uranium and Its Alloys with Refractory Oxides, Nuclear Sci. and Eng 6, 504-510, (1959).
7. N. Asami, M. Yamada, and S. Takahashi, **Pressure-temperature Phase Diagram (4) of Uranium Metal**, Nippon Kinzoku Gakkaisi 31, 389-94 (1967).
8. D.B. Tracy, Argonne National Laboratory, private communication (1985).
9. H. A. Saller, R. F. Dickerson, and W. F. Murr, **Uranium Alloys for High-Temperature Application**, Battelle Memorial Inst. Ohio Report, BMI-1098 (1956).
10. F. A. Rough, **An Evaluation of Data on Zirconium-Uranium Alloys**, Battelle Memorial Inst., Columbus, Ohio Report BMI-1030, (1955)..
11. R. Boucher and P. Barthelemy, **Comparison of the Alloys U-Pu-Mo, U-Pu-Nb, U-Pu, Ti, U-Pu-Zr**, ANL-Trans-138 (1964), translation by B. Blumenthal, CEA-R-2531 (1964).
12. (a) Argonne National Laboratory, Metallurgy Division, Annual Progress Report for 1965, ANL-7155, 14-25 (1965).  
(b) L. R. Kelman, H. Savage, C. M. Walter, B. Blumenthal, R. J. Dunworth, and H. V. Rhude, **Status of Metallic Plutonium Fast Power-Breeder Fuels**, Plutonium 1965, A. E. Kay and M. B. Waldron, eds., Chapman and Hall, London, 458 (1967).

13. D.R. Harbur, J. W. Anderson, W. J. Maraman, Studies on the U-Pu-Zr Alloy System for Fast Breeder Reactor Applications, Los Alamos, LA-4512 (1970).

**Section B.4**

**Surface Tension**

(This section incomplete at this time)

**Section C.1**  
**Thermal Conductivity**

## C. TRANSPORT

### C.1 Thermal Conductivity\*

#### C.1.1 Uranium-Zirconium Alloys (Unirradiated)

Touloukian et al.[1] have summarized the data for U-Zr alloys. Based on the data they present, the following correlation has been developed:

$$k_0 = A + BT + CT^2, \text{ W/m}\cdot\text{K} \quad (1)$$

where  $A = 17.5 (1 - 2.23 W_Z)/(1 + 1.61 W_Z)$   
 $B = 1.54 \times 10^{-2} (1 + 0.061 W_Z)/(1 + 1.61 W_Z)$   
 $C = 9.38 \times 10^{-6}$   
 $W_Z$  = weight fraction of Zr  
 $T$  = temperature in K.

In the temperature range of interest (300-900°C) for fuel performance under normal operating conditions, the correlation shows excellent agreement with the U-Zr data for  $0.015 \leq W_Z \leq 0.20$  with an average deviation from the data of less than 1%. However, the correlation yields values lower than the U-40Zr data by ~20%. If it is assumed that the data are accurate to within  $\pm 20\%$ , then the accuracy of Eq. 1 is taken to be the same as that for the data for  $W_Z \leq 0.20$ . Table C.1-1 gives the data and the values predicted by Eq. 1 for several temperatures and Zr weight fractions. The same information is given in Fig. C.1-1 in graphical form. The thermal-conductivity values for pure uranium [1] are included in Fig. C.1-1 and Table C.1-1 for reference.

\* The reference list for Section C.1 is on page C.1-22.

**TABLE C.1-1. Summary of U-Zr Alloy Thermal-conductivity Data and Values (in Parentheses) Calculated from Eq. 1.**

T (°C)	$k_o$ (W/cm <sup>2</sup> °C)					
	U	U-1.5Zr	U-5Zr	U-10Zr	U-20Zr	U-40Zr
20	0.270 (0.228)	0.226 (0.217)	0.19 (0.194)	---	0.11 (0.116)	0.07 (0.048)
100	0.291 (0.245)	0.240 (0.234)	0.21 (0.210)	---	0.13 (0.130)	0.08 (0.060)
200	0.311 (0.269)	0.260 (0.257)	0.23 (0.232)	---	0.15 (0.150)	0.10 (0.078)
300	0.334 (0.294)	0.285 (0.282)	0.25 (0.256)	---	0.17 (0.171)	0.12 (0.097)
400	0.358 (0.321)	0.310 (0.309)	0.28 (0.282)	---	0.20 (0.195)	0.14 (0.118)
500	0.382 (0.350)	0.340 (0.337)	0.31 (0.310)	---	0.22 (0.220)	0.17 (0.142)
600	0.406 (0.380)	0.370 (0.368)	0.34 (0.340)	---	0.25 (0.247)	0.20 (0.167)
700	0.432 (0.413)	0.405 (0.400)	0.37 (0.371)	---	0.28 (0.277)	0.24 (0.193)
800	0.457 (0.448)	0.445 (0.434)	0.41 (0.405)	---	0.31 (0.307)	0.28 (0.222)
900	0.483 (0.484)	--- ---	0.44 (0.440)	---	0.34 (0.340)	0.33 (0.253)

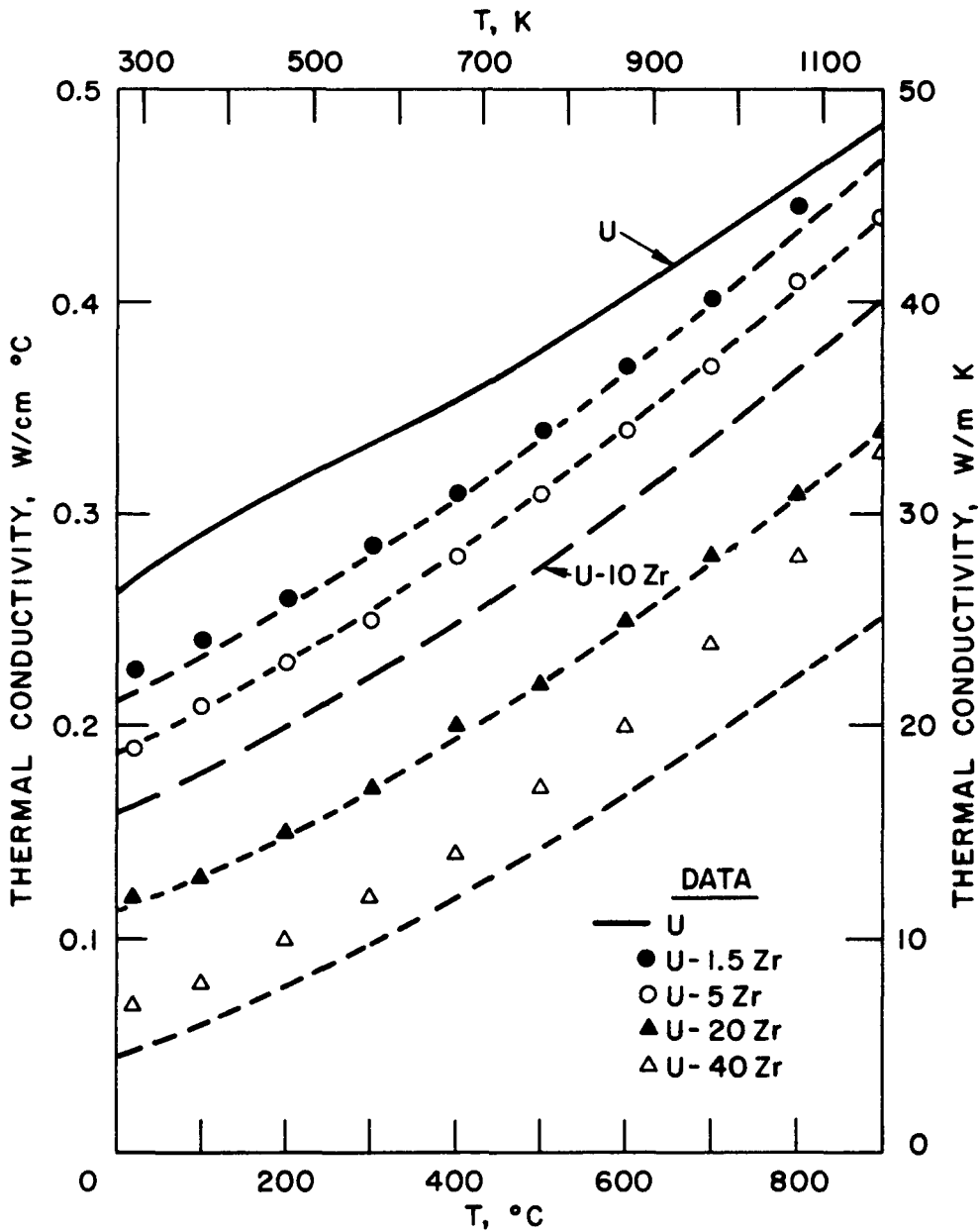


Fig. C.1-1. Comparison Between U-Zr Thermal-conductivity Data and the Recommended Correlation (Eq. 1). The thermal conductivity of pure uranium is also included for reference purposes. The dashed lines are calculated from the correlation.

### Justification

In reviewing the data for U-Zr alloys, it appeared that the decrease in thermal conductivity with increasing Zr content correlated better with atom fraction than with weight fraction, particularly for low Zr content. The coefficients (A, B, and C) in Eq. 1 were chosen to vary linearly with Zr atom fraction at several temperatures for the U-1.5Zr, U-5Zr, and U-20Zr cases. The coefficients were then converted to weight-fraction dependencies because of the more common use of weight fraction in specification of fuel parameters.

As indicated in Table C.1-1 and Fig. C.1-1, the correlation is a very good representation of the data for  $0.015 \leq W_Z \leq 0.20$ . This gives considerable confidence in using the correlation to interpolate the data for  $W_Z = 0.1$ . However, there is less confidence in extrapolating the correlation to  $W_Z = 0.0$  or  $W_Z = 0.4$ .

### Irradiated U-Zr

No data are available on the effects of irradiation on the thermal conductivity of U-Zr. The unirradiated thermal conductivity of U-Zr with 5 to 10 wt.% Zr is comparable to that of U-5Fs (see C.1.3). If it is assumed that U-10Zr behaves in a similar manner under irradiation conditions to U-5Fs with regard to fission-gas swelling and sodium logging, then the same porosity correction factor may be used from startup to major interlinkage of porosity (see C.1.3):

$$f_p = k/k_o = (1 - P)/(1 + \beta P), \quad (2)$$

where P is porosity fraction and  $1.5 \leq \beta \leq 2.5$ . The minimum value for  $f_p$  is taken as  $0.5 \pm 0.1$ . The long-time value of  $f_p$  is taken as  $0.7 \pm 0.1$  to account for the combined effects of gas-filled and sodium-filled porosity. For design studies, an uncertainty of  $\pm 30\%$  is arbitrarily assumed.

Several other effects must also be considered in calculating the in-reactor thermal conductivity of U-Zr fuels in the context of the IFR application. While negligible weight fractions of Pu are produced in EBR-II, the opposite is true for U-Zr in an IFR. Transmutation of U to Pu results in lowering of the thermal conductivity of the fuel (see C.1.2). Physics calculations can be used to provide input on the amount of Pu produced as function of burnup. The coefficients in Eq. 1 can then be modified (as has been done in C.1.2) to reflect the change in conductivity due to Pu generation:

$$\begin{aligned} A &= 17.5 [(1 - 2.23 W_z)/(1 + 1.61 W_z) - 2.62 W_p] \\ B &= 1.54 \times 10^{-2} [(1 + 0.061 W_z)/(1 + 1.61 W_z) + 0.90 W_p] \\ C &= 9.38 \times 10^{-6} (1 - 2.70 W_p) \end{aligned}$$

where  $W_p$  = the weight fraction of Pu.

Another phenomenon that will affect the local thermal conductivity of U-Zr is the redistribution of U and Zr (and Pu and fission products) under the thermal gradient. Work is in progress to model this phenomenon to provide input to the thermal-conductivity equation as a function of burnup and operating conditions.

### C.1.2 Uranium-Zirconium-Plutonium Alloys (Unirradiated)

Thermal-conductivity data for U-Pu-Zr fuels have been summarized in ANL-AFP-38 [2]. The correlation recommended to describe the thermal conductivity of unirradiated, 100%-dense U-Pu-Zr fuels is

$$k_0 = A + BT + CT^2, \text{ W/m}\cdot\text{K}, \quad (1)$$

where  $A = 17.5 [(1 - 2.23 W_Z)/(1 + 1.61 W_Z) - 2.62 W_P]$   
 $B = 1.54 \times 10^{-2} [(1 + 0.061 W_Z)/(1 + 1.61 W_Z) + 0.90 W_P]$   
 $C = 9.38 \times 10^{-6} (1 - 2.70 W_P)$   
 $W_Z$  = Zr weight fraction  
 $W_P$  = Pu weight fraction  
 $T$  = temperature in K.

Table C.1-2 and Fig. C.1-2 summarize the data [2] used in developing the correlation. The data are assumed to be accurate within  $\pm 20\%$ . In the temperature range of interest (300-900°C), the maximum deviation between the correlation and the data is 10%. Thus, the accuracy of the data is taken as the accuracy of the correlation. For design calculations, an uncertainty of 20% is recommended.

#### Justification

The form of the correlation represented by Eq. 1 was chosen on the basis of the data set for U-Zr alloys (see C.1.1), which is more extensive than the data base for U-Pu-Zr alloys. The coefficients (A, B, and C) were modified slightly to give reasonably good agreement at 300°C and 800°C. It is interesting to note that the curvature suggested by the U-Pu-Zr data is different in sign from that suggested by the U-Zr data. No fundamental reason for this can be found. While better fits to the U-Pu-Zr data can be determined to match the temperature, no additional confidence would be realized, because of the uncertainty in the data.

**TABLE C.1-2. Summary of Thermal-conductivity Data for Unirradiated, 100%-dense U-Pu-Zr Alloys. The values calculated from the recommended correlation (Eq. 1) are included in parentheses.**

T (°C)	$k_0$ (w/cm °C)			
	<u>U-16.2Pu-6.2Zr</u>	<u>U-14.7Pu-9.7Zr</u>	<u>U-18.4Pu-11.5Zr</u>	<u>U-15Pu-10Zr</u>
20	--- (0.115)	--- (0.101)	--- (0.075)	--- (0.098)
100	0.109 (0.131)	0.100 (0.117)	0.092 (0.090)	--- (0.114)
200	0.142 (0.152)	0.132 (0.137)	0.117 (0.110)	--- (0.134)
300	0.177 (0.173)	0.164 (0.158)	0.144 (0.130)	--- (0.155)
400	0.210 (0.196)	0.196 (0.181)	0.171 (0.152)	--- (0.177)
500	0.241 (0.220)	0.225 (0.204)	0.197 (0.174)	--- (0.201)
600	0.264 (0.245)	0.253 (0.229)	0.219 (0.198)	--- (0.226)
700	0.280 (0.271)	0.278 (0.255)	0.234 (0.222)	--- (0.253)
800	0.293 (0.298)	0.301 (0.282)	0.248 (0.247)	--- (0.278)
900	--- (0.327)	--- (0.310)	--- (0.274)	--- (0.306)

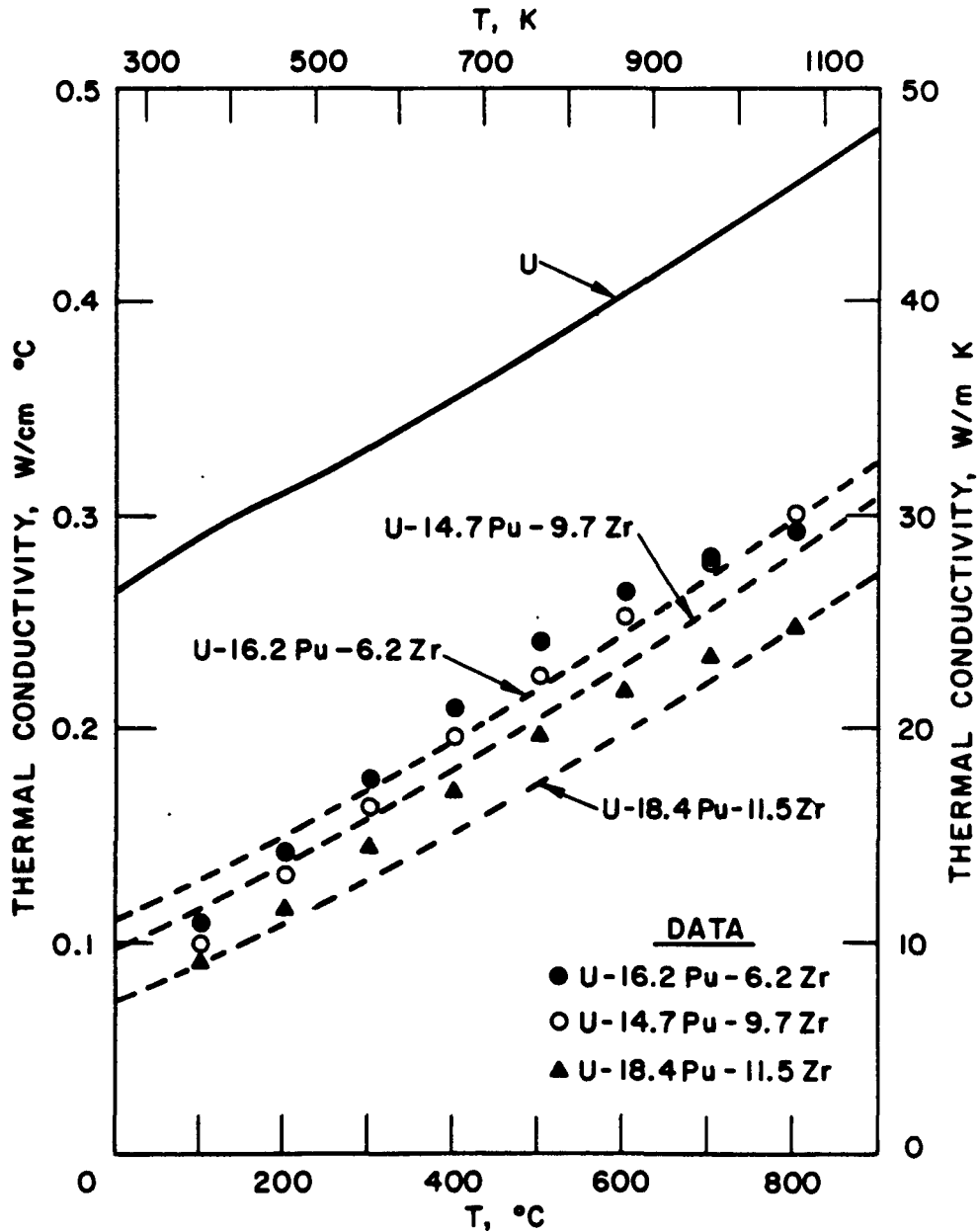


Fig. C.1-2. Comparison Between Correlation Predictions (Dashed Lines) and Data for the Thermal Conductivity of Unirradiated, 100%-dense U-Pu-Zr Alloys. A curve based on the data for pure U is also included [1].

### Irradiated U-Pu-Zr

As in the case for U-Zr, no data are available for the thermal conductivity of irradiated U-Pu-Zr. Based on the behavior of U-5Fs (see C.1.3), it is assumed that up until porosity interlinkage, the decrease in conductivity with increasing fission-gas porosity can be represented by

$$f_p = k/k_0 = (1 - P)/(1 + \beta P) \quad (2)$$

where  $P$  is porosity fraction and  $1.5 \leq \beta \leq 2.5$ .

The minimum value of  $f_p$  is  $0.5 \pm 0.1$  and the long-time value is  $0.72 \pm 0.1$  to reflect the influence of sodium logging and fuel hot pressing.

Additional effects that should be considered are increased Pu (or Zr) weight fractions with burnup, redistribution of U, Pu, and Zr, and local concentrations of solid (and liquid) fission products. For IFR design studies in which it is primarily the Pu that fissions, no further degradation of thermal conductivity with fission-product generation is recommended. However, in test runs employing highly enriched U, the replacement of the highly conducting U with fission products may cause additional degradation of thermal conductivity with burnup. More work needs to be done in this area. The interim recommendation is that Eqs. 1 and 2 be used for prediction of U-Pu-Zr thermal conductivity and that physics calculations be used to determine the weight fractions of U, Pu, Zr as a function of burnup. No recommendation is made at this time with regard to fuel-constituent redistribution and solid-fission-product concentration. An uncertainty of  $\pm 30\%$  is arbitrarily assumed for the in-reactor thermal conductivity of U-Pu-Zr alloys.

C.1.3 Others

Unirradiated 100%-dense U-5Fs

The recommended equation for unirradiated, 100%-dense U-5Fs is

$$k_0 = 6.26 + (2.77 \times 10^{-2} T) + (3.91 \times 10^{-6} T^2), \text{ W/m K} \quad (1)$$

where T is temperature in K. Numerical values and uncertainty estimates are listed in Table C.1-3. Figure C.1-3 is a graph of the correlation with a comparison to the results for pure uranium [1] and the U-5Fs data of Saller et al. [3], Zegler and Nevitt [4], and di Novi [5].

**TABLE C.1-3. Correlation Values and Uncertainty Estimates for the Thermal Conductivity of Unirradiated, 100%-dense U-5Fs**

T		Correlation (Eq. 1) (W/m K)	Uncertainty Estimate (±%)
<u>K</u>	<u>°C</u>		
293	20	14.7	30
373	100	17.1	25
473	200	20.2	10
573	300	23.4	6
623	350	25.0	6
673	400	26.7	6
723	450	28.3	6
773	500	30.0	5
823	550	31.7	5
873	600	33.4	5
923	650	35.2	5
973	700	36.9	5
1023	750	38.7	5
1073	800	40.5	5
1123	850	42.3	5
1173	900	44.1	5
1223	950	46.0	5
1273	1000	47.9	5

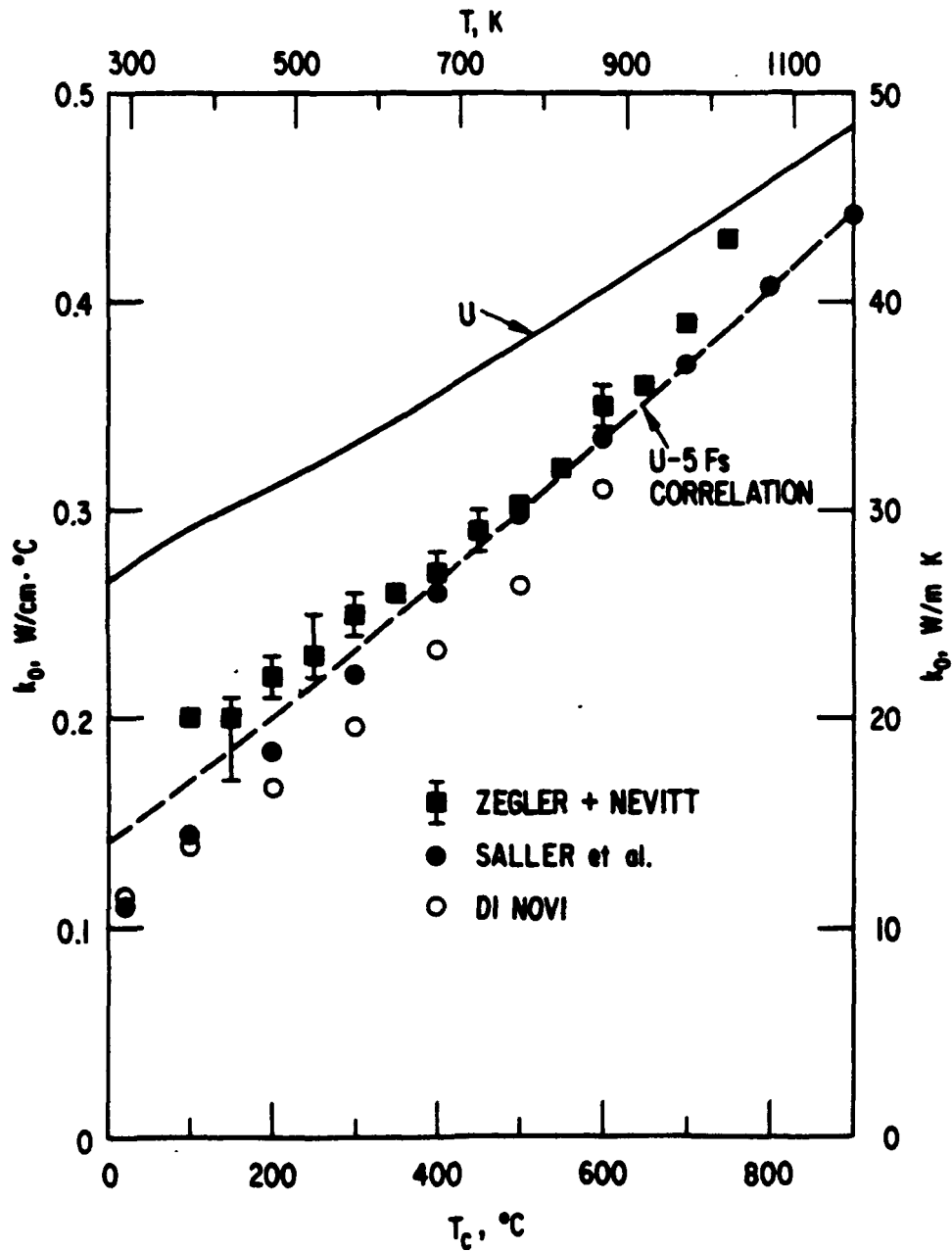


Fig. C.1-3. Comparison Between Measured Thermal Conductivities of Unirradiated, 100%-dense U-5Fs and Values Calculated From the Correlation (Eq. 1). The thermal conductivity of pure U is included for reference purposes.

Justification

Table C.1-4 summarizes the experimental thermal-conductivity values for unirradiated U-5Fs. Saller et al. [3] used a steady-heat-flow method. Each thermal-conductivity value in the table represents an average of 20 readings (five thermal couples and four equilibrium runs). The authors estimate the absolute accuracy to be within  $\pm 5\%$ .

**TABLC C.1-4. Measured Thermal Conductivities of U-5 wt.% Fs**

T (°C)	$k_o$ (W/cm °C)		
	Saller et al. <sup>a</sup>	Zegler & Nevitt <sup>b</sup>	di Novi <sup>c</sup>
20	0.110	---	0.116
100	0.143	0.20	0.138
150	---	0.20 (0.17-0.21)	---
200	0.183	0.22 (0.21-0.23)	0.167
250	---	0.23 (0.22-0.25)	---
300	0.221	0.25 (0.24-0.26)	0.196
350	---	0.26	---
400	0.260	0.27 (0.26-0.28)	0.233
450	---	0.29 (0.28-0.30)	---
500	0.298	0.30	0.264
550	---	0.32	---
600	0.334	0.35 (0.34-0.36)	0.311
650	---	0.36	---
700	0.370	0.39	---
750	---	0.43	---
800	0.407	---	---
900	0.44	---	---

<sup>a</sup>Composition: 2.5 wt % Mo, 0.1 wt % Zr, 1.5 wt % Ru, 0.3 wt % Rh and 0.5 wt % Pd.

<sup>b</sup>Composition: 2.45 wt % Mo, 0.069 wt % Zr, 2.08 wt % Ru, 0.3 wt % Rh, and 0.209 wt % Pd.

<sup>c</sup>EBR-II Mark IA fuel. Values obtained from graph of  $\alpha(k_o = \rho C_p \alpha)$ .

Zegler and Nevitt [4] employed a comparative method based on steady-state thermal gradients in U-5Fs and Armco iron. The authors quote a precision of  $\pm 4\%$ . The absolute accuracy is probably of the order of  $\pm 10\%$  for temperatures below  $700^\circ\text{C}$ . The data above  $700^\circ\text{C}$  are suspect because of the possible formation of a U-Fe eutectic in the region of contact between the U-5Fs and the Armco iron. The agreement between the two sets of data is quite good in the temperature range of  $300\text{--}700^\circ\text{C}$ .

The di Novi data in Table C.1-4 are based on a transient-pulse method to determine the thermal diffusivity ( $\alpha$ ). However, there is an inconsistency between di Novi's measured thermal diffusivity and calculated thermal conductivity ( $k_o = \alpha\rho C_p$ , where  $\rho$  is density and  $C_p$  is specific heat capacity). The thermal-conductivity values in Table C.1-4 were obtained by using di Novi's  $\alpha$  values and the  $\rho$  and  $C_p$  values presented in this handbook. The absolute accuracy of the thermal diffusivities is estimated to be  $\pm 10\%$ . While the resulting thermal conductivities are consistently lower than those of the other authors for temperatures above  $200^\circ\text{C}$ , the agreement is reasonable if one considers the uncertainties involved.

The correlation represented by Eq. 1 was obtained by matching the mean of the Saller et al. and Zegler and Nevitt data at low temperature and the Saller et al. data at higher temperature. The choice of a parabolic equation is somewhat arbitrary. Zegler and Nevitt's data suggest it, while the data of Saller et al. suggest a linear fit. The agreement between the correlation and the data is very good for temperatures of interest ( $T > 300^\circ\text{C}$ ). The uncertainty of  $\leq 5\%$  indicated in Table C.1-3 for  $T > 300^\circ\text{C}$  is based on the uncertainty in the data. This value is low compared to uncertainties anticipated under irradiation conditions.

### Irradiated U-5Fs

A number of in-reactor phenomena tend to lower the conductivity of the U-5Fs. Fission-gas bubbles and thermal-stress-induced microcracking will lower the density and the conductivity; solid (and liquid) fission-product buildup will tend to lower the thermal conductivity much the same as increasing amounts of fission lower the conductivity; and irradiation damage will degrade the conductivity. From start-up to 1-2 at.% burnup, the dominant factor accounting for the degradation of thermal conductivity is assumed to be the decrease in fuel density due to fission-gas-induced swelling and microcracking. Based on the data of di Novi [5] and Beck and Fousek [6], the recommended porosity-correction factor is

$$f_p = (1 - P)/(1 + \beta P) \quad (2)$$

where  $P$  is porosity fraction,  $1.5 \leq \beta < 2.5$  is an empirically determined factor, and  $f_p$  is the ratio of the irradiated ( $k$ ) to the unirradiated ( $k_0$ ) thermal conductivity.

Equation 2 is a reasonable representation of the data for burnups at which the porosity is essentially isolated. After interlinkage has occurred, the ingress of sodium into the voids may tend to improve the conductivity somewhat as suggested by the data of Beck and Fousek [6] and Betten [7]. If it is assumed that interlinkage occurs at  $P \sim 0.25$ , then  $f_p = 0.50 \pm 0.05$  based on Eq. 2. Beyond this point in burnup, the effective conductivity will tend to increase due to sodium logging and fuel hot pressing and tend to decrease due to solid-fission-product accumulation. While modeling of these phenomena is required to predict the effective fuel thermal conductivity as a function of burnup, some preliminary guidance is offered to assist in design studies. The minimum thermal conductivity for design studies can be taken as  $0.5 \pm 0.1$  of the unirradiated value. The long-time (i.e., intermediate to high burnup) behavior is better estimated by  $f_p = 0.7 \pm 0.1$ .

### Justification

R. A. di Novi [5] also used her thermal-pulse method to perform post-irradiation thermal-conductivity measurements on Mark-IA fuel that had been irradiated to ~0.6 to 1.1 at.% burnup. She reported the fractional decrease in thermal conductivity as a function of temperature for a number of samples. Based on these data, she described the ratio ( $f_p$ ) of irradiated-to-unirradiated thermal conductivity of U-5Fs as

$$f_p = (1 - P)/(1 + \beta P) \quad (2)$$

where  $P$  is porosity fraction based on diametral strain measurements and  $\beta = 1.7$  based on a comparison to the data.

There are several difficulties associated with di Novi's assumptions and calculational methods:

- (1) The porosity fraction was assumed to be directly related to the measured diametral strain  $P = 3(\Delta D/D_0)$ ;
- (2) The swelling due to solid and liquid fission products (at fuel operating temperatures) was assumed to have the same effect on thermal conductivity as gaseous fission products.
- (3) No attempt was made to estimate the effects of changing fuel chemistry on thermal conductivity.

These issues are discussed below.

The calculation of  $P$  from the relationship  $P = 3(\Delta D/D_0)$  is fundamentally incorrect. It is an approximation which is good for small, isotropic swelling due to fission-gas bubbles and microcracks. Let  $(\Delta V/V_0)_p$  be the change in fuel volume (relative to the initial fuel volume) due to porosity formation. Because porosity is referenced to the current fuel volume, the relationship between  $P$  and  $(\Delta V/V_0)_p$  is

$$P = \frac{(\Delta V/V_0)_P}{1 + \Delta V/V_0}, \quad (3a)$$

where  $\Delta V/V_0$  is the total volumetric swelling strain, including the effects of fission products other than Xe and Kr. Hofman [8] has estimated the swelling contribution of these other fission products to be in the range of  $(\Delta V/V_0)_{sl} = 0.6$  to  $1.8\%$ /at.% burnup. Because the degree of anisotropy in the samples is difficult to determine without more information, the assumption of isotropy is used to calculate porosity. In terms of measured quantities, Eq. 3a becomes

$$P = \frac{(1 + \Delta D/D_0)^3 - 1 - CB}{(1 + \Delta D/D_0)^3} \quad (3b)$$

where B is burnup in at.% and  $6 \times 10^{-3} \leq C \leq 1.8 \times 10^{-2}$ .

An estimate is now made of the effects of changing fuel chemistry with burnup. Based on information supplied by Hofman [8] and Porter [9], the increased amount of Fs at 10 at.% burnup is  $\sim 2.4$  wt.%, while the total of other solid (and liquid) fission products is  $\sim 4.2$  wt.% and the weight fraction of plutonium is  $\sim 0.4$  wt.%. If it is assumed (to the first order) that this additional 7 wt.% of fission and transmutation products has the same effect on the thermal conductivity as does Fs, then the estimate can be made based on the thermal conductivity of U-12Fs as compared to U-5Fs. Zegler and Nevitt's [4] data on uranium with 3 to 10 wt % Fs was used to estimate the burnup correction factor as

$$f_B = 1 - 0.024B, \quad (4)$$

where B is in at.%. Thus, for di Novi's low-burnup samples, the decrease in conductivity due to changing fuel chemistry is  $\sim 2\%$ , which is negligible compared to the uncertainty in the data. However, Eq. 4 is

useful for estimating the effect of changing fuel chemistry with burnup at higher burnup levels.

Table C.1-5 shows the  $\Delta D/D_0$  values of di Novi and the range of  $(\Delta V/V_0)_P$  one would calculate using Hofman's solid-fission-product swelling rates. The data imply that the conductivity correlates better with porosity than with burnup. Figure C.1-4 shows that a  $\beta$ -value of -2.5 gives a reasonable fit to the data, particularly for  $P > 3\%$ . This value is higher than the value calculated by di Novi (1.7) and higher than one would expect, for example, for sintered products with isolated spherical porosity ( $\beta = 0.7$  to  $1.0$ ) or for irradiated metal fuel with isolated fission-gas bubbles. It appears likely that most of the porosity for these samples is due to partially interconnected bubbles and/or to microtearing induced by anisotropic growth. Such tearing could cause a larger reduction in thermal conductivity than spherical pores of the same porosity fraction. The question of whether such behavior is particular to the Mark-IA fuel is addressed in the following.

Two sets of in-reactor thermal-conductivity measurements were performed on EBR-II Mark-II fuel. Beck and Fousek [6] analyzed the results of the instrumented CP-59 capsule irradiated in CP-5. Thermocouples were located along the fuel centerlines and in the NaK bath adjacent to the cladding. The data are given in graphical form as a percentage decrease in thermal conductivity with fuel volumetric swelling. The volume increase of the fuel was determined from the change in plenum pressure prior to significant gas release. The data are converted to a  $k/k_0$  vs  $P$  plot in Fig. C.1-5 by using

$$P = \frac{(\Delta V/V_0)_P}{100 + \Delta V/V_0}$$

where  $(\Delta V/V_0)_P = (\Delta V/V_0) - (\Delta V/V_0)_{sl}$

Table C.1-5. Summary of di Novi [5] Data (285T595°C)

Burnup (at.%)	$\Delta D/D_0$ (%)	$(\Delta V/V_0)_P$ (%)	P (%)	k/k <sub>0</sub> (%)
0.58	0.89	1.97 (1.62-2.31)	1.92 (1.58-2.25)	95.2 (87.2-96.8)
0.67	1.83	4.69 (4.28-5.09)	4.45 (4.06-4.83)	86.1 (82.3-87.8)
0.80	1.31	2.97 (2.49-3.45)	2.86 (2.40-3.32)	94.8 (89.7-97.3)
0.90	4.69	13.1 (12.5-13.6)	11.5 (11.0-11.9)	68.6 (64.2-76.8)
0.94	2.26	5.66 (5.09-6.22)	5.31 (4.79-5.83)	83.8 (80.4-89.4)
1.00	1.45	3.15 (2.55-3.75)	3.02 (2.44-3.59)	93.9 (90.5-99.0)
1.04	1.97	4.68 (4.05-5.30)	4.41 (3.82-5.00)	85.8 (82.7-89.2)
1.08	4.10	11.1 (10.4-11.7)	9.88 (9.26-10.4)	73.3 (70.3-76.7)
1.10	1.54	3.31 (2.65-3.97)	3.16 (2.53-3.79)	90.0 (88.3-91.8)

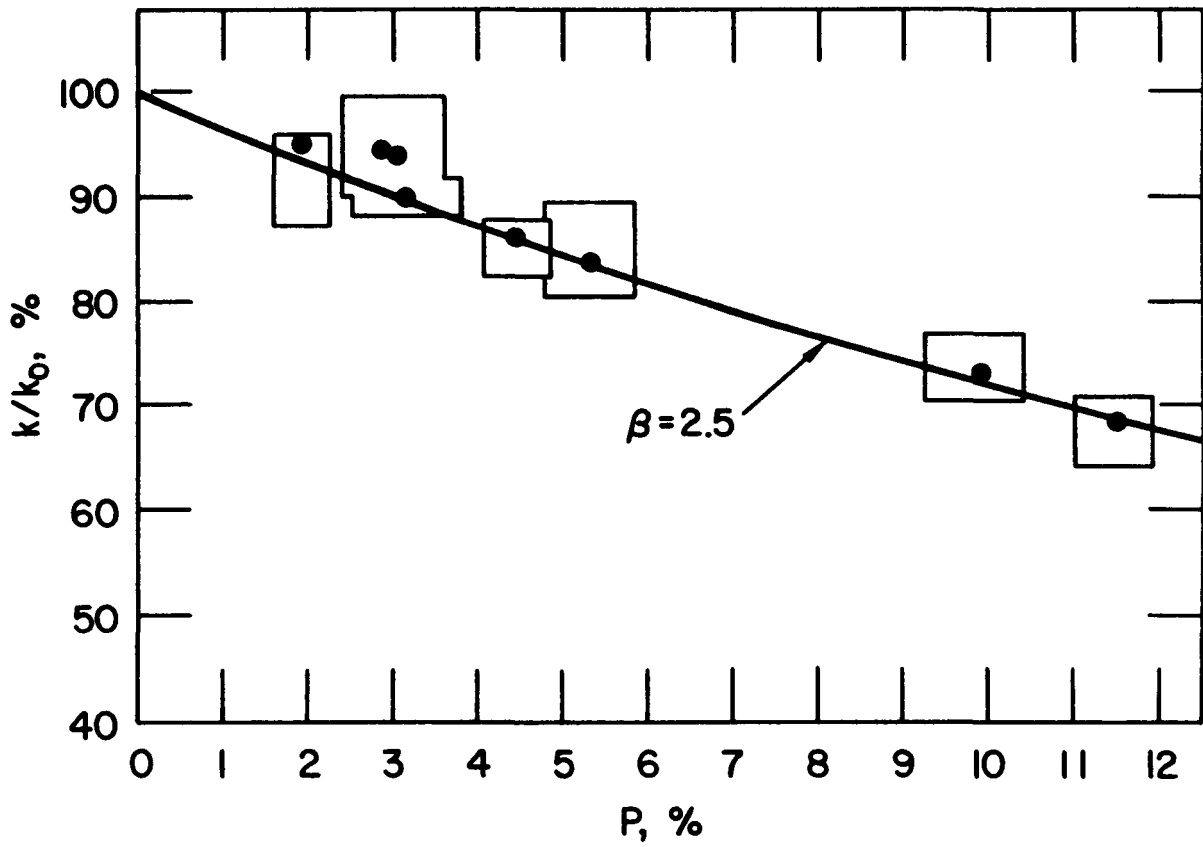


Fig. C.1-4. Comparison Between Analytical Porosity-correction Factor,  $f_p = k/k_0 = (1 - P)/(1 + \beta P)$ , and the Data of di Nova [5] for  $\beta = 2.5$ . The dots represent nominal values while the rectangles encompass the uncertainties based on the scatter in the  $k/k_0$  data and on the uncertainty in the solid (and liquid) fission-product swelling.

$$(\Delta V/V_0)_{s1} = 0.6 \text{ to } 1.8\%/\text{at.}\% \text{ burnup.}$$

Furthermore, the porosity factor,  $(1 - P)/(1 + \beta P)$ , with  $\beta = 2.5$  is tested. As shown in Fig. C.1-5, the porosity-correction factor with  $\beta = 2.5$  predicts a larger decrease in thermal conductivity than indicated for  $P < 23\%$  and a smaller decrease for  $P > 23\%$ . A better fit to the data for  $P \leq 20\%$  ( $\Delta V/V_0 \leq 25\%$ ) is given by  $\beta = 1.5$ . A more sophisticated mathematical treatment would be to let  $f_p = (1 - P)/(1 + \beta P^n)$  in order to better fit the data over the full range of porosities tested. There is some physical basis for this, as the reduction factor should increase as the pores change shape and start to interconnect. However, it is not clear whether the data are accurate enough to justify such a treatment. In particular, the calculation of  $\Delta V/V_0$  from the rise in plenum pressure assumes that no gas is released from the fuel until the bubbles interconnect at  $\Delta V/V_0 \sim 33\%$  ( $P \sim 25\%$ ).

Betten [7] has reported the results of instrumented subassembly XX08 in which fuel and coolant thermocouple measurements were made as a function of time to a peak subassembly burnup of 8.8 at.%. He identifies three general regions of behavior. In region 1 (0 to 1 at.% burnup), the thermal conductivity shows the expected decrease with burnup due to porosity formation. In region 2 (1 to 2 at.% burnup) two temperature peaks are observed, indicating minimum values of fuel thermal conductivity. In region 3 (burnup  $> 2$  at.%), the effective conductivity levels off to a steady-state value. The minimum value of  $k/k_0$  during the temperature peaking is 0.475 with a standard deviation of 0.111. The long-time value of  $k/k_0$  is 0.720 with a standard deviation of 0.059. Work is in progress to further analyze the data and to develop models to rationalize the behavior of these fuel rods.

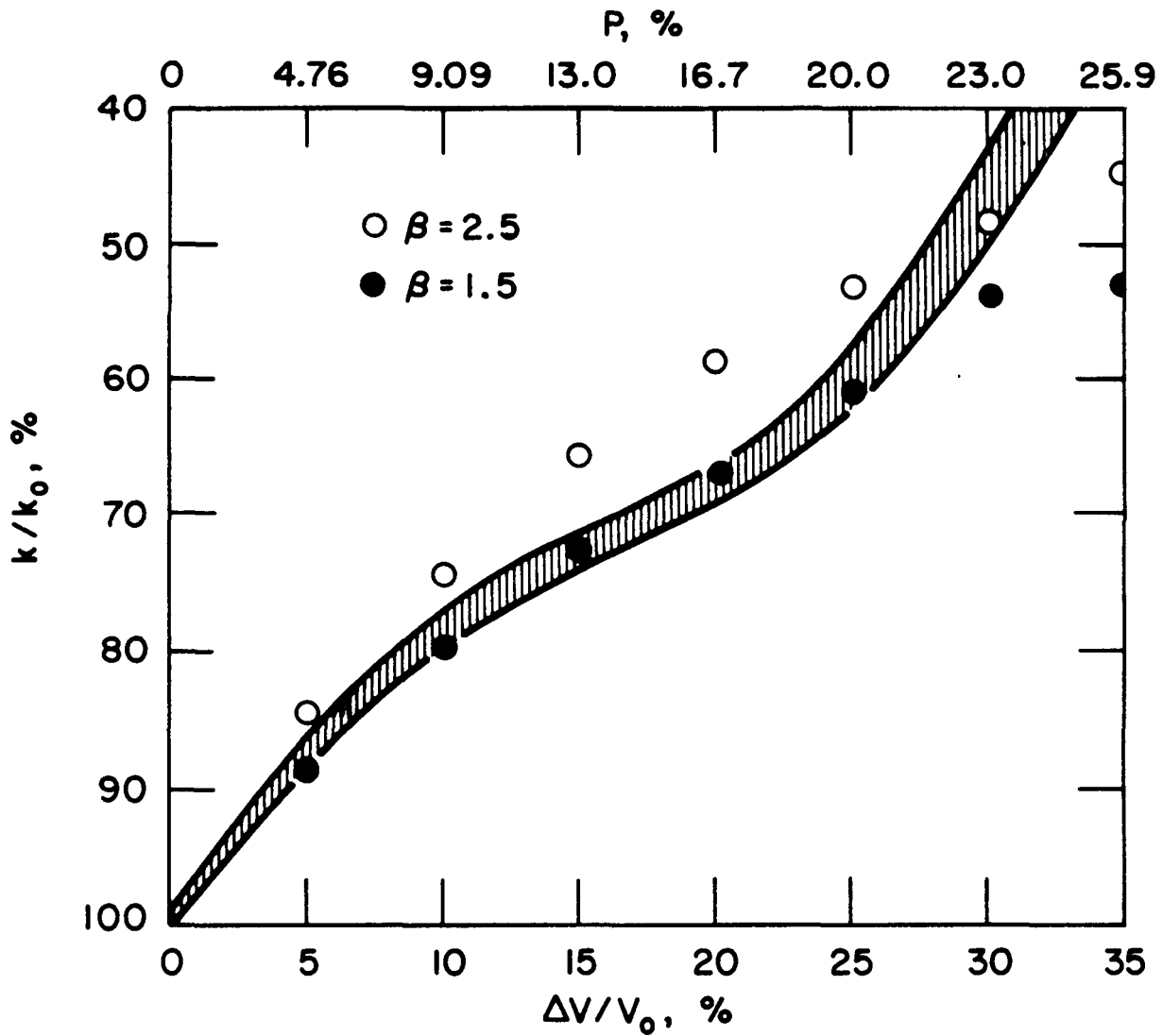


Fig. C.1-5. Comparison of the Analytical Porosity-correction Factor,  $f_p = k/k_0 = (1 - P)/(1 + \beta P)$ , With the In-reactor Data of Beck and Fousek for  $\beta = 1.5$  and  $\beta = 2.5$ .

References for Section C.1

1. Y. S. Touloukian, R. K. Kirby, R. E. Taylor, and P. D. Desai, Thermophysical Properties of Matter, Thermal Conductivity, Metallic Elements and Alloys I, IFI/Plenum, New York (1970).
2. J. H. Kittel et al., Properties of Fuels for Alternate Breeder Fuel Cycles, Argonne National Laboratory Report, ANL-AFP-38, 134 (1977).
3. H. A. Saller, R. F. Dickerson, A. A. Bauer, and N. E. Daniels, Properties of a Fission-Type Alloy, Battelle Memorial Inst. Report BMI-1123 (1956).
4. S. T. Zegler and M. V. Nevitt, Structure and Properties of Uranium-Fission Alloys, Argonne National Laboratory Report ANL-6116 (1961).
5. R. A. Di Novi, Effect of Burnup, Swelling, and Irradiation Temperature on Thermal Diffusivity and Conductivity of Uranium-Fission Alloy, Argonne National Laboratory Report ANL-7886 (1972).
6. W. N. Beck and R. J. Fousek, In-Pile Measurement of Fission Gas Release and Change in Thermal Conductivity for U-5 wt.% Fs Alloy, Trans. Am. Nuc. Soc. 23, 1-78 (1969).
7. P. R. Betten, In-core Measurements of U-5 wt.% Fission Alloy Thermal Conductivity, submitted for presentation at the ANS 1985 Winter Annual Meeting, San Francisco (1985).
8. G. L. Hofman, A Reexamination of the Role of Fission Products in Mk-II Fuel Behavior, Argonne National Laboratory Memo (1979).
9. D. L. Porter, Argonne National Laboratory, personal communication (1985).

**Section C.2**

**Viscosity**

(This section incomplete at this time)

**Section C.3**

**Diffusion Coefficients**

## C. TRANSPORT

### C.3 Diffusion Coefficients\*

#### C.3.1 Uranium-zirconium Alloys

Diffusion in the high-temperature phase of the U-Zr system has been measured by Adda [1] and Muller [2]. The chemical diffusion coefficient

$$\bar{D} = \bar{D}_0 \exp \frac{-Q}{RT}$$

was measured as a function of composition and temperature in both studies, which were in good agreement. The coefficients obtained by Adda are given in Table C.3-1.

TABLE C.3-1. Diffusion Coefficients in Gamma U-Zr

Zr Concentration (at.%)	Q (kcal mole <sup>-1</sup> )	D <sub>0</sub> (cm <sup>2</sup> s <sup>-1</sup> )
10	32	9.5 x 10 <sup>-4</sup>
20	28.6	1.3 x 10 <sup>-4</sup>
30	26.3	3.5 x 10 <sup>-5</sup>
40	27.4	4 x 10 <sup>-5</sup>
50	29.7	8 x 10 <sup>-5</sup>
60	29.7	6.3 x 10 <sup>-5</sup>
70	29.7	5.5 x 10 <sup>-5</sup>
80	34.3	3.2 x 10 <sup>-4</sup>
90	41	7.8 x 10 <sup>-3</sup>
95	47	0.7 x 10 <sup>-2</sup>

\* The reference list for Section C.3 is on page C.3-12.

Measurement of the diffusion couple's interface displacement,  $v$ , as a function of time allowed the calculation of intrinsic diffusion coefficients for uranium and zirconium by means of the following relations:

$$v = (D_u - D_{Zr}) \, dN/dx$$

and

$$\bar{D} = N_u D_{Zr} + N_{Zr} D_u$$

As shown in Fig. C.3-1, the diffusivity of uranium is much larger than that of zirconium in the  $\gamma$ -phase.

Diffusion in the lower-temperature phases has not been studied in much detail. A few experiments at the zirconium-rich side of the system have been reported by Schope [3] and Mash [4]. For temperatures below 600°C Schope reports

$$D_0 = 3.78 \times 10^{-8} \text{ cm}^2\text{s}^{-1}, \quad Q = 15 \text{ kcal mole}^{-1}$$

This activation energy appears to be rather low, probably because more than one phase was present in the diffusion zone, and the concentration profiles were not detailed enough to determine diffusion coefficients in the separate phases.

The activation energy reported by Mash for temperatures below 600°C is even lower and suffers from the same uncertainty, since this experimenter only determined the total width of the interdiffusion zone as a function of time and temperature.

Both experimenters also reported values above 600°C of 47 kcal mole<sup>-1</sup> and 44 kcal mole<sup>-1</sup> respectively, which agree rather well with the data shown at the beginning of this section (see Table C.1-3).

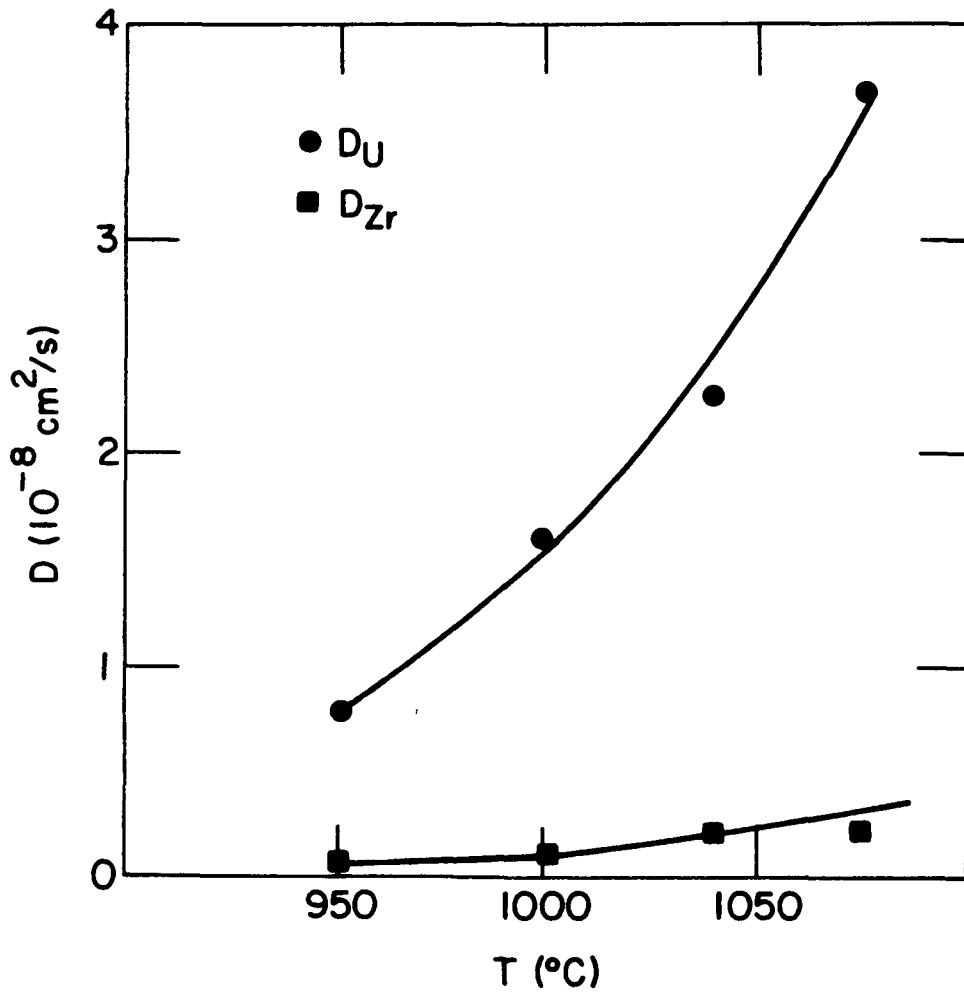


Fig. C.3-1. Intrinsic Diffusion Coefficients of Uranium and Zirconium in Gamma U-Zr.

C.3.2 Uranium-Plutonium-Zirconium Alloys

There are presently no known diffusion data on ternary alloy.

### C.3.3 Others

Available diffusion data on U, Pu, and Zr, as well as the few available data on their binary alloys, are presented in this section to assist the experimenter in estimating diffusivities in the ternary alloy system.

Also offered are limited data on fission-gas diffusion in uranium and thermo-migration in uranium and zirconium.

#### Uranium

Self-diffusion of uranium has been measured in the  $\alpha$ ,  $\beta$ , and  $\gamma$  phases by several experimenters [5,6,7,8], the combined results of which are shown in Fig. C.3-2.

The following coefficients are recommended.

	$\alpha$	$\beta$	$\gamma$
Q (kcal mole <sup>-1</sup> )	40	42	26.5
D <sub>0</sub> (cm <sup>2</sup> s <sup>-1</sup> )	2 x 10 <sup>-3</sup>	1 x 10 <sup>-5</sup>	1.12 x 10 <sup>-3</sup>

#### Plutonium

Self-diffusion of plutonium has been measured in the  $\epsilon$ -phase by Dupuy [9] and in the  $\delta$ - and  $\gamma$ -phases by Tate. [10,26]. The data are shown in Fig. C.3-3. The following coefficients are recommended:

	$\epsilon$	$\delta$	$\gamma$
Q (kcal mole <sup>-1</sup> )	18.5	23.8	16.7
D <sub>0</sub> (cm <sup>2</sup> s <sup>-1</sup> )	2 x 10 <sup>-2</sup>	4.5 x 10 <sup>-2</sup>	2.1 x 10 <sup>-5</sup>

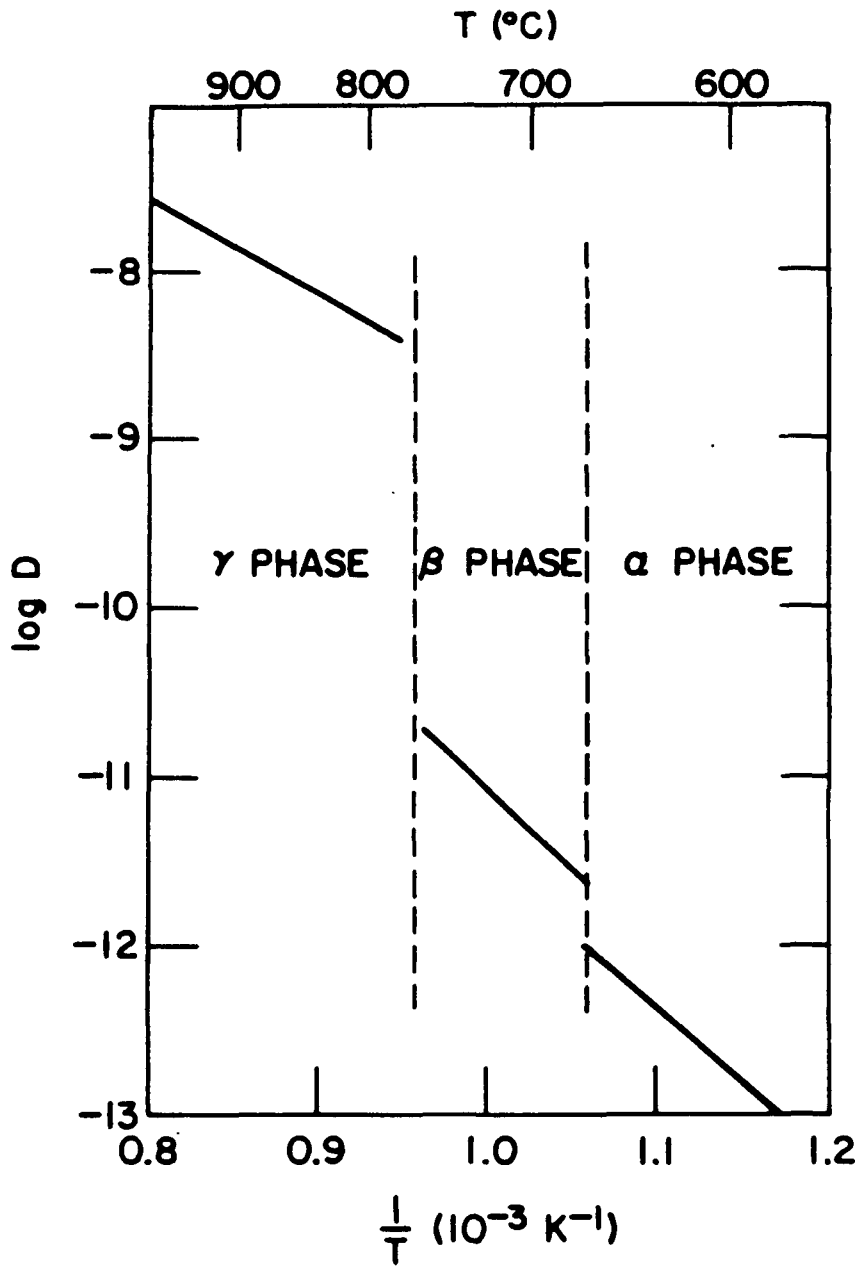


Fig. C.3-2. Self-diffusion Coefficients of Uranium.

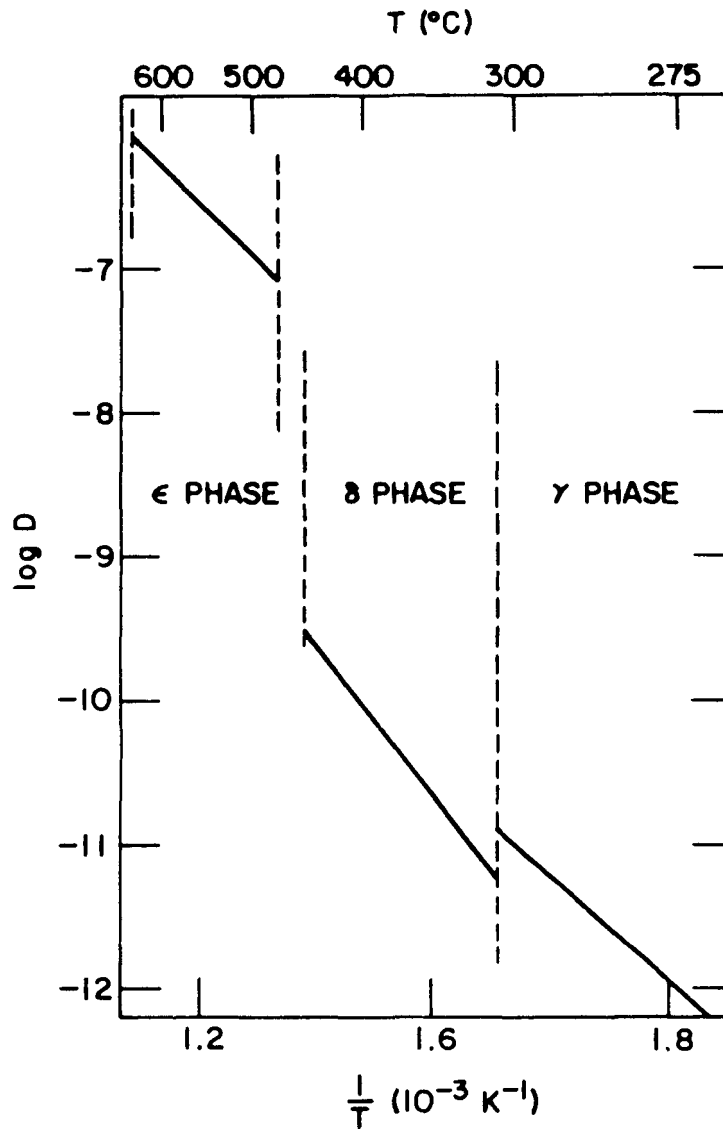


Fig. C.3-3. Self-diffusion Coefficients in Plutonium.

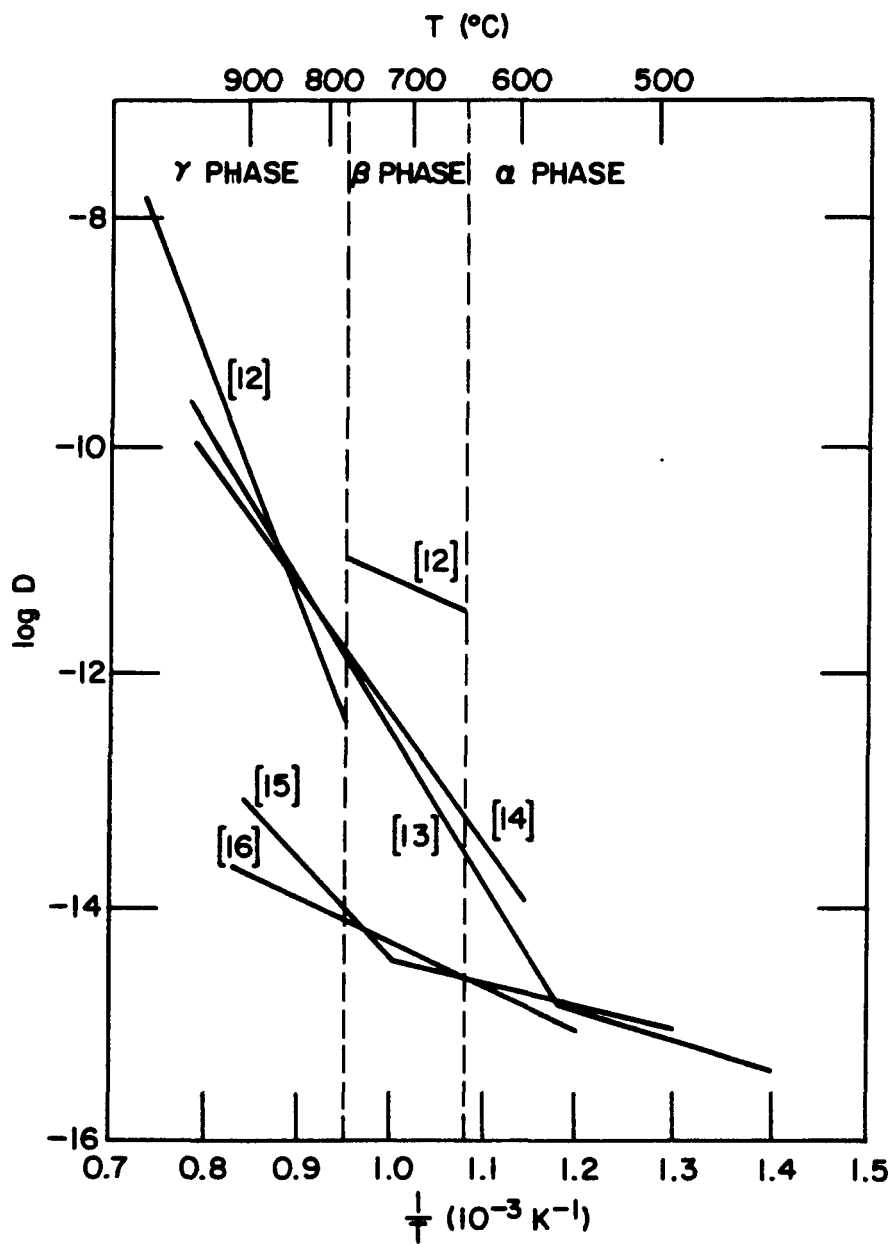


Fig. C.3-4. Xenon-diffusion Coefficients in Uranium.

## Zirconium

Self-diffusion in zirconium ( $\beta$ ) has been determined by several investigators.<sup>23,24,25</sup> The data show a curvature in the Arrhenius plot of  $\log D$  vs.  $T^{-1}$ . Kidson [24] has suggested the following bilinear Arrhenius expression for  $D$  in the  $\beta$ -phase:

$$D = D_{01} \exp \frac{-Q_1}{RT} + D_{02} \exp \frac{-Q_2}{RT}$$

where

$$D_{01} = 1.34 \text{ cm}^2\text{s}^{-1}$$

$$D_{02} = 8.5 \times 10^{-5} \text{ cm}^2\text{s}^{-1}$$

$$Q_1 = 65.2 \text{ kcal mole}^{-1}$$

$$Q_2 = 27.2 \text{ kcal mole}^{-1}$$

Self-diffusion measurements in the  $\alpha$  phase vary widely; however the most recent determination, as follows, is recommended:

$$D_0 = 2.1 \times 10^{-7} \text{ cm}^2\text{s}^{-1}$$

$$Q = 27 \text{ kcal mole}^{-1}$$

## U-Pu

Chemical diffusion coefficients in U-Pu up to a concentration of 17.5% Pu over a temperature range of 400°C to 540°C have been measured by Dupuy [11]. The data are shown in Table C.3-2.

TABLE C.3-2. Diffusion Coefficients in Uranium-plutonium Alloys Between 400°C and 540°C

Pu (wt %)	$D_0$ ( $10^{-7}$ cm <sup>2</sup> /s)	Q (kcal/mole)
0.35	--	--
1.75	0.14	13.4
3.50	0.15	13.7
5.25	0.18	14.1
7.00	0.28	15.2
8.75	0.44	16.3
10.50	0.88	17.9
12.25	1.18	18.8
14.00	2.00	20.0
15.75	2.57	20.6
17.15	--	--

#### Pu-Zr

Plutonium self-diffusion was measured in a 40 at.% Zr alloy over a temperature range of 640°C to 600°C ( $\epsilon$ -phase) [12]. The following coefficients were obtained:

$$D_0^{\text{Pu}} = 4 \times 10^{-2} \text{ cm}^2 \text{ s}^{-1}$$

$$Q = 30 \text{ kcal mole}^{-1}$$

#### Fission-gas Diffusion

Fission-gas diffusion data derived from Xe and Kr release, measured in out-of-pile annealing tests of irradiated uranium, have been reported by several experimenters. The results of the most thoroughly reported experiments are shown in Fig. C.3-4. The data fall in two rather distinct groups. One group is characterized by higher diffusivities in the  $\gamma$ -phase and very high activation energies, e.g., 60 kcal mole<sup>-1</sup> [14] to 98 kcal mole<sup>-1</sup> [13]. This group is probably representative of diffusion of Xe in the U matrix, while the other group

[14,15] that is characterized by a much lower activation energy and lower diffusivities is probably a reflection of primarily grain-boundary diffusion [17]. The different diffusion behavior in the  $\beta$ -phase reported by Perrailon [13], cannot be dismissed, as the experimental work appears to be of excellent quality.

#### Thermomigration

Redistribution of alloy constituents in a temperature gradient called thermomigration or sometimes thermotransport or Soret effect is characterized by a parameter called heat of transport,  $Q^*$ .

Thermomigration experiments in U-Zr and U-Pu-Zr have not been done, and only very limited information is reported on pure uranium and zirconium.

D'Amico [18] reported a value for uranium ( $\gamma$ ) of

$$Q^*/f = +4.7 \pm 0.5 \text{ kcal mole}^{-1}$$

where  $f$  is the tracer diffusion correlation factor. The positive value for  $Q^*$  indicates that uranium migrates to the colder end of the sample.

Campbell [19] and Dubler [20] have reported data on zirconium ( $\beta$ ). Campbell reports a value of

$$Q^*/f = -34 \pm 11 \text{ kcal mole}^{-1}$$

indicating transport to the hotter end of the sample.

#### Surface Diffusion

The recommended surface-diffusion coefficient is obtained from "homologous temperature" arguments by using the low-temperature

correlation given by Gjostein [27], augmented by a high-temperature correlation from the data reported by Gjostein. The result is

$$D_s = 16.6 \exp(-40T_m/RT) + (1.4 \times 10^{-6}) \exp(-13T_m/RT) \text{ m}^2/\text{s}.$$

References for Section C.3

1. Y. Adda, J. Philibert and H. Faraggi, Study of Intermetallic Diffusion Phenomena in the Uranium-Zirconium System, Revue DeMetallurgie 54, 597-610 (1957).
2. N. Muller, Diffusion Studies in the Uranium-Zirconium and Uranium-Nickel Systems, Z. Metallk 50, 652-60 (1959).
3. A. D. Schope and L. R. Jackson, Diffusion Studies of Zirconium-Uranium System, Battelle Memorial Inst. Report BMI-T-24 (1950).
4. D. R. Mash and B. F. Disselhorst, Uranium-Zirconium Diffusion Studies, California Research and Development Co., Livermore Research Lab. LRL-143, AECD-3701 (1954).
5. Y. Adda and A. Kirianenko, Reduction of Self-Diffusion Coefficients in  $\lambda$  Phase of Uranium by Additions of Molybdenum, Zirconium or Niobium, J. Nucl. Mat. 6, 135-6 (1962).
6. S. J. Rothman, L. T. Lloyd, and A. L. Harkness, Diffusion in Uranium, Trans. Am. Inst. Mech. Eng. 218 (1960).
7. A. A. Bochvar et al., Properties of Reactor Materials, Peaceful Uses of Atomic Energy, Proc. 2nd Int. Conf., Geneva, United Nations 5 (1958).
8. G. Martin and B. Perrailon, Grain-boundary, Structure and Kinetics, American Society for Metals, Metals Park, Ohio, Papers, 239 (1980).
9. M. Dupuy and C. R. Head, Study of the Self Diffusion of Plutonium in the  $\epsilon$  Phase, CEA-CEN/FAR, Fontenay-aux-Roses, France, Compt. Rend., Ser. C, 263, 35-8 (1964).
10. R. E. Tate and E. M. Cramer, Self-Diffusion Studies of Delta Plutonium, Trans. Amer. Inst. Met. Engr. 230, 639-44 (1964).
11. M. Dupuy and D. Calais, Chemical Diffusion in the Plutonium-Uranium System, Compt. Rend 260, 1412-15 (1965).
12. J. P. Zanghi and D. Calais, C. R. Head, La Correlation Fusion-Diffusion Dans les Alliages Plutonium-Zirconium, J. Nucl. Mat. 60, (2), 145-150 (1976).
13. B. Perrailon, J. Levy and Y. Adda, Mem. Sci. Rev. Met., L X III, 3 (1966).

14. K. E. Zimen and L. Dahl, The Diffusion of Fission-Xe from U Metal, Zeitschrift fuer Naturforschung (West Germany), 12a, 167-9 (Feb. 1957).
15. F. H. Spedding et al., Thermal Diffusion of Fission Products from Uranium + Uranium Oxide, MUC-NS-3067 (1957).
16. J. C. Bates and A. C. Clark, The Diffusion Xenon in Uranium, FRDC/P-108, (March 1955).
17. C. E. Curtis, Swelling and Inert Gas Diffusion on Irradiated Uranium, Peaceful Uses of Atomic Energy, Proc. 2nd Int. Conf., Geneva, United Nations, 15/P/81 Section 4.1 (1958).
18. J. F. D'Amico and H. B. Huntington, Electromigration and Thermomigration in Gamma-Uranium, J. Phys., Chem. Solids 30, 1607-21 (1969).
19. D. R. Campbell and H. B. Huntington, Thermomigration and Electromigration in Zirconium, Phys. Rev. 179, 601-12 (1969).
20. H. Dubler and H. Wever, Thermo- and Electrotransport in  $\beta$ -Titanium and  $\beta$ -Zirconium, Phys. Status Solidi 25, 109-18 (1968).
21. D. Calais and J. A. Cornet, Self-Diffusion of the fcc  $\epsilon$  Pu Under Hydrostatic Pressure, Mem. Sci. Rev. Met., 69, 493 (1972).
22. American Society for Metals, Diffusion in Body Centered Cubic Metals, International Conference on Diffusion in Body-Centered Cubic Materials, Gatlinburg, Tenn., 1965).
23. E. V. Borisov et al., Metallic Metallov, Izd-Vo AN SSSR, Moscow (1958).
24. C. Kidson and J. McGurn, Self-Diffusion in Body-centered Cubic Zirconium, Canadian Journal of Physics (Canada), 39, (AECL-1271), 1146-57 (1961).
25. J. I. Federer and T. S. Lundy, Diffusion of  $Zr^{95}$  and  $Cb^{95}$  in Bcc Zirconium, Trans. Am. Inst. of Met. Engr. 227, 592-7 (1963).
26. R.E. Tate and G. R. Edwards, Self-diffusion Studies of Gamma-Plutonium, Symposium on Thermodynamics with Emphasis on Nuclear Materials and Atomic Transport in Solids, International Atomic Energy Agency, Vienna (1965).
27. N. A. Gjostein, Surface Self-diffusion in FCC and BCC Metals, Surfaces and Interfaces, 13th Sagamore Army Materials Research Conf., eds. J. J. Burke, N. L. Reed, and V. Weiss: Syracuse University Press, New York 1, 271-304 (1967).
28. R. E. Gruber and J. M. Kramer, Gas Bubble Growth Mechanisms in the Analysis of Metal Fuel Swelling, Argonne National Laboratory ANL/RAS-85-81 (1985).

## D. MECHANICAL

### D.1 Elastic Constants\*

#### D.1.1 Unirradiated 100%-dense U-Zr

F. A. Rough [1] has reported the dynamic Young's modulus (E) for uranium-zirconium alloys as a function of composition and temperature ( $20 < T < 500^{\circ}\text{C}$ ). Figures D.1-1 and -2 summarize the data for induction-melted and arc-melted U-Zr alloys. The Young's modulus for the induction-melted samples is consistently higher than that for arc-melted, indicating the possible role of impurities (e.g., carbon) from the graphite crucibles used.

In order to develop a correlation to predict E as a function of temperature and Zr weight fraction ( $W_z$ ), the temperature dependencies of pure uranium [2] and pure zirconium [2] were considered. The law of mixtures was used to derive

$$E = E_u \left[ \frac{(1 + 0.17 W_z)}{(1 + 1.34 W_z)} \right] \left[ 1 - 1.06 (T - 588) / T_{mu} \right], \quad (1)$$

where  $E_u = 1.60 \times 10^5$  MPa is the Young's modulus of pure U at 588 K ( $315^{\circ}\text{C}$ ) and  $T_{mu} = 1405$  K ( $1132^{\circ}\text{C}$ ) is the melting temperature of pure uranium. The temperature coefficient of 1.06 is consistent with the range of values for metals when the actual temperature is normalized with respect to the melting temperature [2]. The reference temperature of 588 K ( $315^{\circ}\text{C}$ ) was chosen over room temperature because it is the lowest in-reactor temperature for which there are data.

Table D.1-1 shows the comparison between the correlation and the data [1] for arc-melted U-Zr alloys. The Young's modulus varies

---

\* The reference list for Section D.1 is on page D.1-12

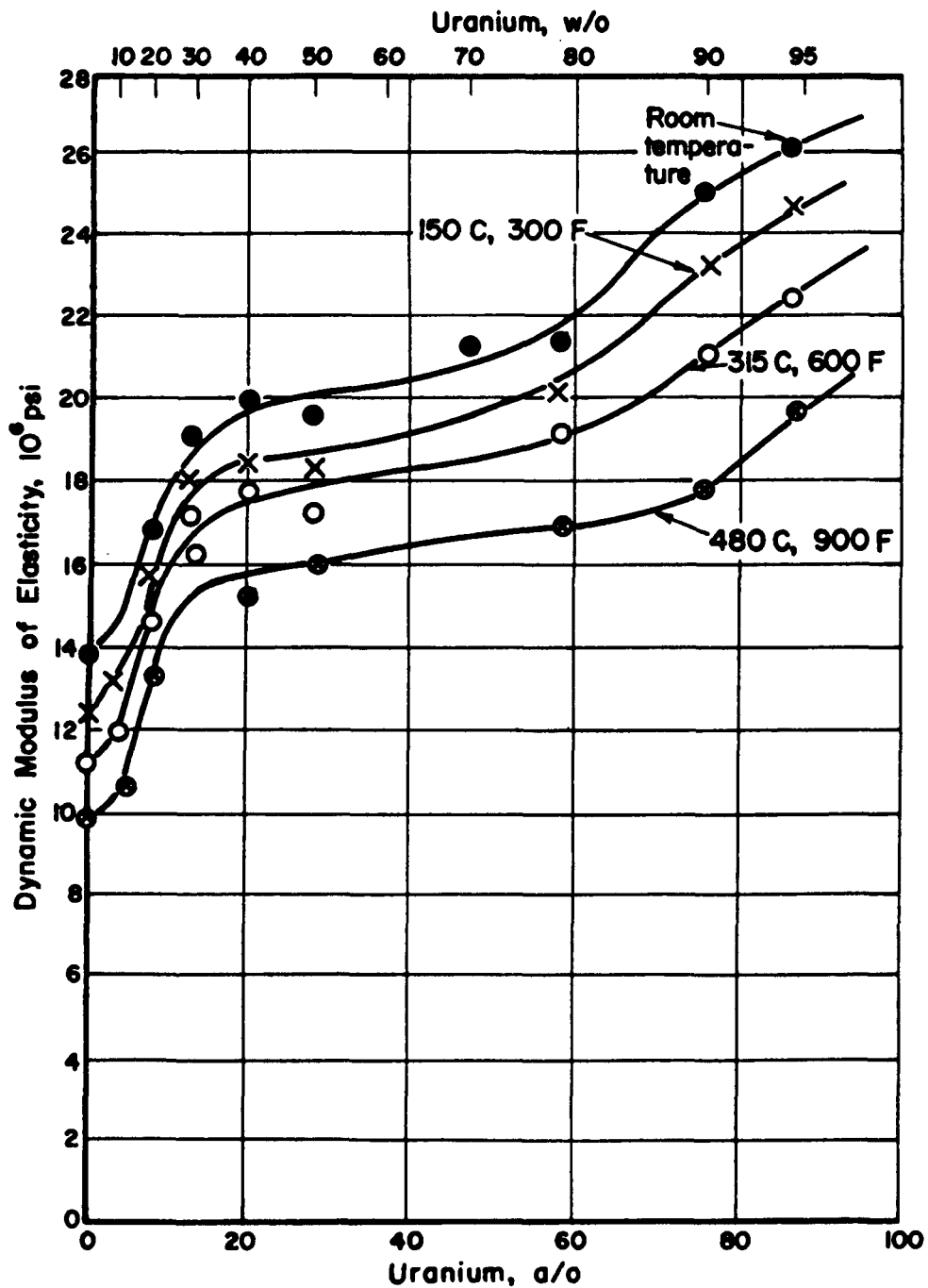


Fig. D.1-1. Variation of Dynamic Modulus of Elasticity at Various Temperatures With Uranium Content in Induction-melted U-Zr Alloys (from Ref. 1).

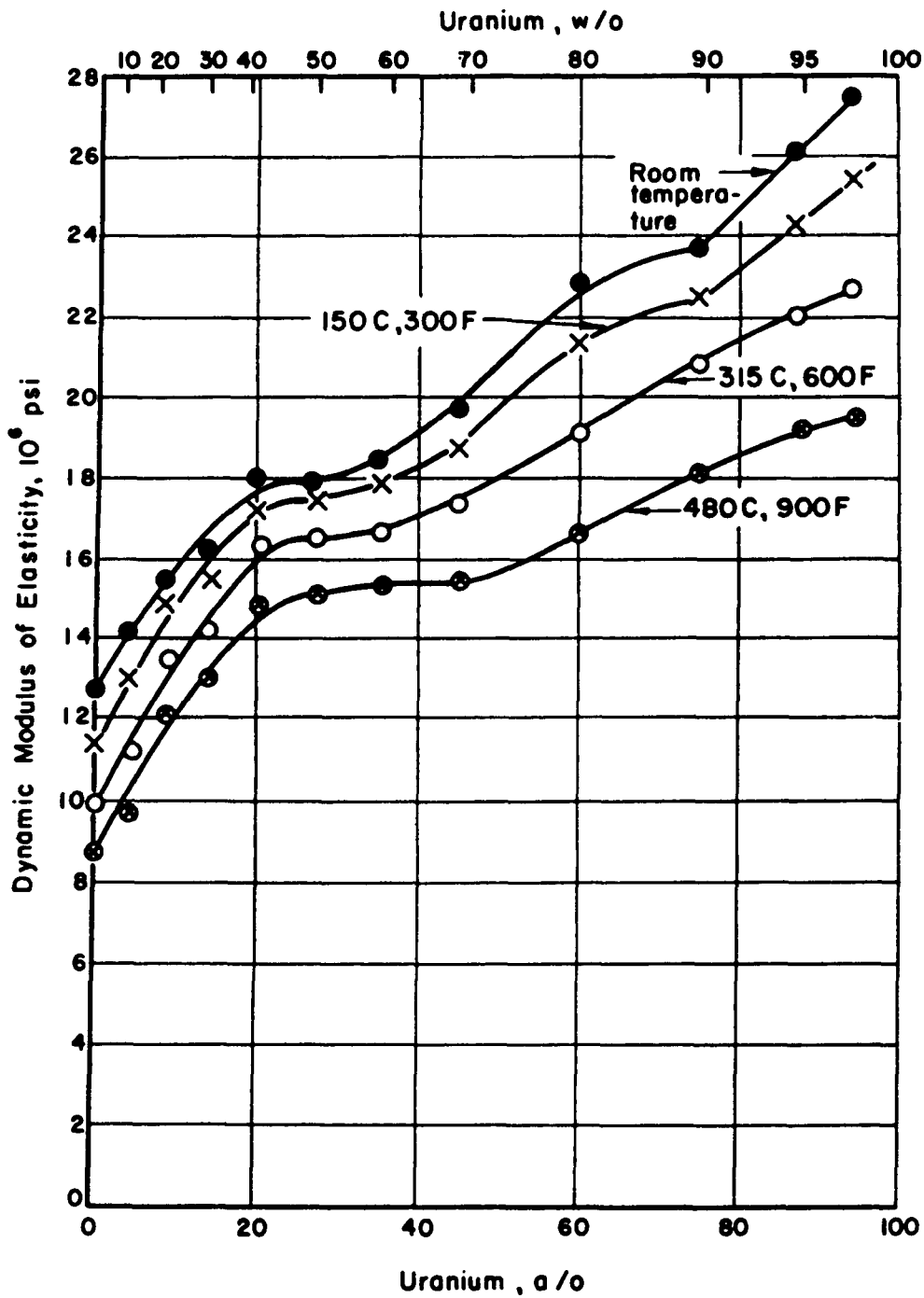


Fig. D.1-2. Variation of Dynamic Modulus of Elasticity at Various Temperatures With Uranium Content In Arc-melted U-Zr Alloys (from Ref. 1).

inversely with both temperature and Zr weight fraction. The maximum deviation between the correlation and the data is 9% for  $W_Z \leq 0.4$  and  $293 \leq T \leq 753$  K. No estimate is available on the accuracy of the data. The major uncertainty is associated with impurity content and fabrication procedures.

**Table D.1-1. Comparison Between the Correlation Values and Experimental Data (from Fig. D.1-1) for U-Zr Alloys. Correlation values are in parentheses.**

<u>T (K)</u>	<u>T (°C)</u>	<u>0<sup>a</sup></u>	<u>2.5</u>	<u>5</u>	<u>10</u>	<u>20</u>	<u>30</u>	<u>40</u>
293	20	1.97 (1.98)	1.89 (1.90)	1.81 (1.85)	1.63 (1.75)	1.58 (1.61)	1.36 (1.47)	1.27 (1.27)
423	150	1.81 (1.80)	1.75 (1.75)	1.68 (1.70)	1.55 (1.61)	1.47 (1.47)	1.29 (1.35)	1.23 (1.25)
588	315	1.60 (1.60)	1.57 (1.56)	1.52 (1.51)	1.43 (1.43)	1.32 (1.30)	1.20 (1.20)	1.15 (1.11)
753	480	1.37 (1.40)	1.34 (1.36)	1.32 (1.32)	1.26 (1.26)	1.14 (1.14)	1.07 (1.05)	1.06 0.97

<sup>a</sup> Extrapolated values from curves in Fig. D.1-1

Equation 1 is recommended for the Young's modulus of 100%-dense U-Zr alloys for temperatures below the phase-change temperature (~650°C). The effects of the phase change and porosity will be discussed subsequently.

A similar approach was used to estimate Poisson's ratio ( $\nu$ ) for U-Zr alloys. Based on the  $\nu$  values [3] for pure uranium and pure zirconium, the law of mixtures was used to derive

$$\nu = 0.24 [(1 + 3.4 W_Z)/(1 + 1.9 W_Z)][1 + 1.2 (T - 588)/T_{\mu}] \quad (2)$$

The Poisson's ratio for pure Zr varies from -0.33 at room temperature to -0.35 at the  $\alpha$ -to- $\beta$  phase-transition temperature of 862°C. The Poisson's ratio for pure U varies from -0.19 at room temperature to -0.29 at 300°C, which is the limit of the data base. Both of these results are dependent on the method of fabrication and, in turn, on the preferred orientation of these anisotropic materials.

No data for the Poisson's ratio of U-Zr alloys are available for comparison with Eq. 2. However, Eq. 2 is recommended for 100%-dense U-Zr alloys for temperatures below the phase-change temperature (e.g., ~650°C for U-10Zr). A maximum value of  $\nu = 0.5$  should also be invoked. For U-10Zr at 650°C, Eq. 2 predicts  $\nu = 0.35$  which is reasonable. The effects of phase change and porosity are discussed in the following.

The effective elastic properties ( $E$ ,  $\nu$ ) generally decrease with increasing porosity. Correction factors of the form

$$f_e = E/E_{100} = 1 - \beta_e P \quad (3)$$

and

$$f_\nu = \nu/\nu_{100} = 1 - \beta_\nu P \quad (4)$$

have been used in the modeling of ceramic nuclear fuels [4,5]. The  $\beta_e$  values for UC, UN, and  $UO_2$  (based on experimental data) are 1.54, 2.72, and 1.66, respectively. Similarly, the  $\beta_\nu$  values are 0.21, 1.31, and 0.91 for UC, UN, and  $UO_2$ , respectively. Averaging these values gives  $\beta_e = 1.2$  and  $\beta_\nu = 0.8$ . It is recommended that these  $f_e$  and  $f_\nu$  factors be applied to Eqs. 1 and 2, respectively, in order to estimate the decrease in effective elastic properties with increasing fission-gas porosity.

The change in elastic properties with phase change is more complicated to unravel because of the sparsity of the data base. Zirconium exhibits a decrease of ~13% in Young's modulus from 862°C to

900°C [2]. No information was found on the change in shear modulus or Poisson's ratio beyond the phase-change temperature. In Fig. D.1-3 the shear modulus of pure U is shown to change slope at the  $\alpha$ -to- $\beta$  transition temperature of  $-670^\circ\text{C}$  and the  $\beta$ -to- $\gamma$  transition temperature of  $-775^\circ\text{C}$  [6]. If the  $\beta$  phase is ignored because it is suppressed in U-Zr alloys, then it appears that one would expect a decrease in shear modulus of  $\sim 30\%$  if the  $\alpha$ -to- $\gamma$  phase change occurred at  $-650^\circ\text{C}$ . In the absence of more data, the preliminary recommendation is that  $E$  be decreased by  $30\%$  at the phase-change temperature and  $\nu$  be held continuous through the phase change. This approach is consistent with the data for  $G$ , but it is certainly not a unique solution to the problem.

In summary, the following equations are recommended for the Young's modulus of U-Zr alloys:

$$E = E_u (1 - 1.2P) \left[ \frac{1 + 0.17 W_z}{1 + 1.34 W_z} \right] \left[ 1 - 1.06 (T - 588)/T_{\text{mu}} \right], \quad (5a)$$

where  $T$  = temperature ( $<$  phase-change temperature) in K

$P$  = porosity fraction

$W_z$  = Zr weight fraction

$T_{\text{mu}}$  = 1405 K, the melting temperature of pure U

and

$E_u = 1.6 \times 10^5$  MPa, the Young's modulus for pure U at the chosen reference temperature of 588 K.

For  $T > T_p$  where  $T_p$  is the  $\alpha$ -to- $\gamma$  phase-change temperature, the recommended Young's modulus ( $E_\gamma$ ) for  $\gamma$ -phase U-Zr is

$$E_\gamma = E - 0.3E_p, \quad (5b)$$

where  $E_p = E(T_p)$  and  $E$  is defined by Eq. 5a.

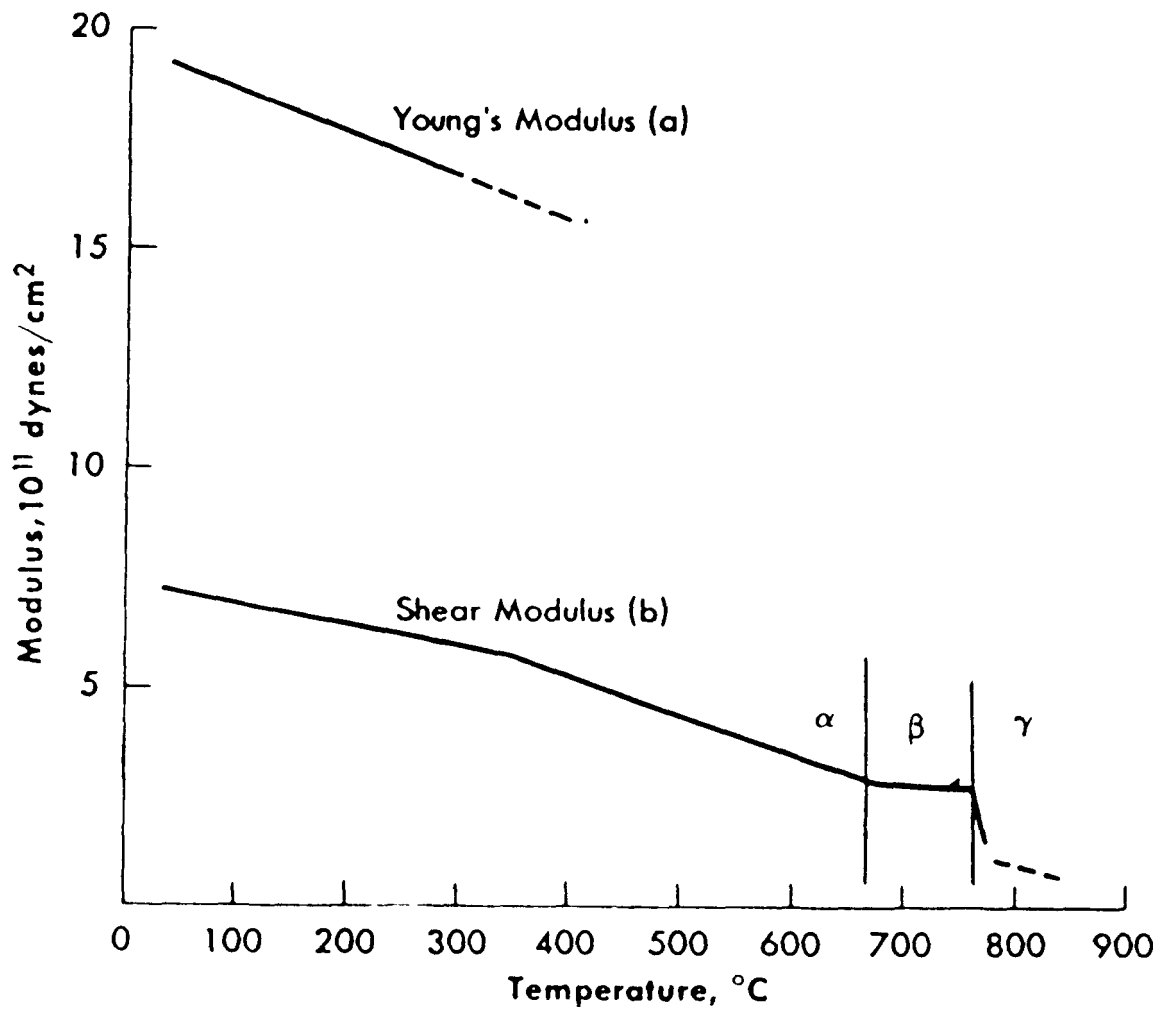


Fig. D.1-3. Effect of Temperature on Elastic Moduli of U (From Ref. 6).

For the Poisson's ratio of U-Zr alloys, the recommended equation is

$$\nu = \nu_u (1 - 0.8P) \left[ \frac{1 + 3.4 W_z}{1 + 1.9 W_z} \right] [1 + 1.2 (T - 588)/T_{\mu}], \quad (6)$$

where  $\nu_u = 0.24$  is the Poisson's ratio of pure U at the chosen reference temperature of 588 K.

### D.1.2 Uranium-Plutonium-Zirconium Alloys

No dynamic data are available for the elastic properties of U-Pu-Zr alloys. The static (i.e., tensile-test) data are generally believed to be unreliable because of the effect of other deformation mechanisms which dominate even at room temperature. Even pure U does not have a well defined static modulus at room temperature [6]. The static data for Young's modulus of U-Pu-Zr alloys are summarized in Table D.1-2 [7]. Most of these data imply at least an order of magnitude decrease in Young's modulus for a Pu weight fraction of 15%.

The Young's modulus for pure Pu is less than that for U [3]. Based on a simple law of mixtures, it is reasonable to expect the Young's modulus of U-Pu-Zr alloys to vary inversely with Pu weight fraction ( $W_p$ ). In order to attempt to quantify this dependency, the room-temperature data for cast U-11Pu-6.3Zr are used to estimate the decrease in E with  $W_p$ . This results in the following correlation for E:

$$E = E_u (1 - 1.2P) \left[ \frac{1 + 0.17 \frac{W_z}{W_p}}{1 + 1.34 \frac{W_z}{W_p}} - W_p \right] [1 - 1.06 (T - 588)/T_{mu}], \quad (7)$$

where  $E_u$ , P,  $W_z$ , T, and  $T_{mu}$  have the same definition as in Eq. 5a and  $W_p$  is the Pu weight fraction. For temperatures above the  $\alpha \rightarrow \gamma$  phase change temperature, Eq. 5b is recommended.

No data are available for the Poisson's ratio of U-Pu-Zr alloys. The room-temperature value for Pu( $\alpha$ ) [3] is less than that for U( $\alpha$ ). However, as Pu goes through so many phase changes between room temperature and typical U-Pu-Zr phase-change temperatures, it is difficult to use the law of mixtures in this application. Thus, Eq. 6 is recommended for U-Pu-Zr alloys.

TABLE D.1-2. Static Young's-modulus Values for Several U-Pu-Zr Compositions (from Ref. 7).

<u>Alloy</u>	<u>Fabricated Method</u>	<u>T (K)</u>	<u>E (10<sup>5</sup> MPa)</u>
U-15Pu-10Zr	Extruded	298	0.15
		573	0.14
		623	0.062
		673	0.028
U-15Pu-12.2Zr	Cast	298	0.097
U-11Pu-6.3Zr	Cast	298	1.70
		948	0.14

D.1.3 Others

Saller et al. [8] have reported some values of Young's modulus for U-5Fs alloys. For as-rolled flat-plate specimens tested statically at 563 K and 813 K, the respective values for E are  $0.68 \times 10^5$  MPa and  $0.63 \times 10^5$  MPa. Because static methods are not considered as reliable for determining the E values for uranium alloys, these data have not been used to guide the development of U-Zr and U-Pu-Zr correlations for elastic properties. It is recommended that Eqs. 5 and 6 be used to describe U-5Fs behavior with  $W_z = 0.05$ . This would probably give a more accurate representation of the U-5Fs elastic properties than the static U-5Fs data.

References for Section D.1

1. F. A. Rough, An Evaluation of Data on Zirconium-Uranium Alloys, Battelle Memorial Inst. Report BMI-1030 (1955).
2. V. W. Koester, Die Temperaturabhängigkeit des Elastizitäts Moduls Reiner Metalle, Z. Fur Metallkunde 39 (1948).
3. Bernard G. Ryle et al, Uranium, Reactor Handbook, 2nd Ed., Materials, edited by C. R. Tipton, Jr., Interscience Publishers, New York, I, 123-124 (1960).
4. M. C. Billone, UNCLE-T: A Computer Code for the Analysis of Steady-State and Transient Performance of (U,Pu)C and (U,Pu)N Fuels, Argonne National Laboratory, Argonne National Laboratory, ANL-AFP-79 (1979).
5. M. C. Billone et al, The LIFE-III Fuel-Element Performance Code, USEnergy Research and Development Admn. Report ERDA-77-56 (1977).
6. A. N. Holden, Physical Metallurgy of Uranium, Addison-Wesley, Reading, MA, 59-63 (1957).
7. D. R. Harbur et al., Studies of the U-Pu-Zr System for Fast Breeder Reactor Applications, Los Alamos Scientific Laboratory Report, LA-4512 (1970).
8. H. A. Saller et al., Properties of a Fissium-Type Alloy, Battelle Memorial Inst. Report BMI-1123, 31 (1956).

**Section D.1**

**Elastic Constants**

**Section D.2**

**Creep**

## D. MECHANICAL

### D.2 Creep\*

#### D.2.1 Uranium-Zirconium Alloys

Tensile-creep data for U-Zr alloys of various compositions have been reported by Battelle Memorial Institute [1,2]. Both secondary (minimum) creep rate and time to 1% creep were reported. Comparison of the minimum creep rates with a calculated average creep rate to 1% strain indicates that primary creep was not important in these tests. The strain-time curves given in Ref. 2 support this conclusion. Unfortunately, most of the data are for alloys containing greater than 45 wt % zirconium where at low temperatures the equilibrium phases consist of pure  $\delta$  or  $\delta$  plus  $\alpha$  zirconium. Such high concentrations of zirconium are probably not relevant to fast-reactor fuel, even though zirconium migration is expected to increase the zirconium concentration in certain regions of the fuel during irradiation.

Because of the scarcity of data, correlations to estimate the thermal creep of uranium-zirconium alloys have been developed from theoretical models plus available data on uranium and uranium-plutonium-zirconium alloys. These correlations and their fit to the U-Zr data are given in Section D.2-3.

---

\* The reference list for Section D.2 is on page D.2-12.

## D.2.2 Uranium-Plutonium-Zirconium Alloys

The thermal creep of U-Pu-Zr alloys has been measured using cast [3] and extruded [4] tensile specimens. The results reported from these studies are the times to reach 2% strain at constant load (constant engineering stress) and constant temperature, as summarized in Table D.2-1. This table shows that, although the temperature ranges do not overlap, the data for the cast alloys and extruded alloys appear inconsistent, with the extruded samples creeping much more rapidly. Part of the difference may be due to the difference in fabrication methods, since uranium is known to work-harden considerably. However, hardness values for the as-cast material prior to extrusion were identical to the hardness values of the extruded material [4]. Furthermore, the effects of work hardening would be expected to be more important to the low-temperature, high-strain-rate tensile properties than to the high-temperature creep properties. A more likely explanation for the high creep rates of the extruded material is that these tests were performed at much higher stresses, lower temperatures, and shorter times, where primary and tertiary components of the creep strain dominate the lower-rate secondary creep strain.

Most of the times to 2% strain reported for creep of cast U-Pu-Zr [3] were extrapolated from tests terminated at about 1% strain. It was established that the strain-time relationship for this material was approximately linear on log-log coordinates to at least 5% strain so the extrapolation was meaningful. Data for times to creep to 1, 2, 3, 4 and 5% strain at 650°C given in Fig. 8 of Ref. 3 indicate that the slope is about 1, suggesting that most of the creep strain accumulated in the constant-rate secondary regime. As with U-Zr alloys, correlations for creep of U-Pu-Zr are included in the general discussion of creep of metallic fuels given in the following section.



### D.2.3 Others

In the  $\alpha$ -uranium-rich regimes of U-Zr and U-Pu-Zr alloys, creep appears to be dominated by creep of the  $\alpha$  uranium matrix. Data on creep of uranium is therefore included in the present discussion. As pointed out by Holden [5, Section 5-5] much of the early uranium creep data was extremely inconsistent due to poor control of grain size and grain orientation and control of temperature fluctuations during the tests. It is known in this regard that polycrystalline uranium samples elongate when repeatedly heated and cooled in the  $\alpha$  temperature range [6] even without load.

More reliable data on creep of uranium has been measured by Shober, Marsh, and Manning [7]. Minimum creep rates were reported for temperatures ranging from 100 to 500°C and stresses yielding creep rates ranging from  $2 \times 10^{-5}$  to  $2.5 \text{ h}^{-1}$ . Secondary creep data at 500°C reported in the Reactor Materials Handbook [8] and the creep data of McIntosh and Heal [9] for tests at 400, 500 and 600°C appear consistent with the data of Shober et al.

The form of the secondary creep equation used here to correlate the data for all metallic fuels is the form used by Solomon, Routbort, and Voglewede to represent creep of  $\text{UO}_2$  [10]. The total plastic strain rate  $\dot{\epsilon}$  is given by

$$\dot{\epsilon} = C_1(d)\sigma \exp(-Q_1/RT) + C_2\sigma^n \exp(-Q_2/RT) \quad (1)$$

where

- $\dot{\epsilon}$  = secondary creep rate,  $\text{s}^{-1}$
- $\sigma$  = equivalent stress, MPa
- $T$  = absolute temperature, K
- $R$  = universal gas constant =  $1.987 \text{ cal g-mole}^{-1} \text{ K}^{-1}$
- $Q_1, Q_2$  = activation energies,  $\text{cal g-mole}^{-1}$
- $d$  = grain size,  $\mu\text{m}$
- $C_1, C_2$  = material functions

In Eq. 1 the first term represents diffusional creep and the second term dislocation creep. In-reactor fission effects and low-temperature deformation mechanisms such as dislocation glide and twinning, which are important in  $\alpha$  uranium at temperatures less than 400°C, are not considered here.

The temperature dependence of creep of uranium in the  $\alpha$  regime has been determined by Shober et al. to obey an Arrhenius relationship with an activation energy  $Q$  of 52,000 cal g-mole<sup>-1</sup>. This value of  $Q$  is approximately equal to the value of the activation energy for self-diffusion (55,000 cal g-mole<sup>-1</sup> [11, p. 296]) in  $\alpha$  uranium, as would be expected from theory. All of the low-temperature creep data for both uranium and the cast U-Pu-Zr have therefore been reduced using the Zener-Holloman parameter

$$Z = \epsilon \exp (52,000/RT)$$

as shown in Fig. D.2-1. The data are seen to follow the same curve with a slope of 1 at low stresses and a slope  $n = 4.5$  at higher stresses, as predicted by Eq. 1. It is noted that the power-law slope of 4.5 has been frequently observed for other metals [12]. The constants  $C_1$  and  $C_2$  have been chosen here to minimize the least-squares error between the calculated and measured values of  $\log Z$ . The final form of Eq. 1 for creep in the  $\alpha$  regime,

$$\epsilon = 0.5 \times 10^4 \sigma \exp (-52,000/RT) + 6.0 \sigma^{4.5} \exp (-52,000/RT) \quad (2)$$

is compared with the data in Fig. D.2-1. The root-mean-square error in  $\log Z$  is 0.4 for the 47 data points.

The grain-size dependence of the linear diffusional creep term in Eq. 1 is expected to vary from  $d^{-2}$  to  $d^{-3}$  depending on whether Nabarro creep or Coble creep dominates. In addition, Harper-Dorn dislocation creep has the same linear stress dependence but is independent of grain size.

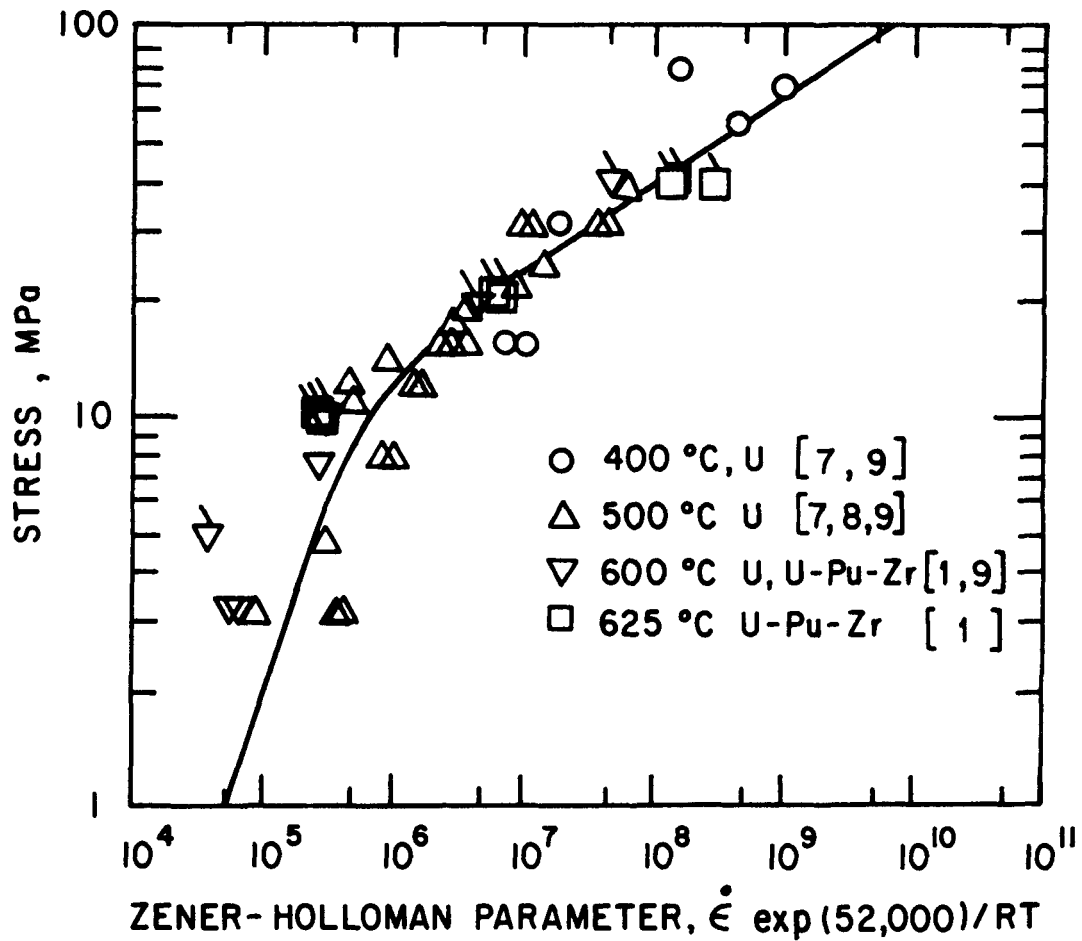


Fig. D.2-1. Secondary Creep of Metal Fuels. Open symbols are data for uranium. Symbols with flags were calculated for cast U-Pu-Zr alloys of various compositions using the reported times to 2% strain. References are given in the brackets. The curve is the least-squares fit to the data using Eq. 1.

Most of the data in the low-stress range in Fig. D.2-1, where the creep rate is linear in stress, come from the experiments of McIntosh and Heal [9]. The grain size in these experiments was controlled to about 160  $\mu\text{m}$ . Although small variations in grain size show the expected behavior of decreasing creep rate with increasing grain size, the variations are not sufficient to determine the power of the dependence. Other experiments on uranium and uranium alloys with larger variations in grain size gave powers that were intermediate between 1 and 2 [9].

Slattery and Miller [13] also measured the creep strength of  $\alpha$  uranium and dilute alloys with different grain sizes at a test temperature of 500°C. The experiments used beams that were allowed to sag in a furnace under their own weight. Although these experiments are somewhat difficult to interpret, it is noted that at the low stress levels of the tests (0.75 MPa maximum) the strain rate was a linear function of stress, as predicted by Eq. 2. However, Slattery and Miller reported that there was no significant difference in creep strength after different heat treatments to refine the grain size. Compared to their data, Eq. 1 predicts creep rates that are about half an order of magnitude too high.

Most of the uranium and the U-Pu-Zr data appear to be fit reasonably well by Eq. 2. In the absence of more extensive data, it is recommended that Eq. 2 be used to estimate the thermal creep of IFR alloys in temperature regimes where the  $\alpha$  phase is present.

At high temperatures, uranium, zirconium, and plutonium are mutually soluble and form a solid-solution  $\gamma$  phase. The only available data on creep of U-Pu-Zr alloys in the  $\gamma$  regime appears to be the measurements of Savage [3] as reproduced in Table D.2-1. Average creep rates calculated from these data by dividing the creep strain by the time are plotted in Fig. D.2-2. The 600°C and 625°C data are the same data that are plotted in Fig. D.2-1 against the Zener-Holloman parameter for creep at lower temperatures. Note that in Fig. D.2-2

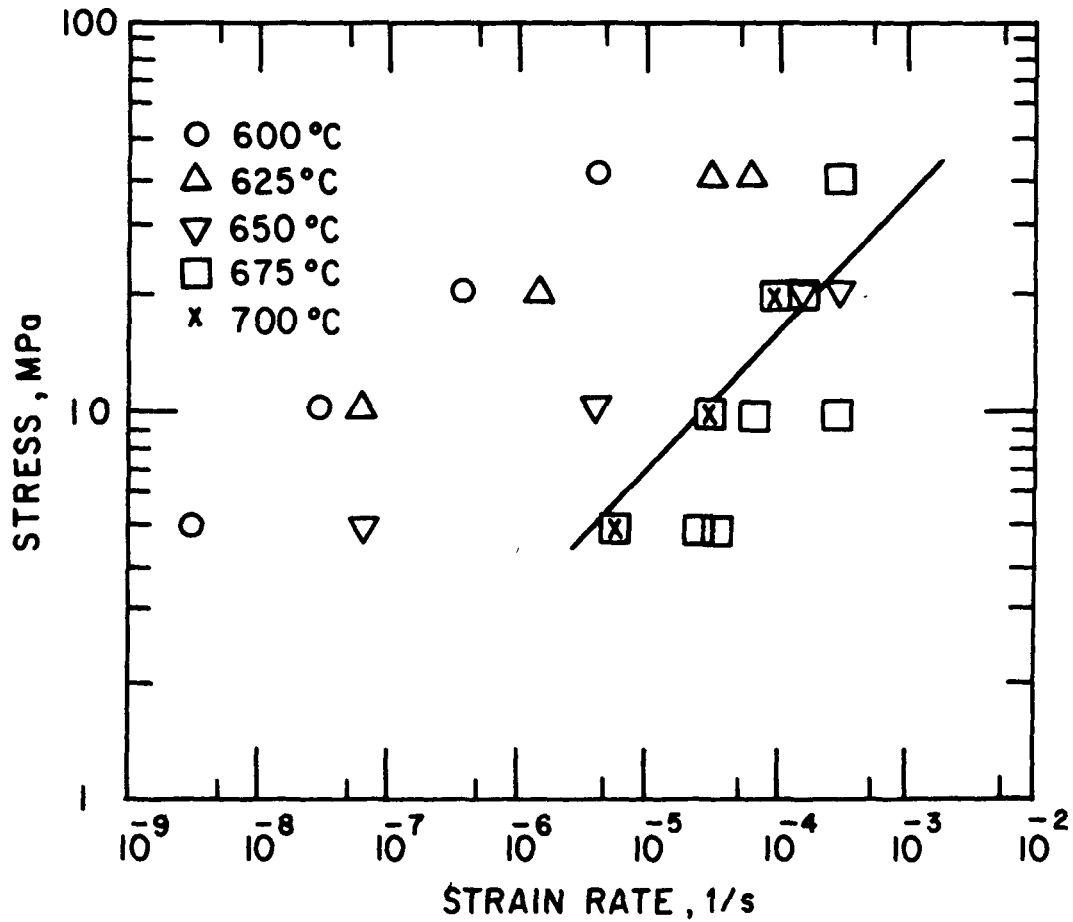


Fig. D.2-2. Secondary Creep of U-Pu-Zr Alloys. Data are given by the symbols. Calculated creep rates at 700°C are represented by the curve.

there is a large increase in the creep rate between 625°C and 700°C. This is not surprising, because the creep mechanisms depend on diffusion and a large increase in the diffusion coefficient might be expected upon transformation to the BCC  $\gamma$  phase. A similar transformation from  $\alpha$  to  $\gamma$  in pure uranium increases the diffusion coefficient by about 5 orders of magnitude [11, p. 299].

**TABLE D.2-2. Measured and Calculated Minimum Creep Rates of Low-Zirconium Binary U-Zr Alloys at 818°C.**

Alloy Composition (wt %)		Stress (MPa)	Measured Creep Rate (%/h)	Calculated Creep Rate (%/h)
U	Zr			
87.4	12.6	9.8	43.0	51.0
92.9	7.1	3.4	0.65	2.2
74.2	25.8	3.4	1.0	2.2

Although in pure metals the ratio of the creep rate on either side of a phase transformation is often directly proportional to the ratio of the self-diffusion coefficients [14, p. 93], the case is not so simple for solid solutions. Here the presence of solute atoms can hinder the rate of dislocation glide, making it possible that the creep rate is governed by dislocation glide rather than climb. Weertman [12] has shown that in this case the creep-rate power is 3. The temperature dependence of creep is again determined by diffusion, but the situation is more complicated in solid solutions than in pure metals because of the different species that are present. In many cases small alloy additions do not change the creep activation energy [14]. In other cases the activation energy is increased or decreased.

We have assumed here that creep of U-Pu-Zr and U-Zr alloys is governed by dislocation glide in the  $\gamma$  regime. The phenomenological creep equation is of the form

$$\epsilon = C_4 \sigma^3 \exp(-Q_4/RT) \quad (3)$$

where  $Q_4$  is the creep activation energy and  $C_4$  may be a function of composition. In lieu of additional creep data we assume that  $Q_4$  is the same as the activation energy for creep of the pure  $\gamma$ -uranium solvent, which in turn is the activation energy for self-diffusion in  $\gamma$  uranium. Thus,

$$Q_4 = 28,500 \text{ cal g-mole}^{-1} \text{ [11, p.296].}$$

The constant

$$C_4 = 8.0 \times 10^{-2} \text{ MPa}^{-3} \text{ s}^{-1}$$

is chosen to fit the 700°C data for U-18.5 wt % Pu-14.1 wt % Zr shown in Fig. D.2-2. Calculated values of strain-rate are compared with the 700°C data in Fig. D.2-2.

A correlation of the form of Eq. 3 was also developed by Walter, Golden, and Olson [15] in their study of U-Pu-Zr slumping in the high-temperature  $\gamma$  regime. The data [16] that were used in this correlation are the same data that were used for the extrapolations of U-18.5 wt % Pu-14.1 wt % Zr creep strain at 675 and 700°C given in Table I. The temperature above which the constituents are mutually soluble at this composition is about 660°C [17]. The creep tests at both 675 and 700°C were therefore probably performed on material in the  $\gamma$  phase, although some of the data given in Table D.2-1 and Fig. D.2-2 do show anomalous behavior. Nevertheless, the creep power  $n = 2.65$  and activation energy  $Q = 27,000 \text{ cal g-mole}^{-1}$  (calculated using Fig. 9 of Ref. [15]) determined from these data are in very good agreement with the values of  $n = 3.0$  and  $Q = 28,500$  that were selected above on the basis of theoretical models.

As a further check on the activation energy and the importance of composition changes, we have also compared calculations using Eq. 3 with data [2] on creep of low-zirconium U-Zr binary alloys at 818°C. The results are shown in Table D.2-2. It would appear from this table that within the range of zirconium contents of interest, the creep rate is not a strong function of the composition. It should be noted, however, that very high zirconium alloys [2] show significantly reduced creep rates with a minimum at 46 wt % for tests at 818°C.

The structure of U-Pu-Zr and U-Zr between the  $\alpha$  and  $\gamma$  regimes discussed here is very complex and depends strongly on composition [17]. The 650°C data and some of the 675°C data shown in Fig. D.2-2 are for alloys in this regime. There is some indication of creep rates greater than would be calculated by extrapolating either the low-temperature or higher-temperature equations given here, although the data are closer to the creep rates for the pure  $\gamma$  phase. It is therefore recommended that Eq. 3 be used to estimate secondary thermal creep rates for U-Zr and U-Pu-Zr alloys at temperatures above which the  $\alpha$  phase is no longer present.

References for Section D.2

1. F. A. Rough, An Evaluation of Data on Zirconium-Uranium Alloys, Battelle Memorial Inst. Report BMI-1030 (1955).
2. H. A. Saller, J. T. Stacy, N. S. Eddy and H. L. Klebanow, Creep Strengths of Uranium Alloys at 1500 and 1800F, Batelle Memorial Inst. Report BMI-834 (1953).
3. H. Savage, Mechanical Properties of U-Pu-Zr and U-Pu-Ti Alloys, Argonne National Laboratory Report ANL-7155, 20 (1965).
4. D. R. Harbur, J. W. Anderson, and W. J. Maraman, Studies on the U-Pu-Zr Alloy System for Fast Breeder Reactor Applications, Los Alamos Scientific Laboratory Report LA-4512 (1970).
5. A. N. Holed, Physical Metallurgy of Uranium, Addison-Wesley, Reading, MA (1958).
6. R. M. Mayfield, Effects of Cycling Variables upon Growth Rate of 300°C Rolled Uranium, Trans. Am. Soc. Metals 50, 926 (1958).
7. F. R. Shober, L. L. Marsh and G. K. Manning, The Mechanical Properties of Beta-Quenched Uranium at Elevated Temperatures, Battelle Memorial Inst. Report BMI-1035 (1955).
8. United States Atomic Energy Commission, Relative Work Hardening Rates of Uranium, Stainless Steel, Nickel and Aluminum, Table 1.22.11, Creep of Uranium at 930°F, The Reactor Materials Handbook, 3, Materials, Section 1, General Properties, AECD-3647, 400 (1955).
9. A. B. McIntosh and T. J. Heal, High Temperature Properties of Uranium and Its Alloys, Peaceful Uses of Atomic Energy, Proc. of the 2nd Int. Conf., Geneva, United Nations, 6, P/49, 413 (1958).
10. A. A. Solomon, J. L. Routbort and J. C. Voglewede, Fission-induced Creep of UO<sub>2</sub> and Its Significance to Fuel-element Performance, Argonne National Laboratory Report ANL-7857 (1971).
11. A.R. Kaufman, Nuclear Reactor Fuel Elements; Metallurgy and Fabrication, Interscience Publishers, New York (1962).
12. J. Weertman, Creep of Indium, Lead and Some of Their Alloys with Various Metals, Trans. Met. Soc., Amer. Inst. of Met. Engr. 218, 207 (1960).
13. G. F. Slattery and W. N. Miller, The Creep Strength of Uranium Containing Small Alloying Additions, J. Nucl. Mat. 22, 320-331 (1967).

14. F. Garofalo, Fundamentals of Creep and Creep-Rupture in Metals, MacMillan Co., New York (1965).
15. C. M. Walter, G. H. Golden and N. J. Olson, U-Pu-Zr Metal Alloy: A Potential Fuel for LMFBR's, Argonne National Laboratory Report ANL-76-28 (1975).
16. L. R. Kelman, H. Savage, C. M. Walter, B. Blumenthal, R. J. Dunworth and H. V. Rhude, Status of Metallic Plutonium Fast Power-Breeder Fuels, Proc. 3rd Int. Conf. on Plutonium, A. E. Kay and M. B. Waldron, eds., Chapman and Hall, London 458-484 (1965)
17. D. R. O'Boyle and A. E. Dwight, The Uranium-Plutonium-Zirconium Ternary Alloy System, Nuc. Met., 17, Part II, 720-732, Plutonium 1970 and Other Actinides, William N. Miner, ed., Proc. 45th Int. Conf. on Plutonium and Other Actinides, Sante Fe, New Mexico, October 5-9, 1970 (1970).